Upgrading Fuel Properties of Biomass by Torrefaction

Shang, Lei; Holm, Jens Kai

Publication date:
2013

Document Version
Publisher's PDF, also known as Version of record

Upgrading Fuel Properties of Biomass by Torrefaction

PhD Thesis

Lei Shang

December, 2012

CHEC

Department of Chemical and Biochemical Engineering

Technical University of Denmark

ABSTRACT

Torrefaction is a mild thermal (200 – 300 ˚C) treatment in an inert atmosphere, which is known to increase the energy density of biomass by evaporating water and a proportion of volatiles. In this work, the influence of torrefaction on the chemical and mechanical properties (grindability and hygroscopicity) of wood chips, wood pellets and wheat straw was investigated and compared. The mass loss during torrefaction was found to be a useful indicator for determining the degree of torrefaction. For all three biomass, higher torrefaction temperature or longer residence time resulted in higher mass loss, higher heating value, better grindability, and less moisture absorption. However, severe torrefaction conditions were found not necessary in order to save energy during grinding, since strain energy and grinding energy decreased tremendously in the first 5 - 25% anhydrous weight loss. By correlating the heating value and mass loss, it was found that wheat straw contained less heating value on mass basis than the other two fuels, but the fraction of energy retained in the torrefied sample as a function of mass loss was very similar for all three biomass. Gas products formed during torrefaction of three biomass were detected *in situ* by coupling mass spectrometer with a thermogravimetric analyzer (TGA). The main components were water, carbon monoxide, formic acid, formaldehyde, methanol, acetic acid, carbon dioxide, and methyl chloride. The cumulative releases of gas products from three biomass fuels at 300 ˚C for 1 h were compared, and water was found to be the dominant product during torrefaction.

The degradation kinetics of wheat straw was studied in TGA by applying a two-step reaction in series model and taking the mass loss during the initial heating period into account. The model and parameters were proven to be able to predict the residual mass of wheat straw in a batch scale torrefaction reactor with different heating rates well. It means the mass yield of solids in the real torrefaction facility can be predicted by simply knowing the temperature curve of the sample.

The pellets pressed from torrefied spruce increased significantly in length after pelletization, which indicates worse quality of inter-particle bonding with correlation to higher torrefaction temperatures. Pine pellets that are torrefied subsequent to pelletization exhibited better durability, no spring back effect or disintegration was observed. A good correlation was found among compression strength of single pellet, durability of the whole batch pellets, and the energy use during grinding. The pellet durability can thus be estimated based on compression strength data of about 25 pellets.

Keywords: Torrefaction, wheat straw, wood chips, pellets, grindability, heating value, kinetics, tensile strength, durability, chemical structure, HGI, FTIR, MS, TGA, hygroscopicity, grinding energy.

Dansk Resume

Torrefaction, der er en mild varmebehandling (200 – 300 ˚C) i inert gas, er kendt for at øge energidensiteten af biomasse ved fordampning af vand samt en mængde flygtige komponenter. I dette studie, er påvirkningen fra torrefaction på træflis', træpillers og hvedehalms kemiske og mekaniske egenskaber (formalingsegenskaber og vandabsorption) undesøgt. Massetabet under torrefaction blev påvist at være en nyttig indikator til bestemmelse af torrefactionsgraden. For alle tre biomasser resulterede højere torrefactiontemperaturer eller længere opholdstid i større massetab, højere brændværdi, bedre formalingsegenskaber samt mindre fugtabsorption. Imidlertid, blev høj torrificerinsgrad fundet unødvendige med henblik på at spare energi under formaling, da belastningsenergien aftog eksponentielt, i løbet af de første 5-25% vandfrit massetab. Ved at korrelere brændværdien med massetabet, blev det fundet, at hvedehalm havde lavere brændværdi på massebasis end de andre to brændsler, samt at andelen af tilbageværende energi i de torreficerede materialer som funktion af massetab, var stort set identisk for alle tre biomasser. Gasprodukter dannet under torrefaction af tre biomasser, blev bestemt *in situ* ved kobling af masse spektrometer med en termo gravimetrisk analysator (TGA). Hovedkomponenterne var vand, kulilte, myresyre, formaldehyd, methanol, eddikesyre, kuldioxid og methylklorid. Den kumulative frigivelse af gas produkter fra tre biomassebrændsler for en times torrefaction ved 300 ˚C blev sammenlignet og det blev fundet at vand var det primære produkt fra torrefaction.

Degraderingenskinetik for hvedehalm blev undersøgt i en TGA ved at anvende en model for en to-trins reaktion i serie og tage hensyn til den dynamiske opvarmnings periode. Det blev eftervist at modellen og parametrene kunne forudsige den tilbageværende masse af hvedehalm i en batchskala torrefactionsreaktor med varieret opvarmningshastighed. Det betyder massetab af faste stoffer i den virkelige torrefaction anlægget kan forudsiges ved blot at kende temperaturkurven af prøven.

Ved pilletering torreficeret grantræ, øgedes længden af pillerne væsentligt jo højere torrificeringsgraden, hvilket indikerer lavere kvalitet af de interpartikulære bindinger som funktion af højere torrefactionstemperatur. Piller af fyr, torreficeret efter pilletering, udviste bedre bestandighed, og hverken tilbagefjedring eller smuldringeffekter blev observeret. En god korrelation blev fundet mellem; kompressionsstyrke af enkelte piller, bestandighed af hele pillepartier og energiforbrug under neddeling. Derfor kan pillers bestandighed estimeres ud fra kompressionsstyrkedata fra ca. 25 piller.

List of publications

This thesis includes the work contained in the following papers, referred to by Roman numerals in the text:

I Changes of chemical and mechanical behavior of torrefied wheat straw

Lei Shang*, Jesper Ahrenfeldt, Jens Kai Holm, Anand R. Sanadi, Søren Barsberg, Tobias Thomsen, Wolfgang Stelte, Ulrik B. Henriksen

Biomass and Bioenergy, (2012), 40: 63-70.

II Physical and chemical property changes of 3 biomass fuels caused by torrefaction

Lei Shang*, Wolfgang Stelte, Jesper Ahrenfeldt, Jens Kai Holm, Rui-zhi Zhang, Yong-hao Luo, Helge Egsgaard, Søren Barsberg, Tobias Thomsen, Lars Stougaard Bach, Ulrik B. Henriksen

Biomass and Bioenergy, under review

III Pelletizing properties of torrefied spruce

Wolfgang Stelte*, Craig Clemons, Jens Kai Holm, Anand R. Sanadi, Jesper Ahrenfeldt, Lei Shang, Ulrik B. Henriksen

Biomass and Bioenergy, (2011), 35: 4690-4698.

IV Quality effects caused by torrefaction of pellets made from Scots pine

Lei Shang*, Niels Peter K. Nielsen, Jonas Dahl, Wolfgang Stelte, Jesper Ahrenfeldt, Jens Kai Holm, Tobias Thomsen, Ulrik B. Henriksen

Fuel Processing Technology, (2012), 101: 23-28.

V Intrinsic kinetics and devolatilization of wheat straw during torrefaction

Lei Shang*, Jesper Ahrenfeldt, Jens Kai Holm, Søren Barsberg, Rui-zhi Zhang, Yong-hao Luo, Helge Egsgaard, Ulrik B. Henriksen

Journal of Analytical and Applied Pyrolysis, (2013), 100: 145-152.

VI A method of predicting the heating value of the solid residues during torrefaction

Lei Shang*, Jesper Ahrenfeldt, Jens Kai Holm, Ulrik B. Henriksen

21th European Biomass Conference and Exhibition. Copenhagen, Denmark, 3-6 June, 2013. Submitted.

* Corresponding author

Publications not included in the thesis:

A. Pelletizing properties of torrefied wheat straw

Wolfgang Stelte*, Lei Shang, Niels Peter K. Nielsen, Anand R. Sanadi

Conference paper: World Sustainable Energy Days 2012, Wels, Austria

B. Recent developments in biomass pelletization – a review

Wolfgang Stelte*, Anand R. Sanadi, Lei Shang, Jens Kai Holm, Jesper Ahrenfeldt, Ulrik B. Henriksen

BioResources, (2012), 7(3): 4451-4490

C. Approach and progress in relation to challenges with the pelletization of torrefied biomass

Wolfgang Stelte*, Niels Peter K Nielsen, Lei Shang, Jonas Dahl, Anand R Sanadi, Hans Ove Hansen

Biomass and Bioenergy, under revision

Conferences and workshops contribution:

Shang L*, Dahl J, Ahrenfeldt J, Holm JK, Nielsen NPK, Stelte W, Thomsen T, Bach LS, Henriksen UB. Quality of pellets from torrefied biomass and pellets torrefied at different temperatures. Poster Presentation at: 20th European Biomass Conference and Exhibition. Milan, Italy, 18-22 June, 2012.

Shang L*, Stelte W, Ahrenfeldt J, Holm JK, Bach LS, Thomsen T, Zhang RZ, Luo YH, Henriksen UB. Physical and chemical property changes of 3 biomass fuels caused by torrefaction. Oral Presentation at: World Sustainable Energy Days – WSEDnext conference, Wels, Austria, 29 February - 2 March, 2012.

Thomsen T*, Bach LS, Shang L, Egsgaard H, Ahrenfeldt J, Holm JK, Henriksen UB. Torrefaction of pine wood chips in a pilot-scale reactor. Poster Presentation at: 19th European Biomass Conference and Exhibition. Berlin, Germany, 6-10 June, 2011.

Shang L*, Ahrenfeldt J, Holm JK, Thomsen T, Henriksen UB. An investigation of the application aspects of torrefaction. Poster Presentation at: Risø International Energy Conference, Roskilde, Denmark, 10-12 May, 2011.

Shang L*, Ahrenfeldt J, Holm JK, Thomsen T, Henriksen UB. Grindability study of torrefied wheat straw. Poster Presentation at: Central European Biomass Conference, Graz, Austria, 26-29 January, 2011.

* Presenting and/or corresponding author

Table of Contents

Abbreviations

HGI --- Hardgrove Grindability Index

STA --- Simultaneous Thermal Analysis

MS --- Mass Spectrometry

EMC --- Equilibrium Moisture Content

ATR --- Attenuated Total Reflectance

FTIR --- Fourier Transform Infrared

AWL --- Anhydrous Weight Loss

TWL --- Total Weight Loss

HHV --- Higher Heating Value

LHV --- Lower Heating Value

TGA --- Thermo Gravimetric Analyzer

HPLC --- High Performance Liquid Chromatography

TIC --- Total Intensity Current

QMS --- Quadrupole Mass Spectrometer

SEM --- Scanning Electron Microscopy

m/z --- mass-to-charge ratio

Chapter 1

Introduction

The work presented in this thesis has been carried out at Technical University of Denmark and Shagnhai Jiaotong University, China. The project was funded by ENERGINET.DK and the ForskEL program (Project 2009-1-1-10202, Torrefaction of Biomass) and DONG Energy Power A/S. The aim of the work has been to understand torrefaction and the property changes of biomass caused by torrefaction at different operation conditions. The goal was to achieve a product which could later be used for co-firing in large scale utility boiler for DONG. Further aims were to combine the pelletizing process with torrefaction to achieve a product with even higher energy density and durability.

This thesis includes six papers. Paper I and II characterize the property changes of wheat straw, pine chips and Scots pine pellets caused by torrefaction. Paper III and IV deal with pellets made from torrefied Norway spruce and Scots pine pellets that are torrefied subsequent to pelletization. In Paper V and VI the degradation kinetics and devolatization of wheat straw was investigated, and a method was developed for predicting the mass yield and energy yield of feedstock in real production.

Background

The role of sustainability in the heat and electricity production continues to increase worldwide. The European Commission has set a binding target of a 20% share of renewables in the energy consumption by 2020 [1]. However, biomass fuels (in forms of straw and industrial biomass waste and wood) are more challenging to utilize than fossil fuel. The low energy density of biomass fuel causes a higher transportation and storage cost compared to coal, and it also reduces the thermal capacity in boilers when co-fired with coal [2]. The high moisture content present in biomass and their ability to absorb moisture from the surrounding atmosphere increase the costs of thermochemical conversion due to the drying stage [3]. The tenacious and fibrous nature of biomass is another important issue when it

comes to grinding the fuels before utilization. Torrefaction is a technique to improve the energy density of biomass, which involves the heating of biomass to moderate temperatures typically between 200 and 300 ˚C in the absence of oxygen and under atmospheric pressure. During the treatment, biomass starts to decompose and release torrefaction gas together with moisture. Thereby, the energy density of the torrefied biomass is increased. Moreover, during the torrefaction the structure of the torrefied biomass is changed to be more brittle and more hydrophobic [4]. All these property changes favour the replacement of fossil fuel with torrefied biomass in connection with co-milling and co-firing with coal in large scale utility boilers.

The process of torrefaction has been known for processing of wood since about 1930. However, it is only recently that it has been claimed to be beneficial for modern biomass utilization due to the increasing demand of fuel and arising concerns of global warming problem. Meanwhile, the knowledge of torrefaction is not clearly defined yet. For example, there is lack of detailed understanding about chemistry occurring during torrefaction, and no mathematical model that can be directly used for predicting the mass yield of solids in real production was developed, etc. Regarding the combination of torrefaction and pelletization, it was first proposed by Energy Research Centre of Netherlands in 2005 [5]. So far only a few studies have been published about the pelletizing properties of torrefied biomass [6-8], and no other publications about the quality of torrefied pellets (different from pellets made from torrefied biomass) have been found.

The plant composition

Straw and woody biomass consists mainly of three groups of organic compounds: cellulose, hemicelluloses, and lignin. In addition to these three main constituents, there are various other organic compounds including small amounts of protein, small quantities of waxes, sugars and salts, and insoluble ash including silica [9].

Cellulose

The most abundant polysaccharide in plant tissue is cellulose. As the structural framework, cellulose is organized into microfibrils, each measuring about 3-6 nm in diameter and containing up to

36 glucan chains having thousands of glucose residues. It is a linear homopolymer of β-(1→4)-linked D-anhydroglucopyranosyl units, which occurs in nature largely in a crystalline form, and organized as fibrils [9] (as shown in Figure 1).

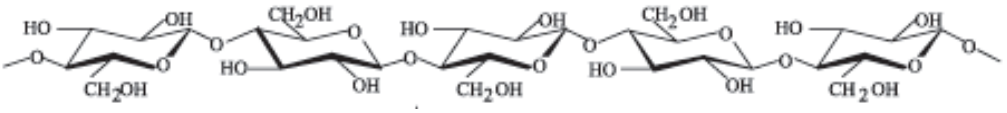

Figure 1: Chemical structure of cellulose [10].

Hemicelluloses

Hemicelluloses rank second to cellulose in abundance in cereal straws. Unlike cellulose, which is a unique molecule differing only in degree of polymerization and crystallinity, the hemicelluloses are non-crystalline heteropolysacharides and defined as the alkali soluble material after removal of the pectic substances. They form hydrogen bonds with cellulose, covalent bonds with lignin, and ester linkages with acetyl units and hydroxycinnamic acids. Hemicelluloses consist of various different sugar units that are arranged in different proportion and with different substituents. The chain may be linear but is often branched [9].

The hemicellulose content of softwoods and hardwoods differ significantly. Hardwood hemicelluloses are mostly composed of highly acetylated heteroxylans, generally classified as 4-*O*-methyl glucuronoxylans. Hexosans are also present but in very low amounts as glucomannans. In contrast, softwoods have a higher proportion of partly acetylated glucomannans and galactoglucomannans, and xylans correspond to only a small fraction of their total hemicellulose content [11]. For wheat straw, the hemicelluloses were confirmed to be a (1→4)-linked β-D-xylan with D-glucopyranosyluronic acid (or 4-O-methyl-α-D-glucopyranosyluronic acid) group attached at position 2, and L-arabinofuranosyl and D-xylopyranosyl groups attached at position 3 [12].

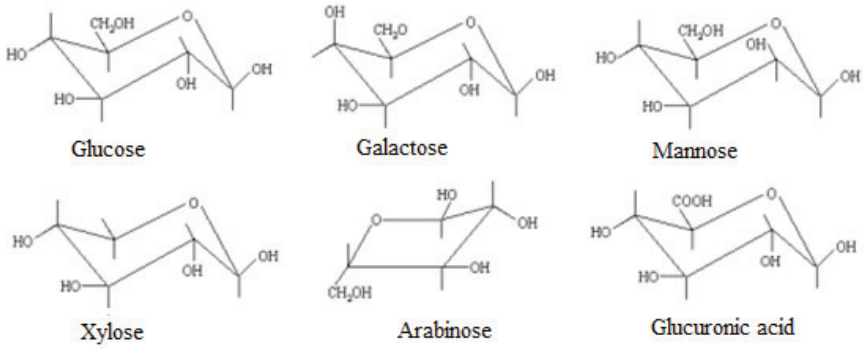

Figure 2: Chemical structures of main components of hemicelluloses [10].

Lignin

Lignin is the encrusting substance binding the wood cells together and giving rigidity to the cell wall [9]. It is a phenolic macromolecule primarily formed by the free-radical polymerisation of *p*-hydroxy cinnamyl alcohol units with varying methoxyl contents. The chemical structure of lignin is very complicated and is based on three monomeric precursors: coniferyl alcohol, sinapyl alcohol, and *p*-coumaryl alcohol (Figure 3). The proportion of these monomers varies among species and this ratio has been used for taxonomic purposes. Depending on the degree of methoxylation, the aromatic group is *p*-hydroxybenzyl (derived from *p*-coumaryl alcohol), guaiacyl (derived from coniferyl alcohol) or syringyl (derived from sinapyl alcohol). The former is not methoxylated, whereas the latter two have one or two methoxyl groups adjacent to the phenolic hydroxyl group, respectively. Softwood lignins are almost exclusively composed of residues derived from coniferyl alcohol (lignin type G), whereas hardwood lignins contain residues derived from both coniferyl and sinapyl alcohols (lignin type GS). In contrast, lignins derived from grasses and herbaceous crops contain the three basic precursors (lignin type HGS). As a consequence, hardwood lignins have higher methoxyl content, are less condensed and are more amenable to chemical conversion than lignins derived from conifers [9].

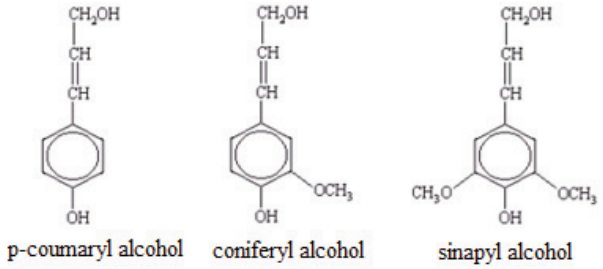

Figure 3: Chemical structures of main components of lignin [10].

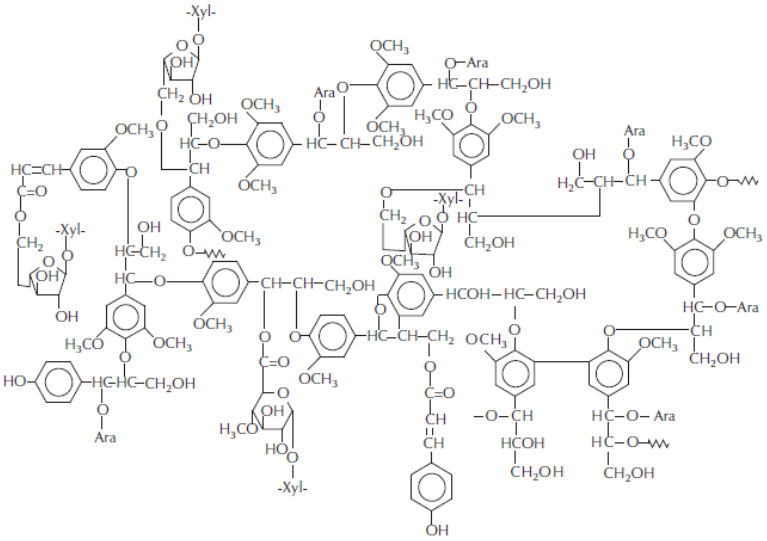

Figure 4: Structure model of wheat straw lignin [9].

Thermal degradation

In studies of heat-induced modifications of biomass properties, Svoboda et al. [13] summarized that the main changes in biomass due to torrefaction involve decomposition of hemicelluloses and partial depolymerization of lignin and cellulose. Bella et al. [14] heated American hardwoods to temperatures between 200 ˚C and 400 ˚C, and found a lower cellulose and hemicelluloses resistance compared to lignin. Gu et al. [15] studied thermal degradation of milkweed plant in the nitrogen atmosphere by using TGA-FTIR. Commercial lignin, cellulose and different hemicelluloses were also

tested. By comparing the weight loss and the temperature where the maximum rate of weight loss happened, it was concluded that hemicelluloses is the least stable component in milkweed floss, cellulose has a higher degradation temperature and degradation onset temperature, lignin begins to degrade at a lower temperature than milkweed floss, but it degrades more slowly as the temperature rises. The FTIR spectra at 300 ˚C in nitrogen show the main degradation products were H_2O and CO_2. The other organic volatile products were formic acid, acetic acid and methanol. Prins et al. [16] analyzed condensable products on HPLC and found that acetic acid and water are the main liquid torrefaction products of willow, while smaller quantities of methanol, formic acid, lactic acid, furfural, hydroxyl acetoneand traces of phenol are found. Šimkovic et al. [17] used TGA-MS to study thermal decomposition of xylan and have also observed these compounds.

In paper I, characterization of chemical changes of wheat straw due to torrefaction was monitored by Attenuated Total Reflectance (ATR) – Fourier transform infrared (FT-IR) spectroscopy, where samples were torrefied before recording the spectra. In paper II, the contents of lignin, cellulose and hemicelluloses for raw and torrefied pine chips, pellets and wheat straw were determined by chemical analysis, and the evolved gas during torrefaction was detected *in situ* by coupling a mass spectrometer with the TGA. In paper V, the relative amount of most gas products from wheat straw when torrefied at 250 ˚C and 300 ˚C were compared, and the amount of water released was quantified based on the MS intensity.

Grindability

A review of grindability study

Grindability is one of the fuel characteristics power plants are concerned most when talking substituting biomass for coal, because it directly decides if the existing coal mills are able to be used for biomass fuels to reduce the particle size efficiently small for a complete combustion. A list of published results regarding grindability study of torrefied biomass is given in Table 1. There are several types of milling equipment available, for example ball mill, pin mill, hammer mill, cutting mill, knife mill/blender, etc. Different mills run by different function principles. Cutting mills work by cutting and

shearing force; hammer mills reduce the particle size by hammering, i.e. impact and shear forces; ball mills perform by the interaction between frictional and impact force caused by difference in speeds between the balls and grinding jars. Because of the Hardgrove Grindability Index (HGI) test, ball mill is widely used in the experiments for grindability of coal and biomass. However, in real production cutting mills and hammer mills are more suitable for grinding biomass materials of a fibrous nature like straw [25,26]. It can be seen in Table 1 that there are several parameters related to size reduction experiments, due to their relevance to the technical and economic feasibility. For example, power consumption of grinding the torrefied biomass is needed for estimating the whole energy balance of torrefaction, pulverizing and pelletization; mill capacity is relevant to deciding the capital investment; and particle size distribution is considered as product quality, which is crucial to the fluidization performance.

As shown in Table 1, all studies showed that grinding energy and particle size distribution decreased with increasing torrefaction temperature or time, but sever torrefaction was approved not necessary by Bergman [28] and Repellin V. [32]. Both Abdullah &Wu [29] and Deng [30] pointed that the shape of biomass fines after grinding is different from biochar and coal. Arias [4] also concluded that the length of the particles reduced with increased torrefaction temperature or time, while the diameter of the particles did not change a lot.

Table 1: A list of experimental conditions and results of grindability study of torrefied biomass given by different authors (T: torrefaction temperature; t: torrefaction time).

Author	Equipment	Material and (Testing items)	Results
Arias [4]	Retsch SK100 Cross beater mill. Feed: < 15 mm; final fineness: < 100 μm; bottom sieve size: 2 mm.	Eucalyptus, 240-280 ˚C, 0-3 h. (Particle size distribution: > 425, 425-150, 150-75, < 75 μm.)	When increasing T and t, the amount of particles passing to the lower size fractions increased. Particle size mainly reduced in length, as the diameter of the particles does not change appreciably with different conditions.
Bridgeman [27]	Retsch PM100 ball mill. Feed: < 10 mm; final fineness: < 1 μm.	Willow, 240 ˚C and 290 ˚C, 10 min and 60 min. (HGI value.)	When increasing T and t, HGI increased.

Bergman [28]	Retsch SM2000 cutting mill. Feed: < 60×80 mm; final fineness: < 0.25-20 mm.	Willow, beach, larch, 230 -270 ˚C, 8 -30 min. (Power consumption, mill capacity, Particle size distribution.)	Power consumption increased when reducing the resulting particle size; power consumption decreased when increasing T and t (but not significant when T > 250 ˚C, t > 8 min); mill capacity increased when increasing T; mass fractions of smaller particle size increased when increase T. Power consumption: willow>beech>larch; while the opposite for the mill capacity.
Abdullah & Wu [29]	Retsch MM400 mixer mill. Feed: ≤ 8 mm; final fineness: ≈ 5 μm	Mallee wood, 300-500 ˚C, 30 min. (Particle size distribution, bulk density, volumetric energy density, SEM images of ground particles.)	The particle size distribution decreased when increasing T (but not significant when T > 330 ˚C); bulk density and volumetric density increased when increasing T (2 min grinding, 600-700 kg m^{-3}; 330 ˚C, 17-23 GJ m^{-3}). Milling energy saving of 73-93% can be achieved by grinding biochar instead of biomass. SEM and image analysis showed short and round particles after grinding biochar, long and fibrous particles after grinding biomass.
Deng [30]	Ball mill	Rice straw and rape stalk, 200-300 ˚C, 30 min. (Particle size distribution: > 450, 450-150, 150-100, < 100 μm.)	The ratio between course and fine particles decreased when T was increased. It was noted that slim powder of biomass is different from the coal particles with spherical or cubic shapes.
Sadaka [31]	(Small and equal pressure for 10 s)	Wheat straw, 200-315 ˚C, 1-3 h. (Visualization of the images.)	Particle size decreased when increasing T and/or t.
Repellin V. [32]	Pre-ground in Retsch SM1 knife mill, sieved between 2-4 mm, and then finely ground in Retsch ZM1 ultra centrifugal mill, equipped with 500 μm grid.	Spruce and beech chips, 160-300 ˚C, 5-60 min. (Grinding energy, Particle size distribution, G value vs. AWL $G = \frac{E}{x_{<200\mu m}}$, E is grinding energy and x is the volumetic fraction of particles smaller than 200 μm.)	Increasing T or t, AWL increased, grinding energy decreased, and particle size distribution decreased linearly. Grinding energy decreased tremendously at 0-8% AWL, but has low impact on particle size distribution. Particle size decreased significantly for treatments of 5 and 20 min, no further variation when duration increased to 40 and 60 min. G value is decreased of 93% when AWL is 28%. Fine grinding of natural wood requires almost 1/6 of its LHV. The effect of torrefaction on powder fineness is stronger for spruce than for beech.

Hardgrove Grindability Index test

The Hardgrove Grindability Index (HGI) was developed as an empirical test to indicate how difficult it is to grind a specific coal to the particle size necessary for effective combustion in a pulverized coal fired boiler [33]. This test has been incorporated into the Standards of different countries, for example ASTM. The HGI value is based on the amount of sample passing through a 75 µm sieve after being ground in a standard Hardgrove ball mill for 60 revolutions for each fixed amount of feed (50 g) with certain range of particle size (0.6 – 1.18 mm). The lower the number, the more difficult the material is to grind. The reason of choosing this particle size is that the preferred particle size range for pulverized coal combustion in a boiler to generate electric power, pulverized coal injection in cement or iron factories, and syngas production is nominally 70% of particles less than 75 µm in diameter and 99.5% of particles less than 300 µm in diameter. In general, particles less than 75 µm react in the volume of gas surrounding them. Particles between 75 and 300 µm require some combination of turbulence at a specific temperature for a defined time for relatively complete combustion. Particles larger than 300 µm do not burn out completely in the time available in the reactor and result in unburned carbon [33]. Joshi [34] and Agus and Waters [35] pointed out that the equal weight approach is unsatisfactory for making direct comparisons among fuels with densities differ a lot. To correct this situation and to bring evenness in grindability ratings of biomass and coal, Bridgeman et al. [27] used the same fixed volume (50 cm^3) for each feed as opposed to a fixed mass (50 g). In paper I and II, a similar method was used for calculating the equivalent Hardgrove Grindability Index (HGI_{equiv}). Particle size distribution analysis was also included as a complement to the HGI test, and grinding energy consumption was measured for wood chips and wood pellets in paper II.

Tensile strength test

As HGI is an empirical method to indicate how difficult it is to grind a specific coal. There is lack of research done for using HGI to indicate the grindability of biomass material, and it is not linked with any known physical property of coal. It is uncertain how well this HGI relates to the grindability of biomass. Therefore, it is important to measure at least one physical property of biomass. Considering the structure of biomass (in form of straw) and the relevance to the grinding process, it was decided to investigate the tensile strength of biomass material before and after torrefaction. Tensile strength is the

maximum stress that a material can withstand while being pulled before breaking. Furthermore, by measuring the elongation of the specimen while pulling it apart, strain energy at fracture per unit volume under tensile force can be calculated. Yigit [36] related the energy absorbed per unit new surface produced in the comminution and the strain energy per unit volume of the solid at fracture, and established mathematical models assuming fracture by tensile stresses. Mathematical models of new surface energy derived from different fracture patterns all have a positive linear relationship with strain energy per unit volume if the starting particle size and the reduction ratio are constants. Although the models cannot represent the fully realistic fracture pattern of a comminution process, they allow using the relative change of the strain energy at fracture under tensile force at different torrefaction temperatures as an indication of how much energy could be saved during grinding with the same circumstances. Some research has been done for measuring the tensile strength of raw biomass material, but not for torrefied biomass. The main difficulty encountered when measuring the tensile strength of biomass like straw was the brittle nature of stems, which caused it to fail at the clamps at each end of a specimen when a tensile force was applied. To solve this problem, Wright [37] prepared specimens with special end grips. O'Dogherty [38] developed a mechanical device, in which short lengths of steel rod were inserted into the specimen ends. The ends were then gripped by rubber jaws which had emery paper inserts interposed between the rubber and the straw. The rubber was mounted in steel clamps which could be rapidly clamped to the specimens. In paper I, tensile strength of wheat straw torrefied at different temperatures was measured by gluing the ends of specimen between 2 pieces of aluminum using 'Loctite super glue', and results were compared with those from literature.

Pelletization

Wood pellets are the only solid biofuels that has a global market, and they are still and will be one of the main feedstock of biomass used in power plants in Denmark. Moreover, pelletization is the future of torrefaction to make it transportable and ready for market. Several studies [5,7,8,39,40] have been made investigating the pelletizing properties of torrefied biomass. Gilbert et al. [8] and paper III indicate that pellet production from torrefied biomass can be challenging and can result in problems during processing and pellet quality. It was shown that torrefaction of biomass increases the friction in the press channel of a pellet mill and that the manufactured pellets are more brittle and less strong

compared to conventional pellets. Wood pellets made from untreated biomass have high mechanical properties which arise from the thermal softening of lignin, its subsequent flow and the formation of what can be referred to as an "entanglement network of molten polymers" [41]. The interpenetration of lignin polymer chains results in strong bonds upon cooling and solidification of the pellet. In paper IV, the quality of torrefied Scots pine pellets (different from pellets made from torrefied biomass) was studied for the first time. The idea behind this was to investigate whether these strong bonds outlast the torrefaction process and whether this might be a feasible method to produce pellets of a high mechanical stability and high energy density. Furthermore, a set of fast and simple laboratory test methods was established for controlling the pellets' quality.

A review of kinetic study

There are plenty of research data [18] relating to pyrolysis of biomass under both dynamic conditions (non-isothermal) and steady-state (isothermal) conditions. The main advantage of determining kinetic parameters by non-isothermal methods rather than by isothermal studies is that only a single sample is required to calculate the kinetics over an entire temperature range in a continuous manner. However, it is widely agreed that multiple heating rates should be adopted to enhance the accuracy of the non-isothermal method [18].

In case of torrefaction, all kinetic studies [19-21] were conducted under isothermal condition. Repellin et al. [20] proposed that torrefaction is kinetically controlled and neglected heat transfer within wood chips in their study, because the time taken for the center of a wood chip to reach the temperature imposed at the surface of these chips is short compared to the heating rate and the residence time of torrefaction (e.g. at 200 ˚C, this characteristic time was 8 s for beech with a size of around 2×15×30 mm and 11 s for spruce with a size of around 5×20×50 mm). It was also concluded that for a residence time of more than 20 min, the Anhydrous Weight Loss (AWL) depends almost entirely on the torrefaction temperature, because AWL is composed of two stages. The first stage is completed within 20 min with a rapid increase, the second stage matches with a slow increase. They used activation energies found in the literature and adjusted kinetic constants for the three models to fit the calculated weight loss to the experimental data using a minimization of least squares method. The

models used were a global one-step reaction model, a Di Blasi and Lanzetta model [22], and a Rousset model [23]. The Rousset model assumes that lignin and cellulose hardly react; hence the decomposition of hemicelluloses is the reason for the overall AWL of wood. However, Repellin et al. [20] only compared the final AWL with experimental results; no comparison was conducted on the degradation of wood as a function of time.

Di Blasi and Lanzetta [22] used a two-step reaction in series model for studying the intrinsic kinetics of isothermal xylan degradation under inert atmosphere in the temperature range of 200-340 ˚C. They found that a one-step global reaction did not fit the experimental results satisfactorily, as the time derivative of the solid mass fraction as a function of temperature exhibited a double peak. In both steps, a competitive volatile and solid formation was taken into account. In a later study done by Branca and Di Blasi on beech wood [24], it was suggested that the first step is due to the degradation of extractives and the most reactive fractions of hemicelluloses, and the second step is due to the degradation of cellulose and part of lignin and hemicelluloses. For temperatures higher than 327 ˚C there is a third step, which can be attributed to the degradation of lignin and small fractions of the other two constituents. Di Blasi and Lanzetta [22] pointed out the usual limitation encountered in order to attain the isothermal stage is that by using slow heating rates to avoid intra-particle temperature gradients usually result in non-negligible weight loss in the heating stage. Therefore, high heating rates (40 - 70 K s^{-1}) were adopted, and the char yield was determined as a function of the sample size prior to the tests to ensure no influence from the temperature spatial gradients. Constant char yields were attained for sample thickness around 100 μm, so particle size of 50 μm was chosen for the test. Di Blasi and Lanzetta [22] used graphical method to determine kinetic parameters by taking logarithm of the relative residual mass over reaction time for each step.

Prins et al. [21] first adopted Di Blasi and Lanzetta [22] model for studying torrefaction of willow, and used a numerical approach (MATLAB) to fit all kinetic parameters by minimizing the sum of squares function of experimental and model results. Different from Di Blasi and Lanzetta [22], bigger particle size (0.7-2.0 mm) and a much lower heating rate (10 ˚C min^{-1} to reach the isothermal part) were used in the experiments in TGA. The kinetic parameters were obtained from the isothermal part of torrefaction by neglecting the degradation of sample during the heating period. The model fit the experimental results obtained with the high heating rate (100 ˚C min^{-1}) at 260 ˚C well at first 14

min. By calculating the Biot number and Pyrolysis number, it was concluded that for pyrolysis of wood with diameter of less than 2 mm below 300 ˚C, the reactions are the rate limiting step and internal heat transfer in the wood particles can be neglected.

Chen and Kuo [19] analyzed the thermal decompositions of the 3 constituents (hemicelluloses, cellulose and lignin) separately using TGA at 200-300 ˚C with 1 h residence time. Kinetic parameters were derived by applying a global one-step reaction model to the weight loss curve for these 3 constituents. With the assumption of no interaction among constituents, the torrefaction of a mixture can be described by the superimposed kinetics. Same as Prins et al. [21], the heating period is not taken into account while using the low heating rate. It can be seen in their experimental results that the conversion of hemicellulose and xylan is already as high as 70% at the beginning of torrefaction at 300 ˚C. So the interpretation of the data lacks an important part of the whole process. And hence the use of this model will be limited if different heating rates are applied.

In paper V, a two-step reaction in series model [21,22] was used to study the kinetics of wheat straw torrefaction. The mass loss during heating period was taken into account when deriving the kinetic parameters from the isothermal part of torrefaction; model results obtained with and without including the non-isothermal part of torrefaction were compared with experimental data at different heating rates. It was also proven that the mass yield of wheat straw from a batch reactor can be predicted accurately by simply knowing the temperature profile of the sample during the reaction. The objective of this paper is to develop a kinetic expression that can predict the mass loss and gas evolution during torrefaction under real production conditions. In paper VI, this model was further related to the heating value and energy yield plot of biomass torrefied at different temperatures. A method of predicting the heating value of the solid products during torrefaction was thus established.

Chapter 2

Materials and methods

The materials and methods used in the papers on which this thesis is based will be introduced briefly in the following. References will be given to the corresponding paper, where a more detailed description of each experiment is found.

Materials

Winter wheat straw (*Triticum aestivum* L.) was used which was the most grown wheat species in Denmark in 2008. It was harvested on the island of Funen, Denmark (55°21′ N 10°21′ E) in August 2008 and cut by hand and stored indoors packed in paper bags.

Pellets made from pine wood (*Pinus sylvestris* L.) were supplied by Verdo's pellet factory in Scotland. The diameter of the pellets was 6 mm.

Wood chips were Danish pine wood from various sources on Zealand, Denmark (55° 30′ N 11° 45′ E). The size of the chips varied from 30×30×20 mm to 100×100×30 mm. The chips were stored for several months in a shielded container with air circulation and had a constant moisture content of around 16% on mass basis.

Norway spruce (*Picea abies* K.) was harvested in southern Sweden (Skåne/Småland) during 2007. Wood stems were collected in autumn, debarked and comminuted into wood chips. The material was dried by free air circulation for four weeks and further chopped into particles < 5 mm in diameter using a hammer mill, then packed in paper bags. The used samples had a particle size between 1 and 2.8 mm and the mass fraction of water was about 8.2%.

Methods

Torrefaction

Samples were dried in the oven at 104 °C for 24 h, and subsequently placed in an air tight metal reactor (15×31×10 cm) with a gas in and outlet (drawing of the reactor and oven refers to paper V). The reactor was placed in an oven (type S 90, Lyngbyovnen, Denmark) and heated up to the desired torrefaction temperature. The heating rate programmed for the oven was 6 °C min^{-1}. Nitrogen flow through the reactor was adjusted to 0.5 L min^{-1} to create an inert atmosphere. A thermocouple placed in the middle of the reactor (noted as 'rotten' in Figure 5) was used for temperature control. The residence time of the torrefaction process was started when the thermocouple inside the reactor ('rotten') has reached the set temperature. Afterwards the oven was shut down and the reactor was allowed to cool down. An example of temperature profiles at different places of the empty reactor during torrefaction of 240 ˚C is shown in Figure 5. The time delay caused by heat transfer from the bottom to the top of the reactor at 240 ˚C was around 15 min, and the temperature difference in the reactor was about 5 ˚C. Such temperature measurements were done at each torrefaction temperature for the empty reactor. The anhydrous weight loss (AWL, %) was determined as the mass loss of dried samples after torrefaction. For detailed equations refer to paper II.

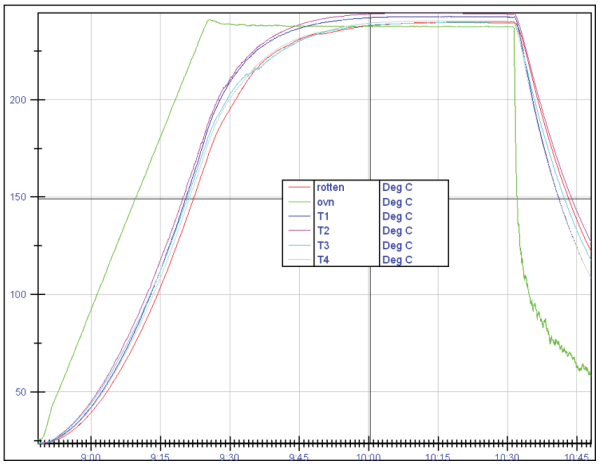

Figure 5: Temperature at different places in the batch reactor without samples during torrefaction of 240 ˚C.

Hardgrove Grindability Index tests

Hardgrove Grindability Index (HGI) test in principle is a simple and widely used measure of grindability for coal. It was performed in a standard Hardgrove grinder (3200LB, AUBEMA, Germany) pursuant to the ASTM D409-51 (1961) standard. The test feed volume was 50 cm^3 with a particle size between 0.6 and 1.18 mm, this was done by pouring the particles into a 50 cm^3 volumetric flask and vigorously stamping on a wooden board to the point where further stamping did not reduce the volume of the material. The loading of the top grinding ring was 290 N and the grinding time was 3 min (60 revolutions). The standard HGI can be determined by Eq. (1) [42] from the mass (in units of gram) of the ground product passing through the 75 µm sieve.

Standard HGI was measured for a reference coal sample (RUKUZN, supplied by DONG Energy, Denmark) at 3 different moisture contents on wet material basis (w.b.) (0%, 6.3%,and 9.0%) by using the same fixed volume (50 cm^3) for each feed according to Eq. (1). Then the relationship between the mass fraction of the coal samples passing through the 75 µm sieve after the grinding (denoted as 'x') and the equivalent HGI (HGI_{equiv}) can be established based on the results from the reference coal sample. The result is given in Eq. (2) with $R^2 = 0.9993$.

$$HGI = 13 + 6.93 \times m_{<75\mu m} \tag{1}$$

$$HGI_{equiv} = \frac{x + 5.2521}{0.3577} \tag{2}$$

Heating value

A Bomb calorimeter (6300, Parr Instrument Company, USA) was used to determine the higher heating value (HHV, MJ kg^{-1}). Initially, the calorimeter was calibrated using benzoic acid tablets. Particles smaller than 1 mm were placed in the crucible and fired inside the bomb calorimeter using an ignition wire in the presence of oxygen. The measurements were repeated at least 2 times, and the average value was used for calculation.

Ash content

Ash content was determined by placing the samples(about 0.4 g each) in a muffle furnace with adequate ventilation (Nabertherm B 180, Germany) at 550 ˚C for 3 h, 2 measurements were taken for each sample. Prior to the measurement, samples were oven dried at 105 ˚C overnight and crucibles were heated at 550 ˚C for 1 h.

For those samples torrefied in TGA, ash content was determined by heating the sample in the atmosphere of air to 850 ˚C at 50 ˚C min^{-1} right after the torrefaction and held for 5 min. According to Mayoral et al. [43], this method gave an ash quantification of an error of ± 0.5% compared to the ASTM method.

Biomass composition

The content of lignin, cellulose and hemicelluloses was determined according to ASTM E 1758-01 [44] and Kaar et al. [45]. A representative sample (about 0.16 g) smaller than 1 mm was dissolved in 72 % H_2SO_4 at room temperature and then hydrolyzed in dilute acid (4 % H_2SO_4) at 121 ˚C by autoclavation for 60 min. Hemicelluloses and cellulose contents were determined by HPLC (Aminex HPX-87H, Bio-Rad, Hercules, CA, USA) analysis of liberated sugar monomers in the filtered liquids, such as xylose, arabinose, galactose, mannose, and glucose, respectively. Klason lignin content was determined based on the residual filter cake corrected for the ash content. Duplicate measurements were mad for each sample.

ATR-FTIR

ATR-FTIR spectroscopy is a facile method which provides direct information from the outer (μm) sample surface layers with no requirement for prior sample preparation. The spectra recorded provide basic and in principle quantitative information on the sample cell wall polymers and their chemical modifications. Samples with size fraction between 250 and 600 μm were used for the FTIR test. Before the test, samples were dried in the oven at 40 ˚C for 24 h. ATR-FTIR spectra (4000 - 650 cm^{-1}) were recorded using a Fourier transform infrared spectrometer (Nicolet 6700 FTIR, Thermo Electron Corporation, USA). The system was equipped with a thermostat controlled ATR unit (T = 30 ˚C) where the sample was pressed against the diamond surface using a spring-loaded anvil. All spectra

were obtained with 128 scans for the background (air) and 100 scans for the sample with a resolution of 4 cm^{-1}. Spectra were recorded from 10 different subsamples for each sample condition, and these spectra were normalized at around 690 cm^{-1} where the spectra are free of distinct IR bands. The average spectrum of the 10 normalized spectra was presented for each sample condition.

Tensile strength

Tensile tests of wheat straw were done using a tensile tester (Vantage, Thwing Albert, USA) with a video extensometer measuring the prolongation of the straw. First, the stem internode was prepared by removing the plant leaf material, and then a flat thin piece was cut from the hollow stem. The ends of the specimen were glued (Loctite super glue, Henkel, USA) into 2 pieces of aluminium, as shown in Figure 6. The length of the specimen was in the range of 3-6 cm, and the width of the specimen was in the range of 1.4-3.1 mm. The elongation rate was 1 mm min^{-1} and stress was recorded using a 250 N load cell. Data from samples that failed close to the aluminium tabs were rejected. Each measurement was repeated at least 4 times, except for wheat straw torrefied at 300 ˚C. Due to the brittleness of the sample, data were collected from only 2 samples. The tensile failure stress (or ultimate tensile strength), σ, of the specimen was calculated from the Eq. (3) [38]:

$$\sigma = \frac{F_t}{A} \tag{3}$$

$$A = \frac{m}{\rho \times l} \tag{4}$$

Where F_t is the tension force at failure and A is the area of the specimen at the failure cross-section. The cross-section area was measured both by an electronic digital micrometer (Digital Micrometer DIN 863, Diesella, Denmark) and calculated from the apparent density by assuming a uniform wall area and structure with length, as shown in Eq. (4), where ρ is the apparent density of the straw, m and l are the mass and length of the specimen, which were measured before the test. Strain energy per unit volume was calculated as the area below the stress-strain curve in the diagram with the percent of elongation as X-axis and stress as Y-axis. [46]

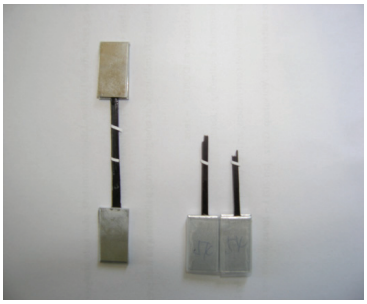

Figure 6: Specimen of tensile test. To the left, a sample before tensile strength is seen. To the right the sample after testing is seen.

Apparent density

Apparent density related to the tensile strength measurement was determined by coating the wheat straw samples (prepared the same way as tensile strength specimen) with paraffin wax, and then used volumetric pipettes and water to measure the volume of wax coated samples in a 25cm^3 volumetric flask. The mass of the straw sample was measured before coating, and the apparent density of wheat straw samples can be calculated by the following equation:

$$\rho_s = \frac{m_s}{V_s} = \frac{m_s}{V_{w+s} - \frac{m_{w+s} - m_s}{\rho_w}} \tag{5}$$

Where ρ means apparent density, V is the volume, m is the mass, 's' means wheat straw, 'w' means wax, and 'w+s' means wax coated straw samples. Since preparing wax coated straw samples were time consuming, and it was difficult to keep samples not floating above the neck of the volumetric flask, apparent density was only measured for wheat straw torrefied at 150 ˚C, which was 0.26 ± 0.03 g cm^{-3}. The apparent densities of wheat straw torrefied at other temperatures were calculated from the bulk densities. Bulk density was measured by filling the wheat straw particles in the range of 0.6-1.18 mm in a 50 cm^3 volumetric flask, and then stamps the flask vigorously on a wooden board to the point where further stamping does not reduce the volume of the content. When the calibration mark of 50 cm^3 is reached, stop and weigh the sample. Because the same size interval was used for all wheat strawparticles, it can be assumed that the volume of air between the particles is a constant for wheat

straw torrefied at different temperatures. By correlating the bulk density and apparent density of wheat straw torrefied at 150 ˚C, the value of this constant 'c' is available.

$$\rho_{bulk} = \frac{m_s}{V_s + c} = \frac{50ml \times \rho_{bulk}}{\frac{50ml \times \rho_{bulk}}{\rho} + c} \tag{6}$$

$$c = 50 \times \left(1 - \frac{\rho_{bulk}}{\rho}\right) = 17.93 \tag{7}$$

The apparent density of wheat straw torrefied at other conditions can be determined by their bulk densities, which were measured related to the Hardgrove grindability test.

Compression test

The internal strength of the pellets was analyzed by compression test and determined as the force at break. The single pellet was laid horizontally on the lower platen, and the upper platen mounted on a load cell was moved down at a certain speed to compress the pellet. The force and the corresponding position (displacement) of the upper plate were logged with 10 ms logging interval. Prior to compressing, the length and pellet mass were determined. At least 5 replications were tested for each sample.

Durability test

The pellet durability was determined according to the EN 15210-1standard [47], also known as tumbling can test. Prior to the testing, pellets were sieved through a 3.15 mm screen (round holes) to remove fines and dust from the samples. The amount of dust is referred to as 'dust in sample', and quantified as the difference in weight of the pellet sample before and after sieving, in percent of the sample before sieving. 500 g dust free pellets were loaded into the chamber of the standard durability tester and exposed to 500 rotations within a time interval of 10 min. The amount of fines formed during the test was determined by sieving the treated sample again through the 3.15 mm screen and determination of the weight difference before and after sieving. The durability value was calculated as the mass fraction of dust free pellets after the treatment in the pellets that was loaded into the tester.

Grinding energy consumption

Energy consumption for grinding was determined using a commercial coffee grinder (Kenia, Mahlkönig, Germany) with a screw conveyer feeding system and a disc grinding system. The distance between the two separate discs could be adjusted manually. The power consumption of the coffee grinder in operation was determined using a wattmeter (THII, Denmark). The meter was connected to a data logging system (NI USB-6009, National Instruments, USA).

Certain amount of sample (50 - 200 g) was fed into the feed hopper and the time required to grind the sample was recorded along with the energy consumed. The idling energy was measured before the material was introduced. The specific energy required for grinding was determined by integrating the area under the power curve corresponding to the time required to grind the sample minus the idling energy [48,49]. Particle size distribution was calculated based on sieve separation of the obtained biomass fraction using a sieve shaker (Retsch, Germany) with nine different sieves (mesh size of 75, 125, 250, 500, 1000, 1400, 2000, 3150, 5000 μm). The sieve shaker was run for 40 minutes and the weight of the individual fractions was determined subsequently.

Hygroscopicity

3 different saturated solutions were prepared in 3 desiccators below the platform using NaCl, KCl, and KNO_3,which gave relative humidity values of 75.5%, 85%, and 92.5% at 25 ˚C, respectively [50,51]. Biomass samples with similar size were selected and packed in one plastic net. These nets, together with 3 empty nets (which accounted for the net sorption) were then put on the platform in the desiccators, which were placed in a well isolated and temperature monitored water bath. Equilibrium moisture contents (EMC) of the biomass samples were measured about once a week, and they were determined by the increase of the mass in the sample nets subtracting the increase of mass in the reference nets.

Pelletization

A single pellet press, which consists of a cylindrical die with 7.8 mm in diameter, was used to produce the pellets used in paper III. The die was heated to 100 ˚C before the test. Small spruce particles equilibrated at 65% relative humidity were loaded stepwise in amounts less than 0.25 g into

the unit, and then compressed at a rate of 2 mm s^{-1} until a maximum pressure of 200 MPa was reached. The pressure was released after 5 s, the piston removed and more biomass was loaded and compressed until the pellet had a length of about 16 mm.

Thermogravimetric analysis

Torrefaction of biomass (in the range of 250 and 300 ˚C) at heating rates of both 10 and 50 ˚C min^{-1} were carried out on a TGA (TG 209 F3, NETZSCH, Germany) with a nitrogen flow rate of 40 cm^3 min^{-1}. Sample (< 0.09 mm) weight varied from 3 to 5 mg, and ceramic crucible was used for the test. In each test, sample was first heated up to 105 ˚C at 20 ˚C min^{-1} and held for 3 min for complete drying, then heated to desired torrefaction temperature and held for 90 min. Afterwards, purge gas was switched from nitrogen to air and sample was heated up to 850 ˚C at 50 ˚C min^{-1}, and kept at this temperature for 5 min for complete combustion. The residual mass is the ash content.

Simultaneous thermal analysis-mass spectrometric analysis (STA-MS)

Torrefaction was also carried out using a simultaneous thermal analyzer (STA 409, NETZSCH, Germany). Approximately 10 mg of the sample was placed in the microbalance and heated at 10 ˚C min^{-1} under 50 cm^3 min^{-1} argon or nitrogen, to a final temperature of 250 or 300 ˚C, and kept at this temperature for 1 h. The evolved gas was analyzed online by a quadrupole mass spectrometer (QMS 403 C, NETZSCH, Germany) coupled to the STA. In order to prevent condensation of evolved gas, the transfer line and inlet system of QMS was kept at ca. 300 ˚C. A small portion of the evolved gas together with the purge gas was led to the ion source of mass spectrometer, since the pressure drops from atmospheric pressure in TGA down to high vacuum in the QMS.

The analysis was focused on selected ions (*m/z*), in particular those which have been detected with high intensity. Since it is difficult to assign a given fragment to a single compound without confirmation by complimentary methods, the main detected *m/z* values were associated with the chemical species that are commonly present in gas products of biomass torrefaction or early stage of pyrolysis. A maximum number of 64 ions could be monitored as a function of time. The mass spectrometric intensities were normalized by the initial sample mass, and the background was subtracted. In order to compare the relative intensity of gas products at different temperatures, the

signals were further normalized by the total intensity current (TIC) of the experiment [52]. However no specific response factors were applied. In order to reach the most reasonable association, the ion traces of both parent and fragment ions of most species have been considered.

Chapter 3

Results and discussion

This chapter summarizes the results and findings from research performed within this project. The different papers included in the thesis are referred to by superscripted Roman numbers: I, II, III, IV, and V.

Characterization

Biomass composition

Results of the sugar composition in both raw biomass (wheat straw, wood chips, wood pellets) and biomass torrefied at 300 ˚C are shown in Table 2. Different monosaccharides were chosen for the determination due to the different biomass species. For wheat straw, hemicelluloses are mainly consisting of a (1→4)-linked β-D-xylan with D-glucopyranosyluronic acid (or 4-O-methyl-α-D-glucopyranosyluronic acid) groups attached at position 2, and L-arabionfuranosyl and D-xylopyranosyl groups attached at position 3 [9]. Hence, only xylose and arabinose were chosen. Glucose is mainly contributed by cellulose; however, it is likely that a small amount of glucose is also present in the hemicelluloses, but this has not been taken into account in this work. It can be seen that the hemicelluloses were totally degraded when torrefied at 300 ˚C (for 2 h) for all 3 biomass species, and cellulose was also strongly degraded under these torrefaction conditions.

Table 2: Mass fraction of sugar composition in both oven dried biomass and biomass torrefied at 300 ˚C for 2 h on dry material basis (d.b.) (paper II).

	Glucose	Xylose	Galactose	Mannose	Arabinose	Acid insoluble fraction	Ash
Wheat straw	34.0	23.4	ND[a]	ND	3.1	20.3[b]	4.6
Wheat straw, 300 ˚C	0.9	0.3	ND	ND	0.0	86.5	12.1
Scots pine pellets	40.5	4.2	2.4	9.8	2.2	32.2[b]	0.7
Scots pine pellets, 300 ˚C	0.2	0.0	0.0	0.0	0.0	98.8	1.1
Pine chips	42.8	6.9	5.3	3.7	0.0	27.5[b]	1.3
Pine chips, 300 ˚C	13.0	0.0	0.0	0.0	0.0	84.6	1.6

[a] *ND, not determined.*
[b] *In case of untreated biomass, the acid insoluble fraction is defined as Klasson lignin content.*

ATR-FTIR

Infrared spectra taken from wheat straw samples torrefied at different temperatures for about 2 h are shown in Figure 7 with the bands of interest being identified by their wavenumbers. The band at 670 cm^{-1} is characteristic for cellulose [53,54] and is an OH torsional vibration band. The fact that a significant decrease of this band is seen only for the highest temperatures between 270 ˚C and 300 ˚C shows that the cellulose component is largely stable until these temperatures are reached. The band at 1160 cm^{-1} is attributed to the antisymmetric stretching of C-O-C glycosidic linkages in both cellulose and hemicelluloses [55,56]. Its decrease is attributed to depolymerization and is most significant at the higher temperatures, and for 300 ˚C the band is practically absent. Gierlinger et al. attributed the band at 1240 cm^{-1} to the anti-symmetric stretching of C-O-C of acetyl groups [56]. There are no acetyl groups existing in the hemicelluloses of wheat straw. However, for both reference xylans a band is found at 1245 cm^{-1} and is of approximately the same strength as the (xylan) 900 cm^{-1} band. The assignment of the 1240 cm^{-1} band to lignin can also not be ruled out. The peak observed at 1505 cm^{-1} is diagnostic of lignin [55,57] and is placed in a spectral region devoid of polysaccharide peaks. No clear change of this peak is observed for most of the temperature range. However, at 300 ˚C it does appear to have diminished. The band at 1732 cm^{-1} is attributed to the carbonyl stretching band of carboxylic acid groups in hemicelluloses [56,57]. It starts to decrease from 250 ˚C, signifying a reduction in the amount of the carboxylic acid groups of hemicelluloses. This reduction is paralleled by the appearance of a new

degradation product band at 1700 cm^{-1}. When torrefaction temperature reaches 300 ˚C, the 1732 cm^{-1} band is completely eliminated, which suggests the complete removal of hemicelluloses. The narrow CH_2- stretching bands (superimposed a broader band) at approximately 2850 and 2920 cm^{-1} are ascribed to the aliphatic fractions of wax [57]. These bands for the C-H stretching can clearly be seen in spectra of extracted wax using hexane by work of Stelte, et al. [58]. These bands appear not to change significantly due to the heat treatment of torrefaction although a small decrease of these bands is suggested for the highest temperatures. It is possible that the higher molecular weight waxes may still be present in the samples torrefied at 300 ˚C, although further work needs to be done to confirm this.

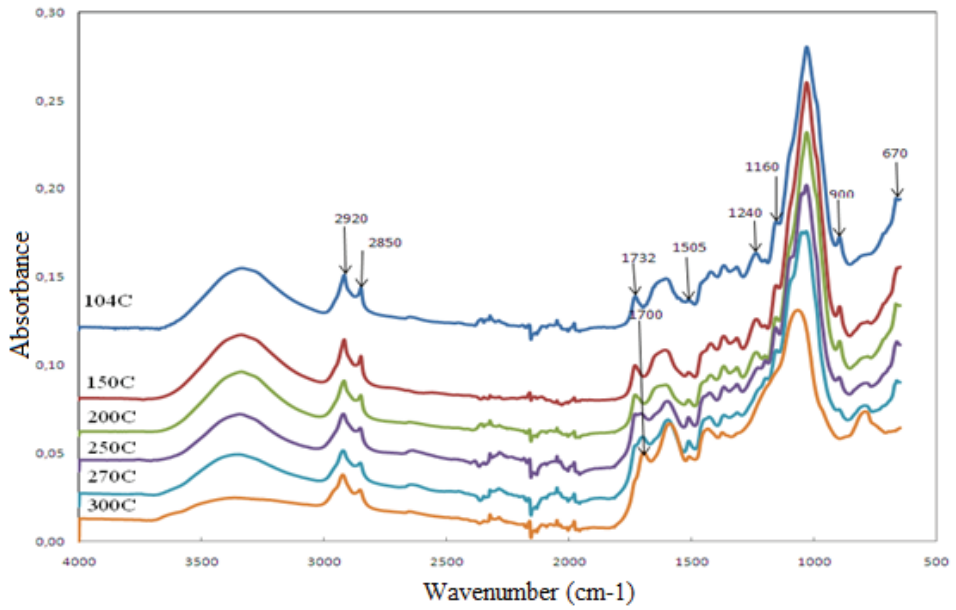

Figure 7: ATR-FTIR spectra of oven dried and torrefied wheat straw samples. All spectra are separated for an easy comparison (paper I).

By analyzing the FTIR spectra of the torrefied wheat straw samples, it can be concluded that there is no major structural change of the wheat straw samples torrefied below 200 ˚C. Increasing the temperature from 200 ˚C to 250 ˚C introduces distinct changes in the spectrum. These appear not to involve lignin or cellulose to any major extent, as the two characteristic bands of these components at

1505 and 670 cm^{-1} do not change. Thus degradation and depolymerization of hemicelluloses is proposed to account for the initial low temperature torrefication effects. A higher temperature effect is most notable for the 270 ˚C to 300 ˚C transition and consists of the degradation of lignin and cellulose.

Heating value and weight loss

As shown in Figure 8, higher torrefaction temperature resulted in higher anhydrous weight loss (AWL) and higher heating value (HHV). On dry and ash free basis, HHV of pellets and wood chips were very close, it increased from about 20 MJ kg^{-1} for oven dried samples to 29 - 30 MJ kg^{-1} for samples torrefied at 300 ˚C, where the AWL was about 50%. The HHV of wheat straw was always about 0.8 MJ kg^{-1} lower than the value of pellets and wood chips at the same AWL. This is in agreement with the experimental results from Prins et al. [59], where straw had the lowest heating value compared to willow, larch and beech, both untreated and at a torrefaction temperature of 250 ˚C. *Energy yield* was defined as the ratio between total energy retained in the torrefied samples and in the oven dried samples (for detailed equations refer to paper II). It is interesting to see that the *energy yield* of torrefied samples as a function of the mass loss was very close for the tested biomass species. It means that the same AWL corresponds to a similar fraction of energy loss in the samples during torrefaction for the tested biomass. It can also be observed that it is not a linear relationship between AWL and HHV/energy yield. There is more energy and mass loss at torrefaction temperatures ranging from 250 to 300 ˚C compared to from 200 to 250 ˚C. It is because hemicelluloses start the decomposition at 200 – 250 ˚C and last until 300 ˚C, while cellulose and lignin start the degradation at 270 – 300 ˚C. So in order to preserve energy in the torrefied material, lower torrefaction temperature and shorter residence time are preferred. If energy condensed material is desired, it is better to have more severe torrefaction conditions.

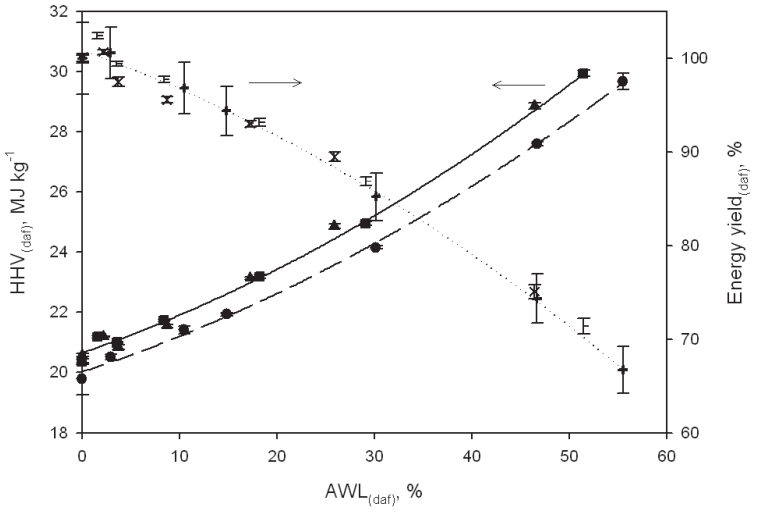

Figure 8: Higher heating value (HHV) for wheat straw (●), Scots pine pellets (■) pine chips (▲), and energy yield for wheat straw (+), Scots pine pellets (-), pine chips (×) vs. anhydrous weight loss (AWL, 0% AWL represents oven dried samples, torrefaction was carried out from 200 to 300 ˚C with every 20 ˚C interval) (paper II).

Grindability

Equivalent Hardgrove Grindability Index (HGI_{equiv})

For all 3 biomass samples, especially for pine chips and wheat straw, higher torrefaction temperatures result in better grindability. In order to achieve similar grindability as coal in wet conditions, a torrefaction temperature of about 240 ˚C is needed for wheat straw and pine chips, while for Scots pine pellets 290 ˚C is required. Below 220 ˚C the grindability of the pellets is almost the same as for pine chips. However, the increase in grindability for pellets is significantly lower than for the other two biomass species and seems not be improved a lot by increasing the torrefaction temperature further. Generally, there's no obvious improvement of grindability for all 3 biomass when torrefaction was conducted below 220 ˚C. The influence of torrefaction residence time on grindability of wheat straw was investigated in paper I, and concluded that there's no obvious improvement of HGI after 2 h torrefaction at 250 ˚C.

Based on the HGI results, the grindability of pine chips is almost as good as wheat straw at low torrefaction temperatures. However, if one takes a look at the particle size distribution results in Figure 10, wheat straw samples have a much higher percentage of fines in the range of 75 to 250 µm compared to pine chips. Therefore particle size distribution measurement is a necessary complement to the HGI test.

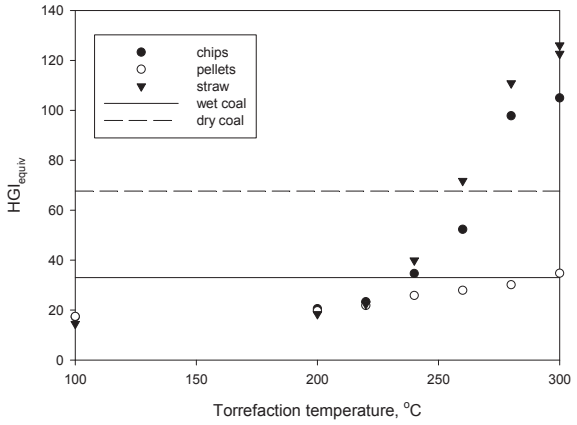

Figure 9: Results of Hardgrove grindability test for oven dried biomass (104 °C) and biomass torrefied at different temperatures for 2 h (HGI tests were repeated for wheat straw torrefied at 300 °C), coal in wet and dry conditions were also tested in the Hardgrove grinder as a reference (paper II).

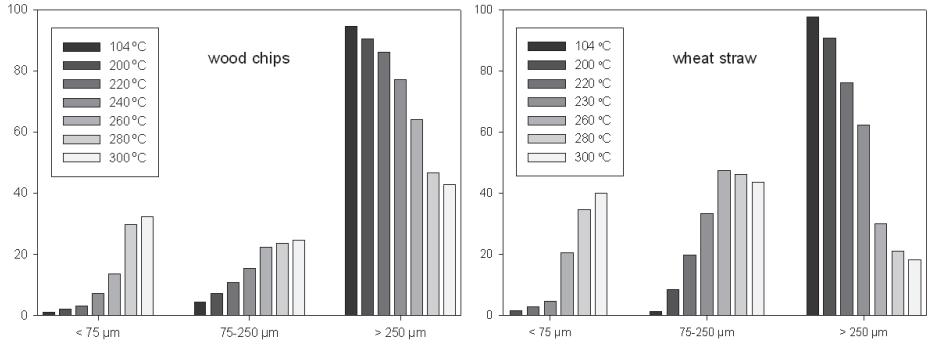

Figure 10: Particle size distribution analysis after HGI test (For wheat straw, particle size distribution wasn't tested on samples torrefied at 240 °C, so the results of samples torrefied at 230 °C are shown here instead) (paper II).

Tensile strength

Tensile strength was measured on oven dried wheat straw and straw torrefied at 150, 200, 250 and 300 ˚C for 2 h. As shown in Figure 11, tensile failure stress decreased from about 55 MPa for oven dried straw and straw torrefied at 150 ˚C to about 24 MPa for straw torrefied at 200˚C, and further to about 4 MPa for straw torrefied at 300 ˚C. By comparing the mean strain energy, it was concluded that wheat straw torrefied at 250 ˚C only required 1/5 to 1/7 of the energy required to pull oven dried wheat straw apart. Tensile strength results showed close relation to the HGI results. However, it was not proved to be more reproducible and repeatable than the HGI test.

Table 3 lists detailed information of tensile tests found in the literature for wheat straw. The data differ a lot mainly due to the different ways of counting the cross-section area (loading rate and moisture content of the specimen, and how the specimen was prepared also influence the results). Burmistrova [60] calculated stalk cross-section area based on the absolute dry weight of the wheat sample, the length of sample and the density of cellulose (1.55 g cm^{-3}). This physical cross-section area is smaller than the geometrical wall area by a factor of 5-10. Therefore the tensile strength is correspondingly larger than the results of the other quoted authors. Comparing the results obtained from oven dried wheat straw in this thesis and the data listed, it is found that the tensile strength is likely underestimated in most of the literature where the whole stalk was used for the test. Because the whole stalk does not break equally at the same time. In most cases, the weakest part break first while the other parts still hold together and only breaks when the force increases. Therefore, the cross-section area of the whole stalk is bigger than the actual area where the break happens, leading to underestimated tensile strength.

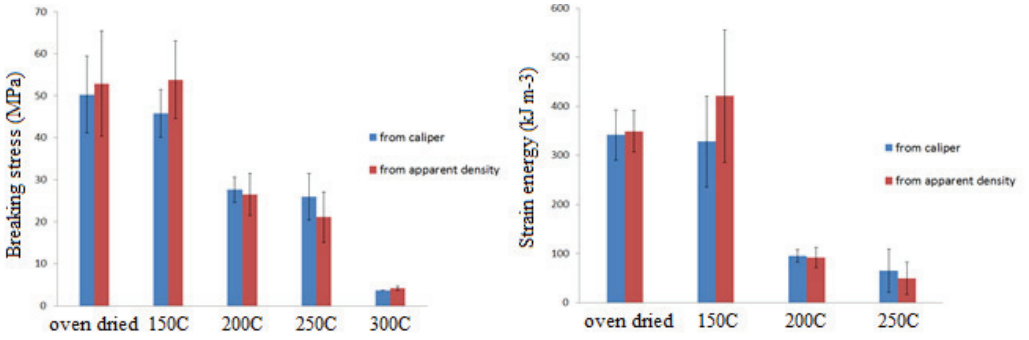

Figure 11: Tensile strength (left) and strain energy (right) of wheat straw samples treated at different temperatures from both direct caliper measurement and indirect apparent density calculation (to determine the cross-section area at break) (paper I).

Table 3: A list of experimental results of tensile test from literature.

Author	Specimen	Moisture content and loading	Tensile stress (MPa)	Cross-sectional area
O'Dogherty [61]	Wheat straw	10-14% (w.b.)	9-32	Not indicated.
Limpiti [62]	Wheat straw (3rd internode)	10-65% (w.b.)	32-38	Outside and inside diameter measured by a moving microscope.
Burmistrova [60]	Wheat varieties		128-399	Stem wall areas excluding the intercellular areas
O'Dogherty [38]	Wheat straw (internode)	8-22% (w.b.), 10 mm min^{-1}	21.2-31.2	Wall area of the specimen at the failure cross-sections
Wright [37]	Wheat/barley straw (2nd internode)	5 mm min^{-1}		Cross sectional area and min/max diameter were optically measured from a stereo-zoom microscope and analysis tools from Image Pro Plus software.
Kronbergs [63]	Wheat stalk	Not indicated	118.7±8.63	Measured by microscope, and assuming cross section as an elliptic ring.
This thesis	Wheat straw (2nd internode, part of the stem)	About 3-5%, due to the storage. 250 N, 1 mm min^{-1}	28-46 (oven dried)	Calculated from Bulk density
			256-422 (oven dried)	Calculated from true density by volume difference after immersing whole straw in the water.

Grinding energy

The energy use for grinding pine chips and Scots pine pellets in a bench scale disc mill (Figure 12) showed a sharp decrease up to approximately 25% and 10% AWL, respectively. Therefore, these two AWLs can be suggested as the optimal torrefaction conditions. Comparing with the results in paper IV, in which the energy consumption of pellets was measured at different setting, it can be concluded that grinding at the finest setting requires ten times as much energy as at the coarsest setting. An exponential decrease of grinding energy with AWL was observed for both conditions.

Contrary to the HGI results, pine chips consumed more grinding energy than pellets, except for the highest AWL (about 50%) where energy use in grinding for these two fuels tends to be close. It means below torrefaction temperature of 220 ˚C the bonding forces in the small particles (0.6-1.18 mm) are similar for pine chips and pellets, but the bonding in the whole pellets is 'weaker' than in the pine chips. For torrefaction temperatures up to 300 ˚C, the HGI results showed that bonding in the small particles outlast torrefaction quite well, but not the bonding in the whole pellets as shown in Figure 12.

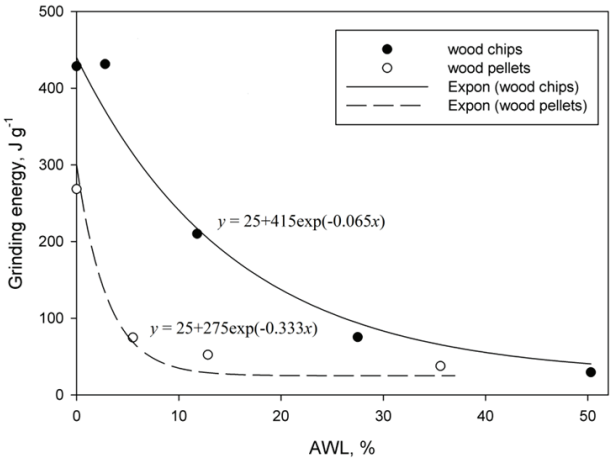

Figure 12: The energy required for grinding Scots pine pellets (torrefied at 230, 250, and 270 ˚C for ca. 1 h) and pine chips (torrefied at 200, 250, 275, and 300 ˚C for ca. 2 h) vs. anhydrous weight loss (0% AWL represents original pellets and oven dried pine chips). The grinding energy of a reference coal sample (RUKUZN, in size range of 2-7.1 mm, oven dried at 104 ˚C overnight) was determined with the same procedure, and it was 25 J g^{-1} (paper II).

Particle size distribution analysis was also done for the samples after the grinding energy measurement in paper II. Consistent with the HGI results, torrefied pine chips ended up with much higher fraction of fines (<75 μm) than pellets after grinding and the higher the torrefaction temperature, the higher the percentage of fines. However, increasing torrefaction temperature from 230 to 270 ˚C does not seem to improve the particle size distribution of pellets significantly, which is in agreement with the energy consumption results.

Hygroscopicity

When the relative humidity was increased, equilibrium moisture contents (EMCs) of all 3 samples (pine chips, Scots pine pellets, wheat straw) increased correspondingly. Samples pre-treated at higher torrefaction temperatures absorbed less moisture, although this trend was disturbed for wheat straw torrefied at the highest temperature due to the experimental error. EMCs of torrefied samples can be reduced by about 5-10%, 7-12% and 13-20% under 75.5%, 85% and 92.5% relative humidity, respectively. All three biomass samples exhibited similar EMCs under a relative humidity of 75.5%. However, when the relative humidity was higher than 75.5% wheat straw samples absorbed most moisture; while pellets and pine chips seemed to have similar EMCs in most cases.

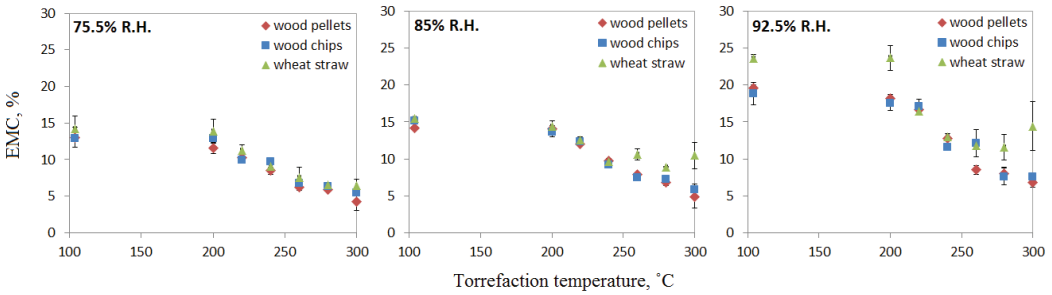

Figure 13: Equilibrium moisture content (EMC, on dry basis) for 3 kinds of biomass torrerfied at different temperatures (104 ˚C means oven dried samples) under 3 relative humidities (paper II).

Pellet property

Figure 14 shows the picture of pellets obtained from two different processes by switching the sequence of pelletization and torrefaction. No pellets could be made from spruce torrefied at 300 ˚C, and even at 275 ˚C the pellets exhibit many defects. It can also be observed that the pellet length increased with an increasing torrefaction temperature. This attributes to a spring-back effect and is a sign of poor adhesion between particles. It was suggested in paper III that the reduced hydrogen bonding sites due to the thermal degradation of hemicelluloses and lignin during torrefaction, together with the increased glass transition temperature of hemicelluloses and lignin caused by lower moisture content of the torrefied wood are the main reason of decreased pellet strength. On the other hand, Scots pine pellets torrefied at different temperatures exhibit good durability, no spring back effect or disintegration was observed. It means the bonds formed during pelletization outlast the torrefaction quite well.

Figure 14: Images of pellets made from torrefied spruce with residence time of ca. 2 h (paper III) and Scots pine pellets that torrefied subsequent to pelletization for about 1 h (paper IV).

Figure 15 shows that both the grinding energy and the compression strength of single pellets have the similar trend of energy decreasing when the mass loss during torrefaction increases. The particle size distribution analysis after grinding indicates that an obvious increase (8% compared to reference sample) of small particles (1 mm) occurred already at torrefaction temperature of 230 ˚C, further increase of temperature (from 230 to 270 ˚C) resulted only in slight increase of small particles

(+5%), but steep decrease of big particle (-10%). Figure 16 illustrates that an exponential function fits the correlation between the durability and the compression strength well. This indicates that if the compression energy is known, a reasonable estimate for the durability can be made and vice versa. It must also be noted that the analysis was based on pellets with diameter of 6 mm only, which means the diameter parameter has not been taken into account.

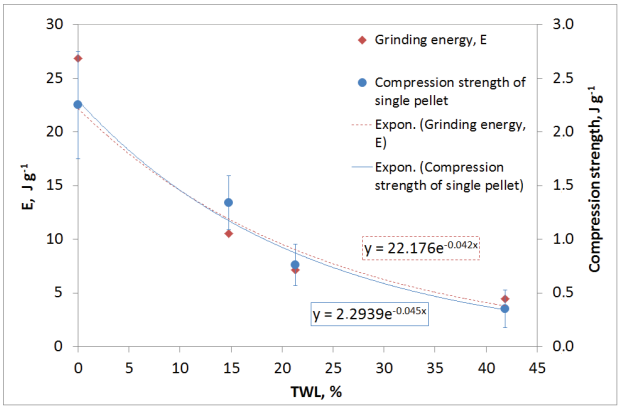

Figure 15: The specific energy required for grinding Scots pine pellets (E, J g^{-1}) and the compression strength of single 15-mm-long Scots pine pellet (J g^{-1}) vs. total weight loss (TWL is the total mass loss during drying and torrefaction) of pellet samples after torrefaction (paper IV).

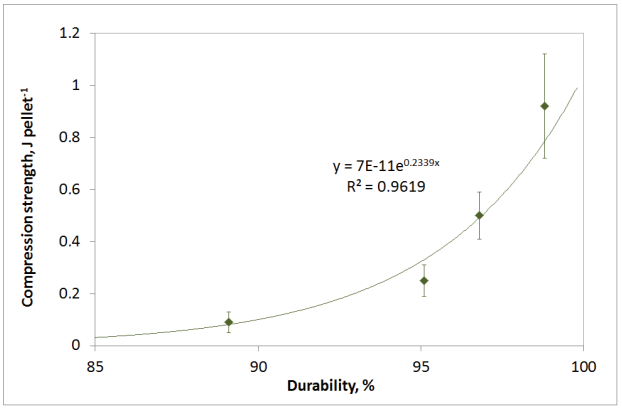

Figure 16: Plot of compression strength of single 15-mm-long Scots pine pellet (J pellet^{-1}) vs. durability. The fit of an exponential function is illustrated (paper IV).

In order to produce pellets (Ø 6 mm) with durability higher than 97.5% as required by ENPlus, compression strength of 0.6 J pellet^{-1} (with length of 15 mm) is needed, and the grinding energy (at coarsest setting) of ca. 15.3 J g^{-1} is expected. At this condition, energy reduction in grinding compared with untreated pellets is 43% (11.6 J g^{-1}), and the energy loss due to the torrefaction is about 4% (730 J g^{-1} based on original mass). However, the HHV is increased by about 1600 J g^{-1} from 18.4 MJ kg^{-1} for reference pellets to 20.00 MJ kg^{-1}, which corresponds to a torrefaction temperature of a bit lower than 230 °C with residence time of 1 h.

Kinetic study

Kinetic model

The two-step first order reaction in series model, as shown in scheme (8), was chosen for studying the wheat straw torrefaction. As opposed to the high heating rate of 40-70 K s^{-1} adopted by Di Blasi and Lanzetta [22], slow heating rate (< 100 K min^{-1}) was used to avoid intra-particle temperature gradients. Therefore weight loss during heating stage needs to be taken into account when deriving the kinetic parameters from the isothermal stage. Prins et al. [21] first used this model, Eq. (8)-(11), for studying torrefaction of willow. But the degradation during the heating period was neglected, that is *at t = 0, [A] = [A], [B] = [C] = 0.*

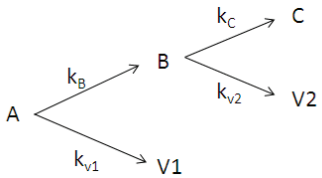

(8)

$$\frac{d[A]}{dt} = -(k_B + k_{v1})[A] \tag{9}$$

$$\frac{d[B]}{dt} = k_B[A] - (k_C + k_{v2})[B] \tag{10}$$

$$\frac{d[C]}{dt} = k_C[B] \tag{11}$$

$$at \quad t=0, \qquad [A]=[A]_0, \qquad [B]=[B]_0, \qquad [C]=[C]_0$$

Integration of Eqs.(9) - (11) with above mentioned initial conditions, and making $K_1 = k_B + k_{v1}$, $K_2 = k_C + k_{v2}$ gives (for details refer to Appendix-1):

$$[A] = [A]_0 \exp(-K_1 t) \tag{12}$$

$$[B] = \frac{k_B [A]_0}{K_1 - K_2} [\exp(-K_2 t) - \exp(-K_1 t)] + [B]_0 \exp(-K_2 t) \tag{13}$$

$$[C] = [C]_0 + \frac{k_C (k_B [A]_0 + K_1 [B]_0)}{K_1 K_2} + \frac{k_B k_C [A]_0 \exp(-K_1 t)}{K_1 (K_1 - K_2)} - \frac{k_B k_C [A]_0 \exp(-K_2 t)}{K_2 (K_1 - K_2)} - \frac{k_C [B]_0 \exp(-K_2 t)}{K_2} \tag{14}$$

$$\left(\frac{M}{M_0}\right)_{theor} = [A] + [B] + [C] \tag{15}$$

$$\left(\frac{M}{M_0}\right)_{\exp} = \frac{m_{TGA} - m_{ash}}{m_0 - m_{ash}} \tag{16}$$

Where the biomass is denoted ‘A’, and ‘B’ is the intermediate compound, which is a solid with a reduced degree of polymerization. ‘V1’ and ‘V2’ are volatiles; ‘C’ is the solid residue. *t* is time in s. *k* is the rate constant for each step, expressed as s^{-1}. *M* and M_0 are the solid residual and the initial sample mass on ash free basis, respectively. Experimentally M/M_0 can be determined by TGA, where m_0 is the initial sample mass, m_{ash} is mass of ash in the sample, and m_{TGA} is the mass measured by TGA as function of time.

A schematic drawing of the algorithm taking into account the chemical composition change at the onset of the isothermal period is shown in Figure 17. In the first iteration it was assumed that the entire solid is A, without B and C. With this initial assumption and a starting guess of k_B, k_{V1}, k_C, k_{V2}, which were based on values found from [21], nonlinear optimization using the MATLAB command ‘lsqcurvefit’ was made with the default tolerance settings. The ‘lsqcurvefit’ is based on the Niedler-Mead optimization algorithm and used to minimize the root mean square of between the calculated and

experimental data. Following this, at each temperature the four pre-exponential factors (*A*) and activation energies (*Ea*) were calculated by means of Arrhenius plot. With these calculated values the initial concentration of the isothermal period for A, B, and C can be obtained, and then used as input for the optimization. The calculations were done by numerical solution of the three coupled first order differential equations, as shown in Eqs. (9) - (11). To account for the heating rate, the chain rule was used to transform the equations into the temperature dependent form shown in Eqs. (17) - (19). From the second iteration and onwards the calculated *A* and *Ea* were used to provide the starting guess for the Niedler-Mead optimization. The procedure was repeated until stable values for the *A* and *Ea* were reached.

$$\frac{d[A]}{dT} = \left(\frac{dt}{dT}\right) \cdot \{-(k_B + k_{v1})[A]\} = \frac{1}{\beta} \cdot \{-(k_B + k_{v1})[A]\} \tag{17}$$

$$\frac{d[B]}{dT} = \frac{1}{\beta} \cdot \{k_B[A] - (k_C + k_{v2})[B]\} \tag{18}$$

$$\frac{d[C]}{dT} = \frac{1}{\beta} \cdot \{k_C[B]\} \tag{19}$$

Where β is the heating rate $\frac{dT}{dt}$, in K s^{-1}, and T is temperature in K.

By using a two-step reaction model and taking the degradation of sample during heating period into account, it allows to derive the kinetic parameters suitable for predicting the solid mass loss over the entire reaction period, especially at the initial stage of the reaction. This is very useful for the real production, where low heating rates are mostly applied. In practice, once the kinetic parameters have been obtained from the TGA test, the mass yield in the real torrefaction facility can be predicted by simply knowing the temperature history of the sample. However, for a biomass feedstock that has heat transfer limitation, e.g. in forms of logs or big chips etc., or biomass with different compositions that may generate heat during torrefaction, a heat transfer model may be coupled to the temperature function in the existing kinetic model for the mass yield calculations.

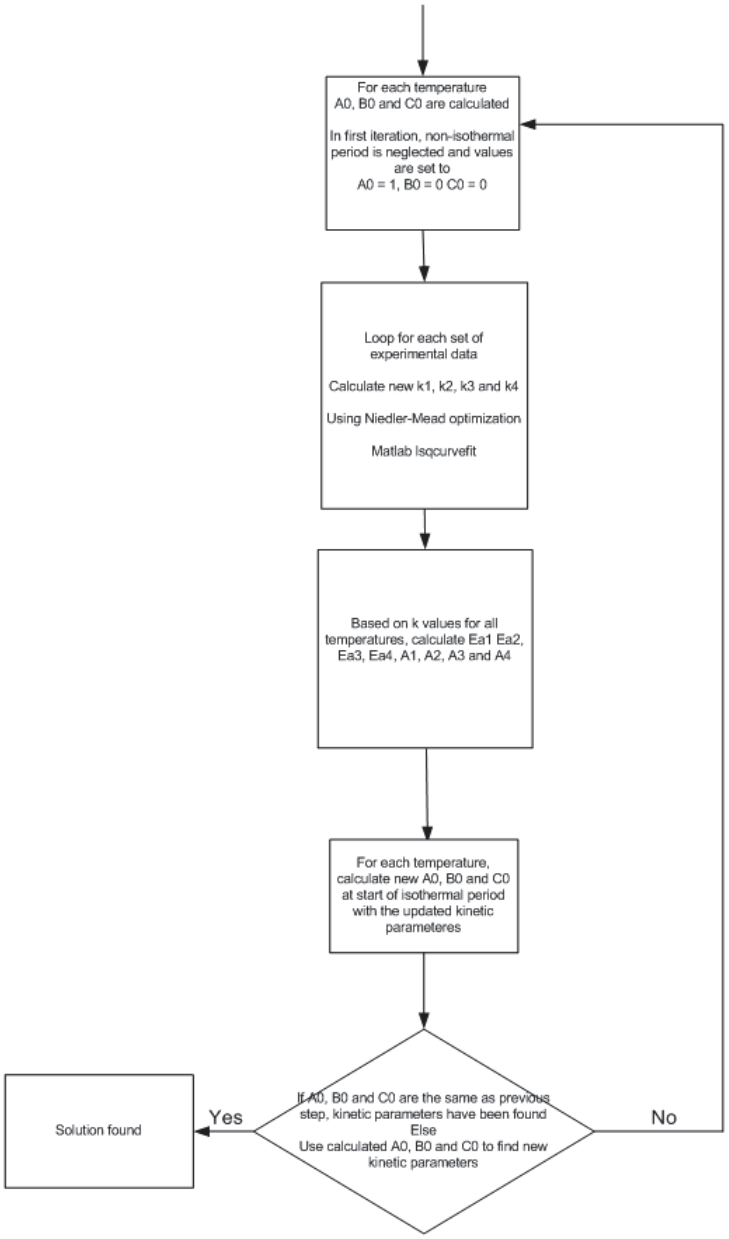

Figure 17: Diagram of algorithm used in MATLAB for calculating kinetic parameters of wheat straw torrefaction.

Model verification

The kinetic parameters of wheat straw obtained by best fitting the experimental data of 250, 260, 275 ˚C (at heating rate of 10 K min^{-1}) and 250, 260, 275, 280 (at heating rate of 50 K min^{-1}) are as follows:

$$k_B = 3.48 \times 10^4 \exp\left(\frac{-70999}{RT}\right) \quad (20)$$

$$k_{v1} = 3.91 \times 10^{10} \exp\left(\frac{-139460}{RT}\right) \quad (21)$$

$$k_C = 4.34 \times 10^3 \exp\left(\frac{-76566}{RT}\right) \quad (22)$$

$$k_{v2} = 3.48 \times 10^7 \exp\left(\frac{-118620}{RT}\right) \quad (23)$$

Where k is the reaction rate constant in unit of s^{-1}, T is the temperature in K, and R is the universal gas constant in J mol^{-1} K^{-1}. In agreement with literature, the first step is much faster than the second step. Solid yields for two reaction steps decreased from 85% and 66% at 250 ˚C to 61% and 46% at 300 ˚C respectively.

In order to verify the model, experimental data were compared with model results for both non-isothermal part (heating period from 200 ˚C to final torrefaction at both heating rates) and isothermal part. Due to the similarity and more relevance of low heating rates to real production, only results from 10 ˚C min^{-1} are shown in Figure 18. Instead, a three-step torrefaction was run from 200 ˚C to 250 ˚C (at 50 K min^{-1}) and held at 250 ˚C for 1 min, then heated to 260 ˚C (at 10 K min^{-1}) and held for 1 min, in the end heated up 270 ˚C (at 10 K min^{-1}) and held for 1 h. The difficulty of distinguishing each step is due to the temperature overshooting problem in the TGA. The higher the set temperature (and/or the faster the heating rates) the larger the overshoot occurs. It can be seen the model described the reaction accurately. The model was also tested on torrefaction of wheat straw conducted in a batch reactor. The temperature recorded in the center of the reactor was used as the input for the model to calculate the residual mass, assuming heat transfer from the wheat straw surface to the center is much faster than the

heating rate of the oven (6 ˚C min^{-1}). Model and experimental results are shown in Figure 19. There is a good correlation between model results and experimental data.

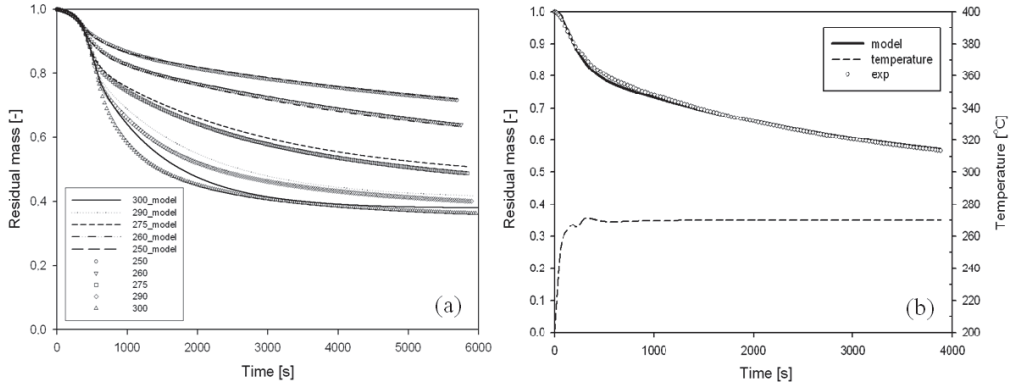

Figure 18: Experimental and modeled relative weight (on ash free basis) of wheat straw vs. time for (a) at heating rate of 10 K min^{-1}. (b) three-step heating at various rates. Starting weight is defined at 200 ˚C; heating period from 200 ˚C to desired torrefaction temperature is included in the plot (paper V).

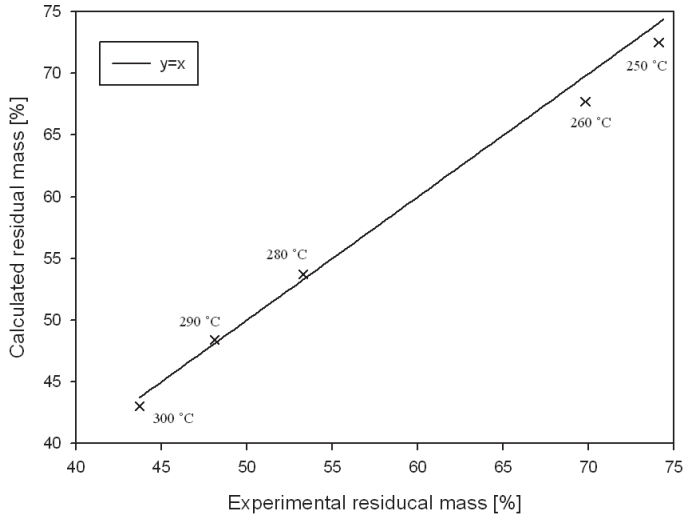

Figure 19: Correlation between experimental residual mass obtained from torrefaction of wheat straw in a batch reactor and calculated results from the model. Both results are on dry and ash free basis (paper V).

Gas evolution with MS analysis

Gas products during torrefaction of wheat straw, at 250 and 300 ˚C, were detected based on selected ions were water (18), carbon monoxide (28), formic acid (46, 45), formaldehyde (30, 29), methanol (31, 32), acetic acid (43, 45, 60), carbon dioxide (44), methyl chloride (50, 52). Traces of hydrogen sulfide (34) and carbonyl sulfide (60, 48) were also found. In addition, relatively large quantities of simple aliphatic hydrocarbons were apparently present, C_xH_y and C_xH_{2x} (15, 27, 39, 41). A trace of acetone (58) was only found at torrefaction of 300 ˚C. Although signal of lactic acid (45) was detected, it was not considered since other compounds also give intensity of *m/z* 45, i.e. formic acid, acetic acid, and alcohols. Figure 20 shows the relative quantity of each gas released from torrefaction temperature of 250 and 300 ˚C for residence time of 1 h. The amount of most gas products from 250 ˚C was about 30% of that at 300 ˚C, except for formic acid (46). It means formic acid is preferentially released at lower temperature compared to other gases. The relative amount of water released during wheat straw torrefaction was also quantified in paper V based on the MS intensity. Agreed with literature [59], water is a main product of torrefaction, and its amount increases with torrefaction temperature. At 300 ˚C, evolution of water accounts for almost half of the overall mass loss.

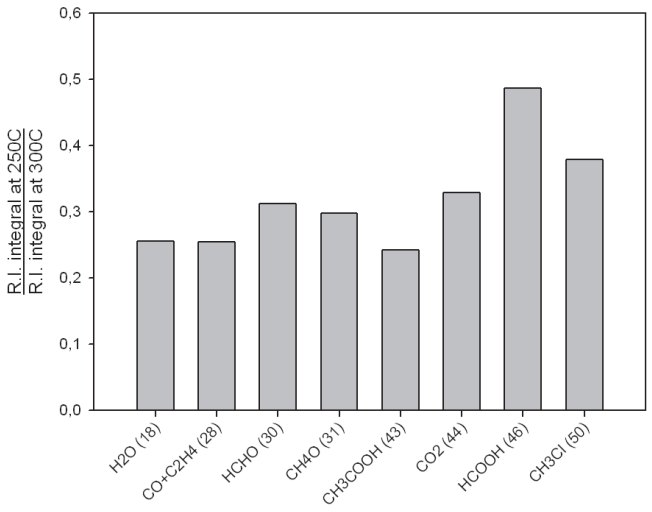

Figure 20: Ratio of each gas product released from wheat straw at 250 and 300 ˚C by calculating the relative intensity (R.I.) integral over the period from 200 ˚C till the end of torrefaction. (Paper V)

The cumulative releases of gas products from three biomass species at 300 ˚C for 1 h were compared in paper II. The evolution of gas started almost simultaneously when temperature reached 200 ˚C. Generally, Scots pine pellets released least gas; wheat straw released more acetic acid, formic acid, carbonyl sulfide, acetone and CO_2 than wood chips; pine chips produced more water, formaldehyde, and methanol than wheat straw and wood pellets. In both studies, it was concluded that water is the dominant product during torrefaction.

Chapter 4

Torrefaction reactors

An overview of torrefaction initiatives is given in Table 4, based on the review paper made by Kleinschmidt C.P. [64]. Basically, these reactors can be divided into following categories: conveyor reactor, moving bed reactor, rotary drum reactor, Turbo-dryer®, Torbed®, microwave reactor. Most of the technologies use direct heating between gas and solid phase. Conveyor reactor can be further divided into screw conveyor (including the paddle conveyor) and belt conveyor, an example is shown in Figure 21. Both Thermya and ECN use moving bed reactor. The one Thermya developed is called TORSPYD technology (as shown in Figure 22), which feed the biomass from the top of the reactor and introduce the hot gas from the bottom. As the biomass travel downwards, they experience the drying zone, volatiles evaporation zone, and torrefaction zone. A model of torrefaction system based on moving bed concept was developed by Tumuluru et al. [65], and a mathematical model specially developed for TORSPYD column was published by Ratte et al. [66]. Rotary drum reactor is composed by a drum and a rotating shaft. The biomass tumbles while the drum rotates, and thus achieves a good heat and mass transfer. Turbo-dryer® (as shown in Figure 23) developed by Wyssmont is a sophisticated dryer typically for chemicals, food, pharmaceuticals, etc. It consists of a stack of slowly rotating circular trays. Material, which is fed onto the top tray, is wiped onto the next lower tray after each revolution. The trays are contained in an enclosure in which heated air or gas is circulated by internal fans. Different from all the above mentioned reactors, Torbed® (as shown in Figure 24) used by TOPELL is a much faster process with residence time of about 100 s. The particles to be processed are held in a shallow bed suspended by jets of the process gas stream that is forced through stationary angled blades at high velocity. As for microwave reactor, limited knowledge of scaling-up is attained so far.

Regarding the kinetic study discussed in chapter 3, in order to model the mass loss of the biomass feedstock it is important to ensure that there is good heat distribution through the reactor,

otherwise temperature measurement at different places including the cooling area in the reactor will be necessary. For technology like TORBED®, which is an extremely fast process for feedstock in a uniform and small size, it will be very relevant to use the developed kinetic model to predict the mass loss of solids during torrefaction. Since our model took the mass loss during heating period into account when deriving the kinetic parameters, and thus the model can predict the mass loss in the initial stage of reaction very well. This is a big advantage of our model.

Table 4: Overview of torrefaction developers in Europe, North America, and Brazil [64].

Developer	Technology	Supplier	Location(s)	Production Capacity (t/a)	Starting
Topell Energy B.V. (NL)	Torbed, direct heating	Torftech Inc. (UK)	Duiven (NL)	60000	Q4 2010
Stramproy Green Investment B.V. (NL)	Vibrating belt, direct heating	Stramproy Green Technology (NL)	Steenwijk (NL)	45000	Q3 2011
Thermya (F), Idema (Lantec)	Moving bed, direct heating	Thermya (Torspyd)	San Sebastian, (ES)	20000	Q4 2011
Thermya (F), LMK Energy	Moving bed, direct heating	Thermya (Torspyd)	Mazingarbe (F)	20000	Q3 2011
Bio Energy Development North AB (S)	Rotary Drum	Metso (FIN)	Örnsköldsvik (S)	25000-30000	2011/2012
Andritz (A)	Moving bed	Andritz (A)	Sdr.Stenderup (DK)	1 t/h demo plant	Q1 2012
Zilkha Biomass Energy (USA)	Unknown	Unknown	Crockett (Texas,USA)	40000	Q4 2010
Keyflame (USA)	Paddle conveyer	Keyflame prop.	Quitman, Mississippi	65000+ (2x350,000t end 2012)	Q4 2011
New Biomass Energy (USA)	Unknown	Unknown	Quitman, Mississippi	65000	Q4 2011
4Energy Invest (B)	Vibrating belt, direct heating	Stramproy Green Technology (NL)	Amel (B)	38000	Q4 2010
Torr-Coal B.V. (NL)	Rotary Drum (indirectly heated) with dechlorination step	TorrCoal Technology	Dilsen-Stokkem (B)	35000	Q3 2010
ECN (NL), Vattenfall(S)	Moving bed	ECN	Unknown	Unknown	Unknown

Foxcoal B.V. (NL)	Screw conveyor (indirectly heated)	Unknown	Winschoten (NL)	35000	2010
Biolake B.V. (NL)	Screw conveyor	Unknown	Eastern Europe	5000-10000	Q4 2010
EBES AG (A)	Rotary Drum	Andritz (A)	Frohnleiten (A)	10000	2011
Atmosclear SA (CH)	Rotary Drum	CDS (UK)	Latvia, New Zealand, US	50000	Q4 2010
Rotawave Biocoal, Ltd. (UK)	Micro wave reactor (TIES)	Group's Vikoma	Terrace, British Columbia	110000	Q4 2011
Ingelia (ES)	Hydrothermal carbonization	Ingelia (ES)	Valencia (ES)	2000	2010
Andritz ACB process (A)	Rotary drum	Andritz (A)	Austria	50000	
Integro Earth Fuels LLC (USA)	TurboDryer	Wyssmont (USA)	Roxboro, Gramling, NC, Eastman, GA	10000 -> 75000	Q1 2012
Agri-Tech Producers LLC (USA)	Belt reactor	Kusters Zima Corporation	Unknown	Unknown	2010
Torrefaction systems, Inc. (USA)	Unknown	Bepex International (USA)	Minneapolis	10000	2013
New Earth Renewable Energy Fuels, Inc. (USA)	Fixed bed/Pyrovac	Pyrovac Group (CA)	Unknown	Unknown	Unknown
WPAC (CA)	KDS processor	Unknown	Unknown	35000	2011
Radian BioEnergy (USA)	Gasification reactor	Radian BioEnergy	Unknown	60000	Unknown
Canadian Bio-coal Ltd. (CA)	TurboDryer	Wyssmont (USA)	British Columbia	180000	Q2 2012
Renewable Fuel Technologies (CA)	Mobil torrefaction unit	Unknown	Unknown	2.7 kg/h	2010
Earth Care Products (USA)	Rotary Drum	Unknown	Unknown	Unknown	Unknown
ERB Brazil	Unknown	Unknown	Unknown	2 units, 1 mill. t/a (Eucalyptus)	2012

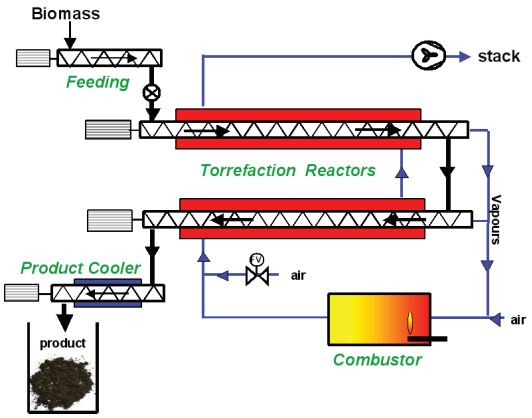

Figure 21: BTG torrefaction process using indirect heating and screw conveyor reactor, a demo-unit was built for a client (100-150 kg/hr input) [67].

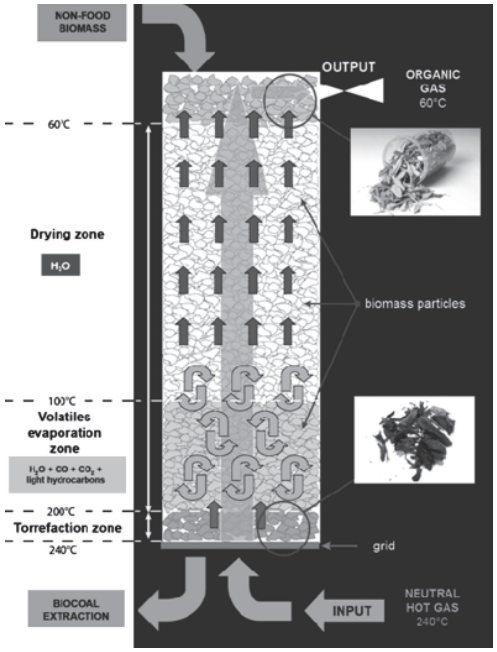

Figure 22: TORSPYD™ column [66].

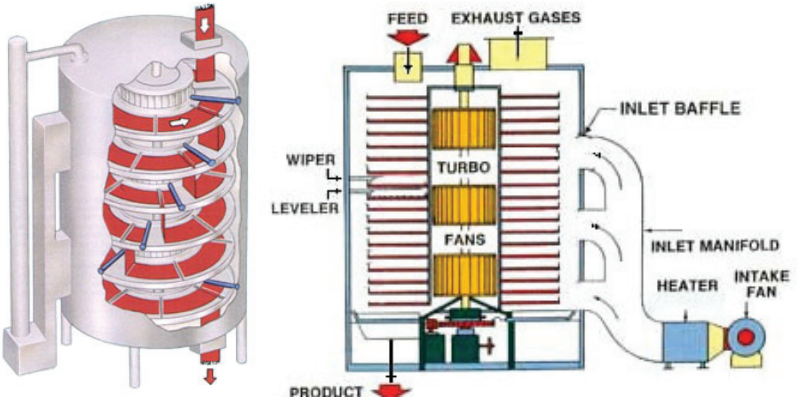

Figure 23: Standard TURBO-DRYER® from Wyssmont [68].

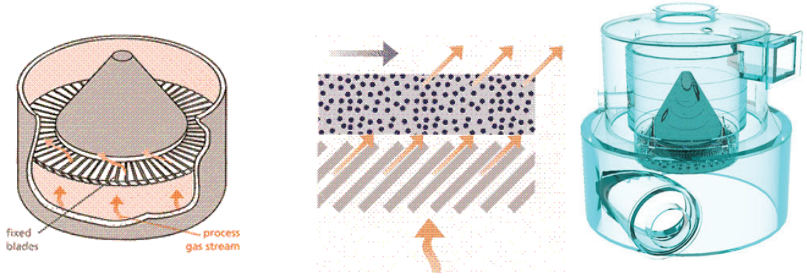

Figure 24: TORBED® Compact Bed Reactor [69].

The torrefaciton reactor built in DTU-Risø campus (as shown in Figure 25 and Figure 26) is a screw conveyor reactor with a feeding capacity of about 6 kg h^{-1}. The reactor is indirectly heated by liquefied petroleum gas. A nitrogen flow of 2.5 L min^{-1} was used as a carrier gas in the torrefaction and collecting unit through the experiment to avoid ignition. The temperature of flue gas is controlled by adjusting the gas and air volume, and the temperature of reaction was monitored by totally 12 thermocouples located in different places through the reactor. The residence time was controlled by adjusting the rotating speed of the screw conveyor. The aim of building this reactor was to produce torrefied biomass for testing in big-scale grinder and boiler. Therefore, the heat integration has not been considered so far. By now, 7 barrels wood chips have been torrefied at 3 different temperatures (250,

270, 280 ˚C). To ensure that treated chips reach the desired degree of torrefaction, the heating value of torrefied chips was compared with the products from lab-scale reactor at different temperatures. It was assured that the variation is within ± 5 ˚C.

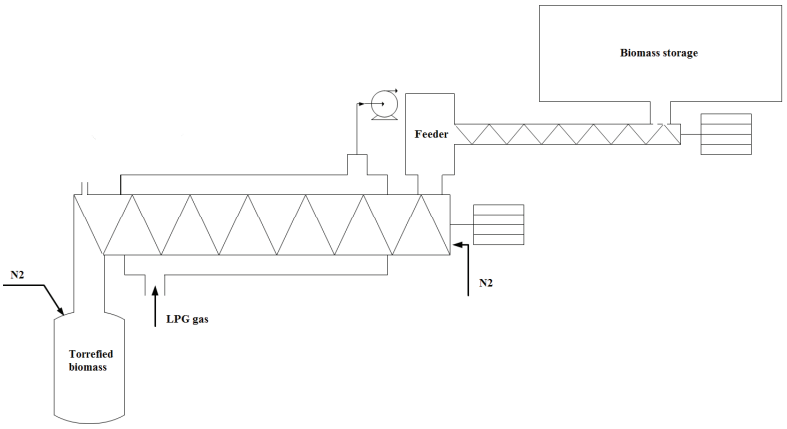

Figure 25: Illustration of the screw conveyor torrefaction reactor and feeding system built in DTU Risø campus.

Figure 26: Picture of the torrefaction unit in DTU Risø campus.

Chapter 5

Concluding remarks

This thesis mainly consists of 3 parts of work: characterization of three different kinds of biomass subject to torrefaction; pellets quality when combining torrefaction and pelletization; and kinetic study of torrefaction. The goal was first to find the optimal operation condition of torrefaction (temperature and time) by analyzing the property changes of different biomass (pine chips, Scots pine pellets and wheat straw) on a lab-scale reactor, and gather the heating value and weight loss data at different temperatures. Then investigate the intrinsic kinetics of torrefaction on TGA and obtain a model that can predict the mass loss at different heating rates. In this way, we hope this thesis can be helpful for the real torrefaction production as a tool for product quality control. As for pellet quality study, it is the next step for torrefaction to be commercialized. Without pelletization, torrefied biomass is limited to on-site usage. However, the pellet study presented in this thesis is only a very preliminary test to compare the different procedures when combining torrefaction and pelletization.

Biomass became darker with increasing torrefaction temperature, and the biomass has lost its shiny surface and smoothness, especially for pellets torrefied at temperatures above 260 ˚C and chips torrefied at 300 ˚C. Wheat straw torrefied at 280 ˚C and above became extremely brittle. For all three biomass, higher torrefaction temperatures result in less moisture absorption and better grindability. Tensile failure stress decreased from about 55 MPa for oven dried straw and straw torrefied at 150 ˚C to 24 MPa for straw torrefied at 200 ˚C, and further to about 4 MPa for straw torrefied at 300 ˚C. Though tensile strength test was not proved to be more reproducible and repeatable than the Hardgrove Grindability Index (HGI) test, strain energy suggested that about 80 – 85% of the energy can be saved when breaking torrefied wheat straw (250 ˚C, 2 h) instead of oven dried samples. As for pine chips and pellets, grinding energy measured on a disc mill showed a sharp decrease for the first 25% and 10% AWL, respectively. Based on HGI, in order to achieve similar grindability as coal, a torrefaction temperature of above 240 ˚C is needed for wheat straw and chips, and 290 ˚C for pellets. However by

comparing the HGI results with other tests, it can be concluded that HGI test is able to predict the relative amount of fines (< 75 μm) generated from different biomass when ground under the same circumstances. But it is not suitable for biomass like pellets, which does not have a uniform structure in different scale. Since pellets are made by compressing pre-ground wood particles together. It was shown that less energy was needed to grind torrefied pellets compared to chips, but more energy would be required to reduce the particle size further for pellets than for chips. Moreover, particle size distribution is a necessary complement to the HGI test.

When studying the pellet property by switching the sequence of pelletization and torrefaction, it was concluded that pine pellets torrefied at different temperatures exhibit better durability than the pellets made from torrefied spruce. It means the bonds formed during pelletization outlast the torrefaction quite well. A good correlation among pellet durability, the compression strength, and the energy required for grinding was observed, which means that compression strength of single pellet can be used as a product quality control method to predict the durability of the whole batch pellets and the energy use in grinding and vice versa. In order to produce pellets (with diameter of 6 mm) with durability higher than 97.5 % as required by ENPlus, compression strength of 0.6 joule per pellet with length of 15 mm (or 1.53 joule per gram pellet with length of 15 mm) is needed, and grinding energy of about 15.3 J g^{-1} is expected. At this condition, energy reduction in grinding compared with untreated pellets is 43 % (11.6 J g^{-1}), and the energy loss due to the torrefaction of pellets is about 4 % (730 J g^{-1} based on original mass). However, the higher heating value (HHV) is increased by about 1600 J $g^{-1}$from 18.4 MJ kg^{-1} for reference pellets to 20.0 MJ kg^{-1}, which corresponds to a torrefaction temperature of a bit lower than 230 ˚C with residence time of 1 h.

By analyzing the FTIR spectra of the torrefied wheat straw, it was concluded that there's no major structural change when torrefaction temperature is lower than 200 ˚C, hemicelluloses degrade at about 250 ˚C while cellulose and lignin degrade at 270 – 300 ˚C. Cell wall composition analysis showed that for all three biomass species, hemicelluloses were totally degraded when torrefied at 300 ˚C for 2 h, and cellulose was also strongly degraded. Gas products detected during torrefaction for three biomass species were water, CO, CO_2, formic acid, formaldehyde, methanol, acetic acid, traces of hydrogen sulfide and carbonyl sulfide were also found. Moreover, methyl chloride was detected in wheat straw torrefaction. This means torrefaction may reduce the chlorine content in the biomass,

which is a benefit for the later combustion, due to the fouling and slagging problem caused by high chlorine and alkali content in biomass. Water was found to be the dominant gas product during torrefaction. At 300 ˚C, evolution of water accounts for almost half of the overall mass loss.

On a dry and ash free basis, higher heating value (HHV) of chips and pellets increased from about 20 MJ kg^{-1} to 29 – 30 MJ kg^{-1} when torrefied at 300 ˚C. While HHV of wheat straw was always about 0.8 MJ kg^{-1} lower than the value of other two fuels at the same anhydrous weight loss (AWL). However, the fraction of energy retained in the torrefied sample as a function of AWL is very similar for all three biomass. Together with the kinetic model developed in this thesis, which is able to predict the mass loss of solids during torrefaction at different heating rates by simply knowing the temperature history of the sample in the reactor, it is possible to know the HHV of the products in advance by just measuring the HHV of the raw material of the feedstock. This method can thus be used for reactor or process design and may supply a solution to the inhomogeneity problem of torrefied products encountered by most torrefaction facilities.

Moreover, medium torrefaction temperatures (240-280 ˚C) and residence time of about 0.5-1 h is recommended for the real production. Because the grindability is improved most and sufficiently at such conditions, more severe torrefaction will lead to more energy loss of the biomass but slight improvement of the grindability. Another reason is that high torrefaction temperatures (f.x. > 275 ˚C) make the pelletization challenging. The methods established in this project for characterizing the fuel properties of torrefied biomass can also be used for quality control of torrefied products from industry.

Acknowledgements

First of all, I would like to say thank you to my supervisors: Jesper Ahrenfeldt, Ulrik Birk Henriksen, both from DTU, Chemical and Biochemical Engineering Department, CHEC, Biomass gasification group, and Jens Kai Holm from DONG Energy. With your guidance and advice, I never felt alone during this 3-year study. Thanks for all the support and effort of creating a good working environment by introducing me to the cooperation partners and letting me participate in the conferences, etc. Thank you also for your understanding and support when I chose Shanghai Jiaotong University for my external research stay. Thank Jens also for the comprehensive list of torrefaction producers. The help from Helge Egsgaard of interpreting the mass spectroscopy is appreciated. Thanks are also due to my colleagues Tobias Thomsen, Freddy Christensen, Kristian Estrup, Lars S. Bach, and Erik Hansen for building the torrefaction reactors and all your help during my phd study. Special thanks to Wolfgang Stelte, who shared an office with me and let me feel welcomed when I started my phd. Thank you for all the help and advice when I had problem with writing papers. Thank you also to my colleagues in the group Hanne Wojtaszewski, Zsuzsa Sárossy, Maria Puig Arnavat, and Benny Gøbel from DONG, for all your help and creating a friendly atmosphere in the daily work.

I would also like to especially thank some people who have contributed to realize this work:

- Professor Yonghao Luo for letting me join your group at Shanghai Jiaotong University and your kindly introduction and arrangement. Yi Su, all your help and effort with organizing my stay are gratefully appreciated. Everyone in the group, Ruizhi Zhang, Wenguang Wu, Chunyuan Liu, Renhao Yin, Yun Wang, Yang Cao, Yunliang Zhang, Pengyun Lin, etc for taking me as a part of your group and kindly introducing me to all your equipments. It was a very good experience with you.

- Professor Anand Sanadi and Søren Barsberg, both from Copenhagen University, Faculty of Life Science, for a very successful cooperation and your patience when corrected my papers.

- Jonas Dahl and Niels Peter K. Nielsen, both from Danish Technological Institute, for great ideas and input from industrial prospect view.

- Tomas Fernqvist, Ingelis Larsen, and Annette Eva Jensen from Bioenergy group in DTU Risø campus for conducting the cell wall composition analysis.

- Peter Arendt Jensen and Suriyati Saleh for a good cooperation after the integration of DTU and Risø. Special thanks to Brian Brun Hansen and Lilian Beenfeldt Holgersen for the assistance of performing the thermogravimetric analysis in your TGA.

- Hans Lilholt, Frank Adrian, Mustafa Aslan, and Xiaodan Zhang from Material Research division (AFM) in DTU Risø campus, for kindly introduction and valuable comments on tensile strength test.

- All my friends in DTU Risø Campus, Shuo Yao, Yuehua Wu, Ming Chen, Yi Zong, Weiwei Zhang, Xiaoli Guo, Keliang Shi, Yunzhong Chen, Jian Wu, etc for the wonderful lunch time and help during these 3 years.

- Many thanks to my friends, Yuqin Jiang, Yuanjing Zheng, and their children Yiyang and Yan, for informing me of the phd position and continuously supporting me during these 3 years by making good food and taking care of my daughter.

- Last but not least, thanks to my family for your love and support, especially for my husband and my parents for always taking me and my study as the first priority. Without your contribution and encouragement, these 3 years won't be easy. Thank you also to my daughter, Anja, who gave me the chance to work efficiently, for bearing my impatience and giving me all your love and happiness.

Appendix

Appendix-1: Derivation of the two-step reaction series model with proposed initial condition

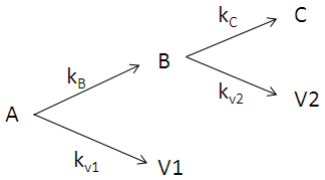

(A-1)

$$\frac{d[A]}{dt} = -K_1[A] \tag{A-2}$$

$$\frac{d[B]}{dt} = k_B[A] - K_2[B] \tag{A-3}$$

$$\frac{d[C]}{dt} = k_C[B] \tag{A-4}$$

$$K_1 = k_B + k_{v1},\ K_2 = k_C + k_{v2} \tag{A-5}$$

$$at \quad t = 0, \quad [A](0) = [A]_0, \quad [B](0) = [B]_0, \quad [C](0) = [C]_0 \tag{A-6}$$

$$\therefore\ [A] = [A]_0 \exp(-K_1 t) \tag{A-7}$$

$$Make \quad V = \frac{[B]}{[A]},\ V_0 = \frac{[B]_0}{[A]_0},\quad then \quad \frac{d[B]}{d[A]} = V + \frac{[A]dV}{d[A]},\quad and \quad \frac{Eq.(3)}{Eq.(2)} = \frac{d[B]}{d[A]} = -\frac{k_B}{K_1} + \frac{K_2}{K_1}\cdot\frac{[B]}{[A]}$$

$$\therefore \int_{V_0}^{V} \frac{dV}{\left[-\frac{k_B}{K_1}+\left(\frac{K_2}{K_1}-1\right)V\right]} = \int_{[A]_0}^{[A]} \frac{d[A]}{[A]}$$

$$\frac{\ln\left[-\frac{k_B}{K_1}-\left(1-\frac{K_2}{K_1}\right)V\right]}{1-\frac{K_2}{K_1}} + \frac{\ln\left[-\frac{k_B}{K_1}-\left(1-\frac{K_2}{K_1}\right)V_0\right]}{1-\frac{K_2}{K_1}} = \ln\frac{[A]}{[A]_0}$$

$$\ln\frac{[-k_B-(K_1-K_2)V_0]}{[-k_B-(K_1-K_2)V]} = \left(1-\frac{K_2}{K_1}\right)(-K_1t)$$

insert $V=\frac{[B]}{[A]},\ V_0=\frac{[B]_0}{[A]_0}$

$$\therefore\ [B]=\frac{k_B[A]_0}{K_1-K_2}[\exp(-K_2t)-\exp(-K_1t)]+[B]_0\exp(-K_2t) \tag{A-8}$$

$$[C]-[C]_0 = k_C\cdot\frac{k_B[A]_0}{K_1-K_2}\left[\int_0^t\exp(-K_2t)dt-\int_0^t\exp(-K_1t)dt\right]+k_C\cdot[B]_0\int_0^t\exp(-K_2t)dt$$

$$=\frac{k_Bk_C[A]_0}{K_1-K_2}\left[-\frac{1}{K_2}\exp(-K_2t)+\frac{1}{K_2}+\frac{1}{K_1}\exp(-K_1t)-\frac{1}{K_1}\right]+k_C[B]_0\left[-\frac{1}{K_2}\exp(-K_2t)+\frac{1}{K_2}\right]$$

$$\therefore\ [C]=[C]_0+\frac{k_C(k_B[A]_0+K_1[B]_0)}{K_1K_2}+\frac{k_Bk_C[A]_0\exp(-K_1t)}{K_1(K_1-K_2)}-\frac{k_Bk_C[A]_0\exp(-K_2t)}{K_2(K_1-K_2)}$$

$$-\frac{k_C[B]_0\exp(-K_2t)}{K_2} \tag{A-9}$$

Appendix-2: MATLAB code for finding the kinetic parameters

```
function dzdT = kinetic(T,z);
global A1 A2 A3 A4 E1 E2 E3 E4 HR_input T_start
HR = HR_input/60;
x1=A1*exp(-E1/(8.3145*(T+T_start+273.15)));
x2=A2*exp(-E2/(8.3145*(T+T_start+273.15)));
x3=A3*exp(-E3/(8.3145*(T+T_start+273.15)));
x4=A4*exp(-E4/(8.3145*(T+T_start+273.15)));
dzdT(1,1)=(-1/HR)*(x1+x2)*z(1);
dzdT(2,1)=(1/HR)*(x1*z(1)-(x3+x4)*z(2));
dzdT(3,1)=(1/HR)*x3*z(2);
```

```
clearall
closeall
clc
global A1 A2 A3 A4 E1 E2 E3 E4 HR_input T_end T_start
%% input
T_start = 200;
HR_vector = [10 10 10 50 50 50 50];
temperatures = [250 260 275 250 260 275 280];
n_samples = [192 194 197 183 184 188 184];
R = 8.3145;
% Original data from experiments 250260275(10+50K)280(50K).All data put in as 1
long vector.x is time in [s].y is residual mass from 0 to 1.
xdata_all = [0   17  47  77  107 137 167 197 227 257 287 317 347 377 …];
ydata_all = [1  0.999309378939252   0.997831766017803   0.995772330744149   …];
%%estimation of the kinetic parameters, assuming A0 is 1.
LB = [0 0 0 0];
UB = [0.06 0.01 0.001 0.001];
k1=0.006300;
k2=0.00270;
k3=0.000271;
k4=0.000176;
initial_guess = [k1 k2 k3 k4];
for ycounter = 1:50;
for s = 1:1:length(temperatures);
clearxxdataydataheat_timeresnormk1k2k3k4
    T_end = temperatures(1,s);
    HR_input = HR_vector(1,s);
    HR = HR_input
if ycounter == 1
       A0 = 1;
       B0 = 0;
       C0 = 0;
guess = initial_guess;
else
%solve equations with calculated kinetic parameters
temp = [T_start-T_start:0.1:T_end-T_start];
       x0 = [1 0 0];
       [T,z] = ode15s(@kinetic,temp,x0);
% Update initial concentration
       A0 = z(end,1);
```

```
B0 = z(end,2);
       C0 = z(end,3);
%Update initial guess of k parameters, using the estimated A and E values
       k1 =A1*exp(-E1/(8.3145*(temperatures(1,s)+273.15)));
       k2 =A2*exp(-E2/(8.3145*(temperatures(1,s)+273.15)));
       k3 =A3*exp(-E3/(8.3145*(temperatures(1,s)+273.15)));
       k4 =A4*exp(-E4/(8.3145*(temperatures(1,s)+273.15)));
guess = [k1 k2 k3 k4];
end
    cell_end = sum(n_samples(1:s));
    cell_start=cell_end-n_samples(1,s)+1;
xdata = xdata_all(cell_start:cell_end);
ydata = ydata_all(cell_start:cell_end);
heat_time = (temperatures(1,s)-T_start)/HR*60;
xdata_negative =xdata-heat_time;
[row,col] = find(xdata_negative>=0);
if col>0
col1 = xdata(length(xdata)-length(col)-1:length(xdata));
else
col1 = xdata;
end
off_set = col1(1,1);
xdata = col1-off_set;
ydata = ydata_all(cell_start+n_samples(1,s)-length(xdata):cell_end);
%solution x(1,2,3,4)=k1,kv1,k2,kv2
[x, resnorm] = lsqcurvefit(@(x,xdata) ((A0*exp(-
1*(x(1)+x(2))*xdata))+(A0*x(1)/((x(1)+x(2))-(x(3)+x(4)))*(exp(-
1*(x(3)+x(4))*xdata)-exp(-1*(x(1)+x(2))*xdata))+B0*exp(-
1*(x(3)+x(4))*xdata))+(C0+x(3)*(x(1)*A0+(x(1)+x(2))*B0)/((x(1)+x(2))*(x(3)+x(4)))+x
(1)*x(3)*A0*exp(-1*(x(1)+x(2))*xdata)/((x(1)+x(2))*((x(1)+x(2))-(x(3)+x(4))))-
x(1)*x(3)*A0*exp(-1*(x(3)+x(4))*xdata)/((x(3)+x(4))*((x(1)+x(2))-(x(3)+x(4))))-
x(3)*B0*exp(-1*(x(3)+x(4))*xdata)/(x(3)+x(4)))),guess,xdata,ydata,LB,UB);
x_store(s,:) = x; %display x
Rsquar(s) = 1-resnorm;  %display R^2
end%belongs to s loop
T_kelvin_reciprocal = 1./(temperatures+273.15);     %makes a vector that is one
divided by the temperatures in Kelvin
lnK_matrix = log(x_store);
%% calculate Arrhenius constants and activation energy
p1 = polyfit(T_kelvin_reciprocal,lnK_matrix(:,1)',1);
E1 = -R*p1(1);
A1 = exp(p1(2));
p2 = polyfit(T_kelvin_reciprocal,lnK_matrix(:,2)',1);
E2 = -R*p2(1);
A2 = exp(p2(2));
p3 = polyfit(T_kelvin_reciprocal,lnK_matrix(:,3)',1);
E3 = -R*p3(1);
A3 = exp(p3(2));
p4 = polyfit(T_kelvin_reciprocal,lnK_matrix(:,4)',1);
E4 = -R*p4(1);
A4 = exp(p4(2));
ycounter_vector(ycounter) = ycounter;
E1_vector(ycounter) = E1;
A1_vector(ycounter) = A1;
```

```
E2_vector(ycounter) = E2;
A2_vector(ycounter) = A2;
E3_vector(ycounter) = E3;
A3_vector(ycounter) = A3;
E4_vector(ycounter) = E4;
A4_vector(ycounter) = A4;
end%belongs to ycounter
x_store;
[E1 E2 E3 E4; A1 A2 A3 A4]
subplot(2,4,1)
plot(ycounter_vector,E1_vector)
xlabel('Iterations')
ylabel('Ea1')
subplot(2,4,2)
plot(ycounter_vector,E2_vector)
xlabel('Iterations')
ylabel('Ea2')
subplot(2,4,3)
plot(ycounter_vector,E3_vector)
xlabel('Iterations')
ylabel('Ea3')
subplot(2,4,4)
plot(ycounter_vector,E4_vector)
xlabel('Iterations')
ylabel('Ea4')
subplot(2,4,5)
plot(ycounter_vector,A1_vector)
xlabel('Iterations')
ylabel('A1')
subplot(2,4,6)
plot(ycounter_vector,A2_vector)
xlabel('Iterations')
ylabel('A2')
subplot(2,4,7)
plot(ycounter_vector,A3_vector)
xlabel('Iterations')
ylabel('A3')
subplot(2,4,8)
plot(ycounter_vector,A4_vector)
xlabel('Iterations')
ylabel('A4')
```

Appendix-3: MATLAB code for verifying the model

```
function dzdT = kinetic(T,z);
global HR
x(1)=34833*exp(-70999/(8.3145*(T+273.15)));
x(2)=3.9101*10^10*exp(-139460/(8.3145*(T+273.15)));
x(3)=4339.8*exp(-76566/(8.3145*(T+273.15)));
x(4)=3.4751*10^7*exp(-118620/(8.3145*(T+273.15)));
dzdT(1,1)=(-1/HR)*(x(1)+x(2))*z(1);
dzdT(2,1)=(1/HR)*(x(1)*z(1)-(x(3)+x(4))*z(2));
dzdT(3,1)=(1/HR)*x(3)*z(2);
```

```
function dydt = kinetic_isothermal(t,y);
global T_end
x(1)=34833*exp(-70999/(8.3145*(T_end+273.15)));
x(2)=3.9101*10^10*exp(-139460/(8.3145*(T_end+273.15)));
x(3)=4339.8*exp(-76566/(8.3145*(T_end+273.15)));
x(4)=3.4751*10^7*exp(-118620/(8.3145*(T_end+273.15)));
dydt(1,1)=(-1)*(x(1)+x(2))*y(1);
dydt(2,1)=(x(1)*y(1)-(x(3)+x(4))*y(2));
dydt(3,1)=x(3)*y(2);
```

```
clearall
closeall
clc
global T_end HR
%% Input values 275step50K%
Time_vector = [0 0.19833 0.69833 0.92666 1.19833 1.69833 2.19833 2.69833 3.19833 …];
Temp_vector = [199.987 211.265 239.64805 249.591 256.56971 261.47182 261.35094
259.35001 256.91011 …];
T_start = Temp_vector(1,1)
for a = 1:1:length(Temp_vector)-1
    HR_vector(a) = (Temp_vector(a+1)-Temp_vector(a))/(Time_vector(a+1)-
Time_vector(a))
    Duration_vector(a) = (Time_vector(a+1)-Time_vector(a))
end
IC1 = 1
IC2 = 0
IC3 = 0
Residual_mass = []
time_total = []
%% Solution to heating period
for Acount = 1:1:length(HR_vector)
    HR = HR_vector(Acount)/60
if HR == 0
%% solution to isothermal
y0 = [IC1 IC2 IC3];
time_end = Duration_vector(Acount)*60
timey = [0:time_end];
[t,y] = ode15s(@kinetic_isothermal,timey,y0);
ytotal = [y(:,1) + y(:,2) + y(:,3)];
clearIC1IC2IC3
IC1 = y(end,1)
```

```
IC2 = y(end,2)
IC3 = y(end,3)
Residual_mass = [Residual_mass', ytotal']'
TF = isempty(time_total)
if TF == 1
time_plus = 0
else
time_plus = time_total(end)
end
time_total = [time_total, (timey/60+time_plus)]
else
cleartimeztemp
z0 = [IC1 IC2 IC3]
T_end = T_start + Duration_vector(Acount)*HR_vector(Acount);
temp(1) =  T_start;
temp(2) = T_end;
[T,z] = ode15s(@kinetic,temp,z0);
for time_count = 1:1:length(T)
timez(time_count) = (T(time_count)-T_start)/(HR*60);
end
TF = isempty(time_total)
if TF == 1
time_plus = 0
else
time_plus = time_total(end)
end
time_total = [time_total, timez+time_plus]
ztotal = [z(:,1) + z(:,2) + z(:,3)];
clearIC1IC2IC3
IC1 = z(end,1)
IC2 = z(end,2)
IC3 = z(end,3)
Residual_mass = [Residual_mass', ztotal']'
T_start = T_end
end
end
[AX,H1,H2] = plotyy(time_total,Residual_mass,Time_vector,Temp_vector)
xlabel('Time [min]')
ylabel(AX(1),'Residual maas [-]')
ylabel(AX(2),'Temperature [°C]')
holdon
%exp data 275Cstep50K%
xdata_exp_sec = [0  12  42  56  72  102 132 162 192 222 …];
ydata_exp = [1  0.998555800278867   0.990452481015536   0.98419841950737
0.974735840750133   0.956255351261298   0.939947475208408   0.926706081666305
0.91710006509206    0.909460517310808   …];
xdata_exp = xdata_exp_sec/60;
scatter(xdata_exp,ydata_exp)
legend('model','exp','temperature')
```

References

[1] Cremers M. IEA Bioenergy Task 32 Deliverable 4 Technical status of biomass co-firing. 2009; Available at: http://ieabcc.nl/publications/09-1654%20D4%20Technical%20status%20paper%20biomass%20co-firing.pdf. Accessed 26.06.2012.

[2] Sami M, Annamalai K, Wooldridge M. Co-firing of coal and biomass fuel blends. Progress in energy and combustion science 2001;27(2):171-214.

[3] Acharjee TC, Coronella CJ, Vasquez VR. Effect of thermal pretreatment on equilibrium moisture content of lignocellulosic biomass. Bioresour Technol 2011;102(7):4849-4854.

[4] Arias B, Pevida C, Fermoso J, Plaza MG, Rubiera F, Pis JJ. Influence of torrefaction on the grindability and reactivity of woody biomass. Fuel Process Technol 2008;89(2):169-175.

[5] Bergman PCA. Combined torrefaction and pelletisation: the TOP process. Petten, The Netherlands: Energy Research Centre of the Netherlands (ECN); 2005 Jul. 29 p.;Report No.: ECN-C--05-073.

[6] van der Stelt MJC, Gerhauser H, Kiel JHA, Ptasinski KJ. Biomass upgrading by torrefaction for the production of biofuels: A review. Biomass Bioenergy 2011;35(9):3748-3762.

[7] Stelte W, Clemons C, Holm JK, Sanadi AR, Ahrenfeldt J, Shang L, et al. Pelletizing properties of torrefied spruce. Biomass and Bioenergy 2011;35(11):4690-4698.

[8] Gilbert P, Ryu C, Sharifi V, Swithenbank J. Effect of process parameters on pelletisation of herbaceous crops. Fuel 2009;88(8):1491-1497.

[9] Sun RC. Cereal straw as a resource for sustainable biomaterials and biofuels: chemistry, extractives, lignins, hemicelluloses and cellulose. 1st ed. UK: Elsevier; 2010.

[10] Savage Research Group. Biogasification in supercritical water. Available at: http://www.engin.umich.edu/dept/che/research/savage/energy.html. Accessed 24.9.2011.

[11] Pereira RL. The chemistry involved in the steam treatment of lignocellulosic materials. Quim Nova 2003;26(6):863-871.

[12] Sun RC, Lawther JM, Banks W. Fractional and structural characterization of wheat straw hemicelluloses. Carbohydr Polym 1996;29(4):325-331.

[13] Svoboda K, Pohořelý M, Hartman M, Martinec J. Pretreatment and feeding of biomass for pressurized entrained flow gasification. Fuel Process Technol 2009 5;90(5):629-635.

[14] Beall F, Blankenhorn P, Moore G. Carbonized wood-physical properties and use as an SEM preparation. Wood Sci 1974;6:212-219.

[15] Gu P, Hessley RK, Pan WP. Thermal characterization analysis of milkweed flos. J Anal Appl Pyrolysis 1992;24(2):147-161.

[16] Prins MJ. Thermodynamic analysis of biomass gasification and torrefaction. 2005.

[17] Šimkovic I, Varhegyi G, Antal Jr MJ, Ebringerová A, Szekely T, Szabo P. Thermogravimetric/mass spectrometric characterization of the thermal decomposition of (4-O-methyl-D-glucurono)-D-xylan. J Appl Polym Sci 1988;36(3):721-728.

[18] White JE, Catallo WJ. Biomass pyrolysis kinetics: A comparative critical review with relevant agricultural residue case studies. J Anal Appl Pyrolysis 2011;91(1):1-33.

[19] Chen WH, Kuo PC. Isothermal torrefaction kinetics of hemicellulose, cellulose, lignin and xylan using thermogravimetric analysis. Energy 2011;36(11):6451-6460.

[20] Repellin V, Govin A, Rolland M, Guyonnet R. Modelling anhydrous weight loss of wood chips during torrefaction in a pilot kiln. Biomass Bioenergy 2010;34(5):602-609.

[21] Prins MJ, Ptasinski KJ, Janssen FJJG. Torrefaction of wood:: Part 1. Weight loss kinetics. J Anal Appl Pyrolysis 2006;77(1):28-34.

[22] Di Blasi C, Lanzetta M. Intrinsic kinetics of isothermal xylan degradation in inert atmosphere. J Anal Appl Pyrolysis 1997;40:287-303.

[23] Rousset P, Turner I, Donnot A, Perré P. The choice of a low-temperature pyrolysis model at the microscopic level for use in a macroscopic formulation. Ann For Sci 2006;63(2):1-17.

[24] Branca C, Di Blasi C. Kinetics of the isothermal degradation of wood in the temperature range 528-708 K. J Anal Appl Pyrolysis 2003;67(2):207-219.

[25] Schell DJ, Harwood C. Milling of Lignocellulosic Biomass: Results of Pilot-Scale Testing. Appl Biochem Biotech 1994;45-46(1):159-168.

[26] Rhodes M. Introduction to particle technology. 1st ed. Chichester.: Wiley; 1998; pp 247-263.

[27] Bridgeman TG, Jones JM, Williams A, Waldron D. Using existing coal milling technologies to process thermally pre-treated biomass. In: Biomass conference and exhibition. EU BC&E 2009: Proceedings of the 17th European Biomass Conference and Exhibition; 2009 June 29 - July 3; Hamburg, Germany. Italy: ETA-Renewable Energies (Ed.); 2009. p. 1689-1693 .

[28] Bergman PCA, Boersma AR, Kiel JHA, Prins MJ, Ptasinski KJ, Janssen FJJG. Torrefaction for entrained-flow gasification of biomass. Available at: www.ecn.nl/docs/library/report/2005/c05067.pdf ; 2005. Accessed 13.01.2012.

[29] Abdullah H, Wu H. Biochar as a fuel: 1. Properties and grindability of biochars produced from the pyrolysis of mallee wood under slow-heating conditions. Energy Fuels 2009;23(8):4174-4181.

[30] Deng J, Wang G, Kuang J, Zhang Y, Luo Y. Pretreatment of agricultural residues for co-gasification via torrefaction. J Anal Appl Pyrolysis 2009;86(2):331-337.

[31] Sadaka S, Negi S. Improvements of biomass physical and thermochemical characteristics via torrefaction process. Environ Prog Sustainable Energy 2009;28(3):427-434.

[32] Repellin V, Govin A, Rolland M, Guyonnet R. Energy requirement for fine grinding of torrefied wood. Biomass Bioenergy 2010;34(7):923-930.

[33] ACARP Publication. Hardgrove Grindability Index. Available at: http://www.acarp.com.au/Downloads/ACARPHardgroveGrindabilityIndex.pdf ; 2008. Accessed 13.01.2012.

[34] Joshi NR. Relative grindability of bituminous coals on volume basis. Fuel 1979;58(6):477-478.

[35] Agus F, Waters P. Determination of the grindability of coals, shales and other minerals by a modified Hardgrove-machine method. Fuel 1971;50(4):405-431.

[36] Yigit E. Three mathematical comminution models based on strain energy. Int J Miner Process 1976;3(4):365-374.

[37] Wright CT, Pryfogle PA, Stevens NA, Steffler ED, Hess JR, Ulrich TH.Biomechanics of wheat/barley straw and corn stover. Appl Biochem Biotechnol 2005;121(1):5-19.

[38] O'Dogherty MJ, Huber JA, Dyson J, Marshall CJ. A Study of the Physical and Mechanical Properties of Wheat Straw. J Agric Eng Res 1995;62(2):133-142.

[39] Uslu A, Faaij APC, Bergman PCA. Pre-treatment technologies, and their effect on international bioenergy supply chain logistics. Techno-economic evaluation of torrefaction, fast pyrolysis and pelletisation. Energy 2008 8;33(8):1206-1223.

[40] Nimlos MN, Looker EBMJ, Evans RJ. Biomass torrefaction studies with a molecular beam mass spectrometer. Prepr.Pap.-Am.Chem.Soc., Div.Fuel Chem 2003;48(2):590.

[41] Gfeller B, Zanetti M, Properzi M, Pizzi A, Pichelin F, Lehmann M, et al. Wood bonding by vibrational welding. J Adhes Sci Technol 2003;17(11):1573-1589.

[42] Mucsi G. Fast test method for the determination of the grindability of fine materials. Chem Eng Res Design 2008;86(4):395-400.

[43] Mayoral M, Izquierdo M, Andres J, Rubio B. Different approaches to proximate analysis by thermogravimetry analysis. Thermochimica Acta 2001;370(1):91-97.

[44] ASTM E 1758-01. Determination of carbonhydrates in biomass by high performance liquid chromatography. Annual Book of ASTM Standards, vol.11.05. ASTM International, West Conshocken, PA. 2003.

[45] Kaar WE, Cool LG, Merriman MM, Brink DL. The complete analysis of wood polysaccharides using HPLC. J Wood Chem Technol 1991;11(4):447-463.

[46] Timoshenko S, MacCullough GH. Elements of Strength of Materials. 3a ed. Toronto; London: D. Van Nostrand Co.; 1949.

[47] DS/CEN/TS 15210-1: Solid biofuels – Determination of mechanical durability of pellets and briquettes – Part 1: Pellets. Danish Standards Association 2005.

[48] Adapa P, Tabil L, Schoenau G. Grinding performance and physical properties of non-treated and steam exploded barley, canola, oat and wheat straw. Biomass Bioenergy 2010;35(1):549-561.

[49] Mani S, Tabil LG, Sokhansanj S. Grinding performance and physical properties of wheat and barley straws, corn stover and switchgrass. Biomass Bioenergy 2004;27(4):339-352.

[50] Winston PW, Bates DH. Saturated solutions for the control of humidity in biological research. Ecology 1960;41(1):232-237.

[51] Apelblat A, Korin E. The vapour pressures of saturated aqueous solutions of sodium chloride, sodium bromide, sodium nitrate, sodium nitrite, potassium iodate, and rubidium chloride at temperatures from 227 K to 323 K. The Journal of Chemical Thermodynamics 1998;30(1):59-71.

[52] Arenillas A, Rubiera F, Pis J. Simultaneous thermogravimetric–mass spectrometric study on the pyrolysis behaviour of different rank coals. J Anal Appl Pyrolysis 1999;50(1):31-46.

[53] Barsberg S. Prediction of Vibrational Spectra of Polysaccharides-Simulated IR Spectrum of Cellulose Based on Density Functional Theory (DFT). J Phys Chem B 2010;114(36):11703-11708.

[54] Liang C, Marchessault R. Infrared spectra of crystalline polysaccharides. II. Native celluloses in the region from 640 to 1700 cm.$^{-1}$. J Polym Sci 1959;39(135):269-278.

[55] Pandey K. A study of chemical structure of soft and hardwood and wood polymers by FTIR spectroscopy.J Appl Polym Sci 1999;71(12):1969-1975.

[56] Gierlinger N, Goswami L, Schmidt M, Burgert I, Coutand C, Rogge T, et al. In situ FT-IR microscopic study on enzymatic treatment of poplar wood cross-sections. Biomacromolecules 2008;9(8):2194-2201.

[57] Kristensen JB, Thygesen LG, Felby C, Jørgensen H, Elder T. Cell-wall structural changes in wheat straw pretreated for bioethanol production. Biotechnology for Biofuels 2008;1(5)doi:10.1186/1754-6834-1-5.

[58] Stelte W, Holm JK, Sanadi AR, Barsberg S, Ahrenfeldt J, Henriksen UB. A study of bonding and failure mechanisms in fuel pellets from different biomass resources. Biomass Bioenergy 2011;35(2):910-918.

[59] Prins MJ, Ptasinski KJ, Janssen FJJG. Torrefaction of wood: Part 2. Analysis of products. J Anal Appl Pyrolysis 2006;77(1):35-40.

[60] Burmistrova M, Komol'kova I, Klemm N, Panina M, Polunochev I, P'yankov A. Physicomechanical properties of agricultural crops. National Science Foundation (U.S.): Israel Program for Scientific Translations; 1963.

[61] O'Dogherty M. A review of the mechanical behaviour of straw when compressed to high densities. J Agric Eng Res 1989;44:241-265.

[62] Limpiti S. Effect of moisture content and stage of maturity on mechanical properties of wheat straw. Thai J Agric Sci 1980;13:277–283.

[63] Kronbergs E. Mechanical strength testing of stalk materials and compacting energy evaluation. Ind Crop Prod 2000;11(2-3):211-216.

[64] Kleinschmidt C. Overview of international developments in torrefaction. 2011; Available at: http://www.bioenergytrade.org/mobile/320/downloads/grazkleinschmidtpaper2011.pdf. Accessed 03.10.2012.

[65] Tumuluru JS, Sokhansanj S, Wright CT, Boardman RD. 2010; Available at: http://www.inl.gov/technicalpublications/Documents/5394124.pdf. Accessed 03.10.2012.

[66] Ratte J, Fardet E, Mateos D, Héry JS. Mathematical modelling of a continuous biomass torrefaction reactor: TORSPYD™ column. Biomass Bioenergy 2011;35(8):3481-3495.

[67] Biomass Technology Group (BTG). Available at: http://www.btgworld.com/en/rtd/technologies/torrefaction. Accessed 15.10.2012.

[68] Wyssmont. Available at: http://www.wyssmont.com/product_detail.php?section=Dryers&id=1. Accessed 15.10.2012.

[69] TORBED® Energy technologies. Available at: http://www.torftech.com/technologies/compact_bed_reactor.html. Accessed 15.10.2012.

Papers (I - VI)

PAPER I

Changes of chemical and mechanical behavior of torrefied wheat straw

Lei Shang, Jesper Ahrenfeldt, Jens Kai Holm, Anand R. Sanadi, Søren Barsberg, Tobias Thomsen, Wolfgang Stelte, Ulrik B. Henriksen

Reprinted from*Biomass and Bioenergy* (2012),40, 63-70,

Available online at www.sciencedirect.com
SciVerse ScienceDirect
http://www.elsevier.com/locate/biombioe

Changes of chemical and mechanical behavior of torrefied wheat straw

Lei Shang [a,*], *Jesper Ahrenfeldt* [a], *Jens Kai Holm* [b], *Anand R. Sanadi* [c], *Søren Barsberg* [c], *Tobias Thomsen* [a], *Wolfgang Stelte* [a], *Ulrik B. Henriksen* [a]

[a] *Department of Chemical and Biochemical Engineering, Technical University of Denmark, 2800 Kgs. Lyngby, Denmark*
[b] *Chemical Engineering, DONG Energy Power A/S, Nesa Alle 1, 2820 Gentofte, Denmark*
[c] *Biomass and Ecosystem Science, Faculty of Life Sciences, University of Copenhagen, Rolighedsvej 23, 1958 Frederiksberg, Denmark*

ARTICLE INFO

Article history:
Received 25 January 2011
Received in revised form
17 January 2012
Accepted 30 January 2012
Available online 22 February 2012

Keywords:
Torrefaction
Grindability
Tensile strength
Hardgrove
ATR-FTIR
Triticum aestivum L

ABSTRACT

The purpose of the study was to investigate the influence of torrefaction on the grindability of wheat straw. Straw samples were torrefied at temperatures between 200 °C and 300 °C and with residence times between 0.5 and 3 h. Spectroscopic information obtained from ATR-FTIR indicated that below 200 °C there was no obvious structural change of the wheat straw. At 200–250 °C hemicelluloses started to decompose and were totally degraded when torrefied at 300 °C for 2 h, while cellulose and lignin began to decompose at about 270–300 °C. Tensile failure strength and strain energy of oven dried wheat straw and torrefied wheat straw showed a clear reduction with increasing torrefaction temperature. In addition, Hardgrove Grindability Index (HGI) of wheat straw torrefied at different conditions was determined on a standard Hardgrove grinder. Both results showed an improvement of grindability in the torrefaction temperature range 250–300 °C, which can be well explained by the findings from FTIR analysis. At a torrefaction temperature of 260 °C and with a residence time of 2 h, wheat straw samples produced similar HGI values as coal (RUKUZN) with 0% moisture content. Under this condition, the Anhydrous Weight Loss (AWL%) of the wheat straw sample was 30% on dry and ash free basis (daf), and the higher heating value of the torrefied wheat straw was 24.2 MJ kg^{-1} (daf). The energy loss compared to the original material was 15% (daf).

1. Introduction

One of the drawbacks of using biomass as a fuel source is the fact that it is more tenacious and less brittle and hence more difficult and energy intensive to grind into fine particles. This problem is especially acute when biomass is to be used in pulverized combustion systems [1]. Torrefaction is a mild temperature (200–300 °C) pre-treatment of biomass in an inert atmosphere, which has received increased attention in recent years [2]. During the process, the biomass looses moisture and a proportion of the volatile content, and becomes dry, darker, and brittle. Torrefied biomass is hydrophobic, has a higher calorific value and is easier to grind [3,4]. At present, a number of studies on grindability of torrefied biomass have been carried out. Arias et al. [3] ground torrefied eucalyptus wood in a cutting mill with a bottom sieve of 2 mm. In all cases, there is an improvement in the grindability characteristics of the treated biomass, as the percentage of particles passing to the lower size fractions greatly increases for the samples subjected to the torrefaction process. Bridgeman et al. [5] measured the Hardgrove Grindability Index (HGI) of willow heated at 240 °C and 290 °C for 10 and 60 min by using a Retsch ball mill. The higher

* *Corresponding author*. Tel.: +45 2132 4979; fax: +45 4677 4109.
E-mail address: lesh@kt.dtu.dk (L. Shang).
0961-9534/$ – see front matter © 2012 Elsevier Ltd. All rights reserved.
doi:10.1016/j.biombioe.2012.01.049

temperatures and longer residence times improved the grindability. Abdullah and Wu [6] investigated the thermal pretreatment (300–500 °C) of mallee wood in a fixed-bed reactor. A laboratory ball mill was used for testing the grindability. They found that thermal treatment below 330 °C leads to significantly better grinding properties and that further temperature increase had only minor effects. Further studies about the torrefaction and grindability of wood samples have been made by [7–10].

Where these studies have shown the beneficial effect of torrefaction of woody biomass, grass samples such as wheat straw present more difficulty. Wheat straw has some unique properties that differ from woody biomass. The tenaciousness of the untreated wheat straw makes it almost impossible to grind in a ball mill, where the tumbling action rather flattens the fibers instead of crushing and breaking them. This is related to the ultra structural differences of the cell wall of wheat straw as compared to woody biomass. For example, wheat straw fiber has a much thicker outer layer in the secondary cell wall based on volume percentage compared to spruce tracheid. The fibrils in this layer are oriented laterally in cross helix making the defibrillation of grassy biomass more difficult [11]. From a chemical point of view, there is also difference between wheat straw and woody biomass. The main hemicelluloses found in hardwood are partially acetylated (4-O-methyl-D-glucuronopyranosyl)-D-xylans, while hemicelluloses in wheat straw are more complex, mainly consisting of a (1→4)-linked β-D-xylan with D-glucopyranosyluronic acid (or 4-O-methyL-α-D-glucopyranosyluronic acid) groups attached at position 2, and L-arabinofuranosyl and D-xylopyranosyl groups attached at position 3. They form hydrogen bonds with cellulose, covalent bonds (mainly α-benzyl ether linkages) with lignin, and ester linkages with acetyl units and hydroxycinnamic acids. The cross-linking of hemicelluloses and lignin by ferulates/diferulates in the wheat straw cell wall enhanced the difficulty of separating these two components [11]. Higher percentage of hemicelluloses in wheat straw compared with woody biomass also contributes to the better linkage between the polymers.

In studies of heat-induced modifications of biomass properties, Svoboda et al. [12] summarized that the main changes in biomass due to torrefaction involve decomposition of hemicelluloses and partial depolymerization of lignin and cellulose. Bella et al. [13] heated American hardwoods to temperatures between 200 °C and 400 °C, and found a lower cellulose and hemicelluloses resistance compared to lignin. Although some decomposition temperatures for these compounds can be found in literature [5,8], there is a lack of experimental data indicating the close relationship between the thermochemical and the grindability changes, especially for wheat straw.

In the present work the heat-induced chemical modifications of biomass is monitored by Attenuated Total Reflectance (ATR) – FTIR spectroscopy, where the samples were heated before recording the spectra. ATR-FTIR spectroscopy is a facile method which provides direct information from the outer (μm) sample surface layers with no requirement for prior sample preparation. The spectra recorded provide basic and in principle quantitative information on the sample cell wall polymers and their chemical modifications. These modifications, obtained at various torrefaction temperatures, are related to the mechanical and grindability properties. Different methods have been used to study these properties. One example is the Hardgrove Grindability Index (HGI), which in principle is a simple measure of grindability.

The HGI was developed as a measure, which indicates how difficult it is to grind a specific coal to the particle size necessary for effective combustion in a pulverized coal fired boiler [14]. In the standard method the HGI value is based on the amount of sample passing through a 75 μm sieve after being ground in a standard Hardgrove ball mill for 377 radians for each fixed amount of feed (50 g). Joshi [15] and Agus and Waters [16] pointed out that the fixed mass approach is unsatisfactory for making direct comparisons among fuels with densities differing a lot. To correct this situation and to bring evenness in grindability ratings of biomass and coal, Bridgeman et al. [5] used the same fixed volume (50 cm^3) for each feed as opposed to a fixed mass (50 g).

As the HGI is based on an empirical method, it is not linked directly with any specific physical property of the sample, and suffers from relative low reproducibility and repeatability. Therefore, as a supplement, it was decided to investigate the tensile strength of the wheat straw samples before and after torrefaction. The tensile strength is the maximum stress that a material can withstand while being pulled before breaking. Furthermore, by measuring the elongation of the specimen while pulling it apart, it is possible to calculate the strain energy at fracture per unit volume. Yigit [17] related the energy absorbed per unit new surface area created during comminution and the strain energy per unit volume of a solid at fracture, and established mathematical models assuming fracture by tensile stresses. Mathematical models of new surface area energy derived from different fracture patterns all have a positive linear relationship with strain energy per unit volume, if the starting particle size and the reduction ratio are constants. Although the models cannot fully represent the realistic fracture pattern of a comminution process, they allow one to use the relative change of the strain energy at fracture under tensile stress at different torrefaction temperatures as an indication of how much energy can be saved during grinding under the same mill conditions.

The objective of this study was to obtain knowledge on the effects of the torrefaction process on the chemical and mechanical behavior. Attenuated total reflectance Fourier transform infrared (ATR-FT-IR) spectroscopy, together with chemical analysis of cell wall composition were used to qualitatively determine the chemical changes in the lignocellulosic material during the torrefication process. HGI and tensile strength test were used to study the mechanical behavior of the straw at different conditions of torrefication. Higher heating value (HHV) was determined to establish a relationship between energy loss and anhydrous weight loss (AWL).

2. Material and methods

2.1. *Torrefaction*

The wheat straw used in this study is from winter wheat (*Triticum aestivum* L.), which was the most grown wheat species in Denmark in 2008. The straw was cut by hand in the field on the island of Funen, Denmark (55°21′N 10°21′E) in August 2008, and

stored indoors packed in the paper bags. Prior to the experiment, wheat straw were selected and cut to about 30 cm long pieces. Samples were first dried in the oven at 104 °C for 24 h, and then placed in an air tight metal container (15 × 31 × 10 cm) that could be heated in an oven (Lyngbyovnen of type S 90, 3 × 380 V, 9 kW) to the desired torrefaction temperature 0.5 dm^3 min^{-1} of nitrogen was pumped through the sample container to create an inert atmosphere. The temperature of the oven was measured in the center of the chamber using thermocouples and this measurement was used for temperature control. The residence time of the torrefaction process starts when the material temperature has reached the set temperature until it starts to cool down. Torrefaction was carried out at 150, 200, 220, 230, 250, 260, 270, 280, 290 and 300 °C with residence time of 2 h. Additional different residence times of 0.5, 1, 2, 3 h were tested at 250 °C.

2.2. ATR-FTIR

For sample preparation wheat straw were comminuted in a Hardgrove ball mill and the particle size fraction between 250 and 600 μm was used for the FTIR test. Before the test, these particles were dried in the oven at 40 °C for 24 h. ATR-FTIR spectra (4000–650 cm^{-1}) were recorded using a Fourier transform infrared spectrometer (Nicolet 6700 FTIR, Thermo Electron Corporation, USA). The system was equipped with a thermostat controlled ATR unit ($T = 30$ °C) where the sample was pressed against the diamond surface using a spring-loaded anvil. All spectra were obtained with 128 scans for the background (air) and 100 scans for the sample with a resolution of 4 cm^{-1}. Spectra were recorded from 10 different subsamples for each sample condition, and these spectra were normalized at around 690 cm^{-1} where the spectra are free of distinct IR bands. The average spectrum of the 10 normalized spectra was presented for each sample condition. A spectrum was also obtained for each of the two xylans (from Birchwood and from oat spelts, both from Sigma) reference samples (results not shown in this paper).

2.3. Tensile strength

Plant leaf materials were removed from the stem internodes, and a flat thin piece was cut from the hollow stem. The ends of the specimens were glued between 2 pieces of aluminum by using 'Loctite super glue, precision' (Henkel, USA). The length of the specimen was in the range of 3–6 cm, and the width of the specimen was in the range of 1.4–3.1 mm.

Tensile tests of wheat straw torrefied at different temperatures were tested using a tensile tester (Vantage, Thwing Albert, USA) with a video extensometer measuring the prolongation of the straw. The elongation rate was 1 mm min^{-1} and stress was recorded using a 250 N load cell. Data from samples that failed close to the aluminum tabs were rejected. Each measurement was repeated 4 times, except for wheat straw torrefied at 300 °C. Due to the brittleness of the sample, data were collected from only 2 samples. The tensile failure stress (or ultimate tensile strength), σ, of the specimen was calculated from the Eq. (1) [18]:

$$\sigma = \frac{F_t}{A} \tag{1}$$

where F_t is the tension force at failure and A is the area of the specimen at the failure cross-section. The cross-section area was measured both by an electronic digital micrometer (Digital Micrometer DIN 863, Diesella, Denmark) and calculated from the apparent density by assuming a uniform wall area and structure with length. The length and weight of each specimen were measured before the test, and the cross-section area was calculated as given in Eq. (2):

$$\text{Area} = \frac{m}{\rho \times l} \tag{2}$$

where ρ is the apparent density that was determined by coating the wheat straw samples (prepared in the same way as the tensile strength specimen) with paraffin wax (with known density). The weight was measured both prior to and after the coating with paraffin wax. Volumetric pipettes and water were used to measure the volume of wax coated samples in a volumetric flask.

Strain energy per unit volume was calculated as the area below the stress-strain curve in the diagram with the percent of elongation as X-axis and stress as Y-axis [19].

2.4. Hardgrove Grindability Index (HGI)

Determination of grindability was performed in a standard Hardgrove grinder (3200LB, AUBEMA, Germany) pursuant to the ASTM D409-51 (1961) standard. The test feed volume was 50 cm^3 with a particle size between 0.6 mm and 1.18 mm, this was done by pouring the particles into a 50 cm^3 volumetric flask and vigorously stamping on a wooden board to the point where further stamping did not reduce the volume of the material. The loading of the top grinding ring was 290 N and the grinding time was 3 min (377 radians of the mill at speed of 2.09 rad s^{-1}). The test sieve had a 75 μm mesh size and the Hardgrove Index was determined by Eq. (3) [20]:

$$\text{HGI} = 13 + 6.93 \times m_H \tag{3}$$

where m_H is the weight (in the units of gram) of the ground product passing the 75 μm sieve. The lower the number, the more difficult the material is to grind.

In addition to the wheat straw samples, a reference coal sample (RUKUZN, supplied by DONG Energy, Denmark) was tested. The sample was dried in an oven at 104 °C for 24 h before the test, and the mass fraction of water was determined to be 9.0% on wet material basis (w.b.). HGI was measured for the original (wet), partially dried and totally dried coal sample according to ASTM standard test procedure as described in [20] by using the same fixed volume (50 cm^3) for each feed.

2.5. Heating value

A Bomb calorimeter (6300, Parr Instrument Company, USA) was used to determine the higher heating value (HHV). Initially, the calorimeter was calibrated using benzoic acid tablets. Torrefied wheat straw was milled in a cutting mill (SM2000, Retsch, Germany) and particles smaller than 0.6 mm were placed in the crucible and fired inside the bomb calorimeter using an ignition wire in the presence of oxygen. The measurements were repeated at least 2 times, and the average

value was used for calculation. Ash content was determined by placing the samples in a muffle furnace at 550 °C for 3 h, 2 measurements were taken for each condition. Sample crucibles were ashed and dried before the measurement, and the dry material content (DM%) of each sample was determined by a moisture analyzer (Halogen moisture analyzer, Mettler Toledo, Switzerland). All data was calculated on dry and ash free basis (daf).

$$\mathrm{AWL\%} = 100 \times \left(1 - \frac{m_a}{m_b}\right) \tag{4}$$

$$\mathrm{AWL\%_{(daf)}} = \frac{\mathrm{AWL\%}}{100 - \mathrm{ash\%_{(r.b.)}}} \times 100 \tag{5}$$

$$\mathrm{ash\%_{(r.b.)}} = \mathrm{ash\%_{(t.b.)}} \times \frac{100 - \mathrm{AWL\%}}{100} \tag{6}$$

$$\mathrm{HHV_{(daf)}} = \frac{\mathrm{HHV/DM\%}}{100 - \mathrm{ash\%_{(t.b.)}}} \times 100 \tag{7}$$

$$\text{energy loss\%}_{(\mathrm{daf})} = \left[1 - \frac{\mathrm{HHV_{(daf)}}}{\mathrm{HHV_{104\ °C(daf)}}} \times \left(1 - \frac{\mathrm{AWL\%_{(daf)}}}{100}\right)\right] \times 100 \tag{8}$$

where m_a and m_b stand for the sample mass after and before the torrefaction respectively. m_b was recorded right after the drying, making AWL% already dry based. $\mathrm{ash\%_{(r.b.)}}$ denotes ash content in the raw material (untorrefied), whereas $\mathrm{ash\%_{(t.b.)}}$ is the ash content in the torrefied material. Both parameters are dry material based. Energy loss is defined as the total heating value loss of the same wheat straw samples after the torrefaction treatment. $\mathrm{HHV_{104\ °C}}$ means the heating value of oven dried (104 °C, 24 h) wheat straw.

2.6. *Cell wall composition*

The content of lignin, cellulose and hemicelluloses were determined for both untorrefied wheat straw and wheat straw torrefied at 300 °C for 2 h according to ASTM E 1758-01 [21] and Kaar et al. [22]. Briefly, a representative sample that was smaller than 1 mm was first made soluble in strong acid (72% H_2SO_4) at room temperature and then hydrolyzed in dilute acid (4% H_2SO_4) at 121 °C by autoclavation. Hemicelluloses and cellulose contents were determined by HPLC analysis of liberated sugar monomers. Klason lignin content was determined based on the filter cake, subtracting the ash content after incinerating the residues from the strong acid hydrolysis at 550 °C for 3 h.

3. Results and discussion

3.1. *ATR-FT-IR*

Infrared spectra taken from wheat straw samples torrefied at different temperatures are shown in Fig. 1 with the bands of interest being identified by their wavenumbers. The band at 670 cm^{-1} is characteristic for cellulose [23,24] and is an OH torsional vibration band. The fact that a significant decrease of

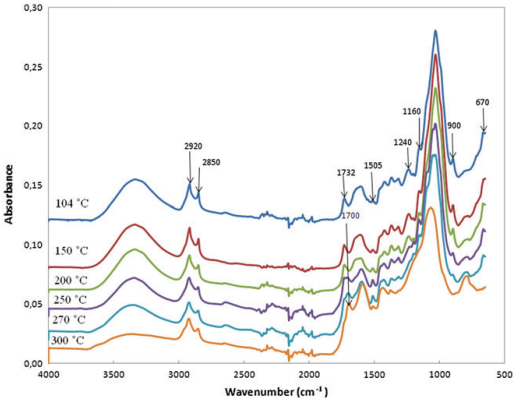

Fig. 1 – ATR-FTIR spectra of oven dried (104 °C) and torrefied wheat straw samples. All spectra are separated to ease the comparison.

this band is seen only for the highest temperatures between 270 °C and 300 °C shows that the cellulose component is largely stable until these temperatures are reached. The band at 1160 cm^{-1} is attributed to the antisymmetric stretching of C-O-C glycosidic linkages in both cellulose and hemicelluloses [25,26]. Its decrease is attributed to depolymerization and is most significant at the higher temperatures, and for 300 °C the band is practically absent. Gierlinger et al. attributed the band at 1240 cm^{-1} to the antisymmetric stretching of C-O-C of acetyl groups [26]. There are no acetyl groups existing in the hemicelluloses of wheat straw. However, for both reference xylans a band is found at 1245 cm^{-1} and is of approximately the same strength as the (xylan) 900 cm^{-1} band. The assignment of the 1240 cm^{-1} band to lignin can also not be ruled out. The peak observed at 1505 cm^{-1} is diagnostic of lignin [25,27] and is placed in a spectral region devoid of polysaccharide peaks. No clear change of this peak is observed for most of the temperature range. However, at 300 °C it does appear to have diminished. The band at 1732 cm^{-1} is attributed to the carbonyl stretching band of carboxylic acid groups in hemicelluloses [26,27]. It starts to decrease from 250 °C, signifying a reduction in the amount of the carboxylic acid groups of hemicelluloses. This reduction is paralleled by the appearance of a new degradation product band at 1700 cm^{-1}. When torrefaction temperature reaches 300 °C, the 1732 cm^{-1} band is completely eliminated, which suggests the complete removal of hemicelluloses. The narrow CH_2- stretching bands (superimposed a broader band) at approximately 2850 and 2920 cm^{-1} are ascribed to the aliphatic fractions of wax [27]. These bands for the C-H stretching can clearly be seen in spectra of extracted wax using hexane by work by Stelte et al. [28]. These bands appear not to change significantly due to the heat treatment of torrefaction although a small decrease of these bands is suggested for the highest temperatures. It is possible that the higher molecular weight waxes may still be present in the samples torrefied at 300 °C, although further work needs to be done to confirm this.

By analyzing the FTIR spectra of the torrefied wheat straw samples, it can be concluded that there is no major structural change of the wheat straw samples torrefied below 200 °C. Increasing the temperature from 200 °C to 250 °C introduces distinct changes in the spectrum. These appear not to involve lignin or cellulose to any major extent, as the two characteristic bands of these components at 1505 and 670 cm^{-1} do not change. Thus degradation and depolymerization of hemicelluloses is proposed to account for the initial low temperature torrefication effects. A higher temperature effect is most notable for the 270 °C–300 °C transition and consists of the degradation of lignin and cellulose. The cell wall composition of both untorrefied wheat straw and wheat straw torrefied at 300 °C were determined, and the results (Table 1) support the findings from FTIR. At 300 °C torrefaction conditions, hemicelluloses are almost completely removed and cellulose is also reduced substantially. Furthermore, although some degradation of wax is indicated, its efficient removal by the heat treatment during torrefaction has not been proved at the current operational conditions (300 °C, 2 h).

3.2. HGI

The reference coal sample at 3 different moisture contents on wet material basis (w.b.) (totally dried: 0%; partially dried: 6.3%; wet: 9.0%) were first ground in the standard Hardgrove grinder, and HGI was determined to be 33, 53, 68 respectively. Then the relationship between the mass fraction of the coal samples passing through the 75 μm sieve after the grinding (x) and the equivalent HGI (HGI_{equiv}) was established in the similar way as Bridgeman et al. [1]. The result is given in Eq. (9) with $R^2 = 0.9993$:

$$HGI_{equiv} = \frac{(x + 5.2521)}{0.3577} \quad (9)$$

This equation was then used to determine the equivalent HGI of the wheat straw samples torrefied at the different temperatures. Meanwhile, standard HGI value was calculated according to Eq. (3). Both standard and equivalent HGI are calculated and plotted in Fig. 2. The standard HGI value of wet coal was measured to be 33, which is close to the value of wheat straw torrefied at 300 °C for 2 h. It means that the mill can produce similar amounts of fine particles by loading the same volume of the two materials. The HGI tests were repeated for the wheat straw samples torrefied at 300 °C. It can be seen from the figure that there was no big improvement of HGI when torrefaction temperature was lower than 200 °C and the HGI value increases sharply when torrefaction temperature goes from 230 °C to 300 °C. FTIR spectra indicate that there is no major structural change of samples torrefied below 200 °C, hemicelluloses start decomposition at 200 °C–250 °C and are removed totally when torrefaction temperature reaches 300 °C, while cellulose and lignin are found to start the degradation at 270 °C–300 °C. It can thus be concluded that the removal of hemicelluloses is the main reason of the increase of HGI, which means a better grindability.

Furthermore, plots of mass fraction of particles passing 75 μm and 250 μm after being ground in the Hardgrove ball mill are given in Fig. 3. It can be seen that there is no big change before 200 °C. The largest increase in the fine particle fraction, which is smaller than 75 μm, happens in the range of 250 °C–300 °C. For particles smaller than 250 μm it happens in the temperature range of 200 °C–250 °C. The mass fraction of reference coal particles at different moisture contents passing through 75 μm and 250 μm after grinding are 6.67%–19.08%, and 31.26%–41.95% respectively. This means that in order to produce similar grindability as coal, the torrefaction temperature should be at least 230 °C. At a torrefaction temperature of 260 °C, wheat straw sample has a similar equivalent HGI value as 'totally dried coal', but a higher percentage of particles passing through 250 μm sieve.

In order to study the influence of residence time on the Hardgrove grindability, tests were also made for wheat straw torrefied at 250 °C for 0.5 h, 1 h, 2 h and 3 h respectively. Results are shown in Fig. 4. It can be seen that for a torrefaction temperature of 250 °C, a 2-h residence time is enough for improving the grindability of wheat straw samples.

3.3. Tensile strength

The results of the tensile strength measurements obtained by using both apparent density and caliper measurements are shown in Fig. 5. From both methods, it can be seen that there is a clear decrease of breaking stress from 150 °C to 200 °C, and from 250 °C to 300 °C. Compared to the HGI results, both tests show a big improvement of grindability at a torrefaction temperature of 250 °C–300 °C, and this finding is consistent with the FTIR analysis results discussed in 3.2. By comparing the mean strain energy (Fig. 6), it can be concluded that wheat straw torrefied at 250 °C for 2 h only requires about 1/5 to 1/7 of

Table 1 – Mass fraction of hemicelluloses, cellulose and lignin in both raw and torrefied wheat straws (dry and ash free basis).

	Lignin	Cellulose	Hemicellulose	Total
Raw wheat straw	21.28	35.64	27.78	84.70
Wheat straw-torrefied at 300 °C for 2 h	98.40	1.02	0.34	99.76

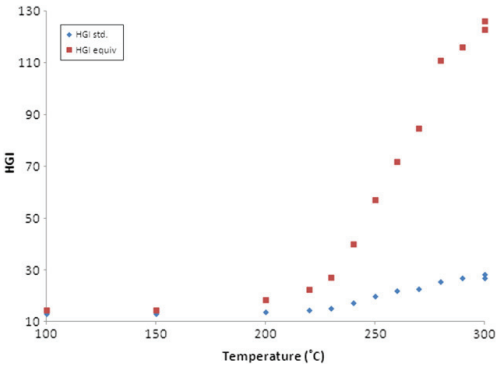

Fig. 2 – HGI of oven dried (104 °C) and torrefied wheat straw.

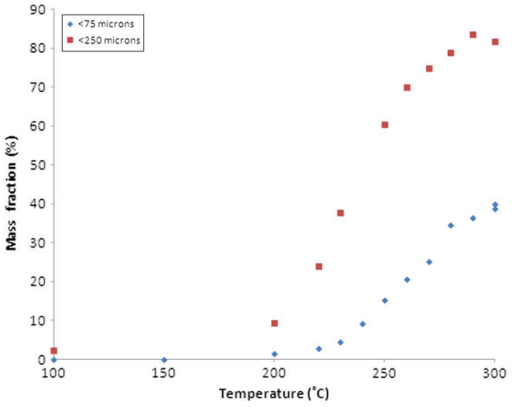

Fig. 3 – Mass fraction of particles passing through 75 μm, and 250 μm after grinding for oven dried and torrefied wheat straw.

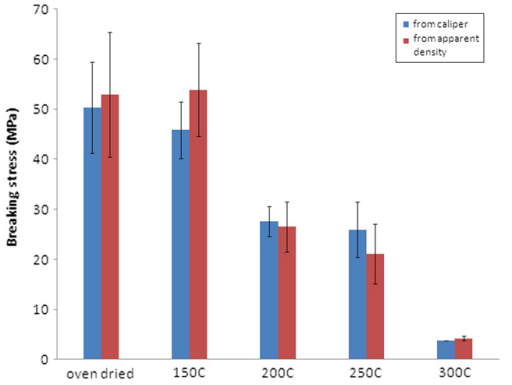

Fig. 5 – Tensile strength of wheat straw dried in oven (104 °C, 24 h) and torrefied under different temperatures for 2 h.

the energy, required to pull untorrefied, oven dried wheat straw apart.

The tensile strength of untreated wheat straw with mass fraction of water in the range of 8–65% on wet material basis (w.b.) found in the literature varies from 9 MPa to 38 MPa [18,29,30]. Contrary to these numbers, Kronbergs [31] reported a much higher value for wheat stalk, found to be (118.7 ± 8.63) MPa. These data are based on the wall area of the whole stalk sample at the failure cross-sections. Besides, Burmistrova [32] calculated stalk cross-section area based on the absolute dry weight of the wheat sample, the length of sample and the density of cellulose (1.55 g cm^{-3}). This physical cross-section area is smaller than the geometrical wall area by a factor of 5–10. Therefore the tensile strength, which was found to be in the range of 128 MPa–399 MPa, is correspondingly larger than the results of the other quoted authors. Comparing the results obtained from oven dried wheat straw in this paper and the data mentioned above, it is found that the tensile strength is likely to be underestimated in most of the literature [18,29,30] where the whole stalk is used for the test. This is because the whole stalk does not break equally at the same time. In most cases, the weakest part breaks first while the other parts still hold together and only break when the force increases. Therefore, the cross section area of the whole stalk is bigger than the actual area where the break happens, leading to underestimated tensile strength.

3.4. *Anhydrous weight loss and energy loss*

The weight loss from the drying process (104 °C, 24 h) is quite constant, which is around 9–10% (w.b.). The weight loss in the torrefaction process can also be called anhydrous weight loss (AWL). The higher torrefaction temperature, the more mass is

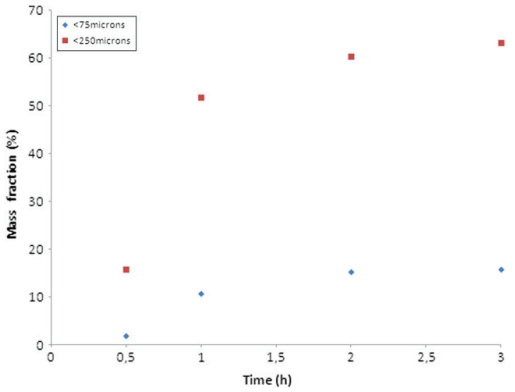

Fig. 4 – Mass fraction of particles passing 75 μm, and 250 μm after grinding for wheat straw torrefied at 250 °C for difference time.

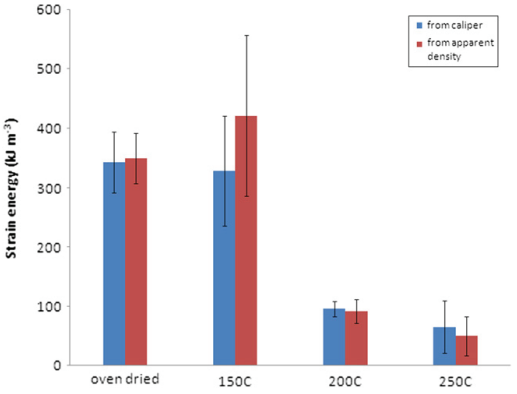

Fig. 6 – Strain energy of same wheat straw as in Fig. 5 from both direct caliper measurement and indirect apparent density calculation.

lost. When the temperature reaches 300 °C, around half of the material is lost.

Fig. 7 shows the experimental and calculated results of ash content. The increase of experimental ash content is only due to the mass loss (non-ash part) from torrefaction. By comparing the calculated ash content, it can be concluded that torrefaction treatment below 300 °C and 2 h has no influence on the ash content of wheat straw samples.

The higher heating value of wheat straw torrefied to different degrees (in form of AWL%) on dry ash free basis is shown in Fig. 8. Data obtained from different residence times at 250 °C are also presented in the plot (triangle markers). As shown, these points are located on the same trend line of HHV as a function of AWL% obtained from different torrefaction temperatures with the same residence time (2 h). This means that the parameter $AWL\%_{(daf)}$ can be used as a parameter to determine the effect of different torrefaction conditions, including temperature and residence time, on the heating value of the biomass. This finding is in agreement with the study done by Almeida et al. [33].

In addition, the influence of the degree of torrefaction as given by the AWL% parameter on the energy loss is also shown in Fig. 8. When the torrefaction conditions get more severe, there is more anhydrous weight loss and energy loss from the original material. The FTIR results show that hemicelluloses start the decomposition at 200–250 °C and it lasts until 300 °C, while cellulose and lignin start the decomposition at 270–300 °C. So there is more energy and mass loss at torrefaction temperatures ranging from 250 °C to 300 °C compared to from 200 °C to 250 °C.

Furthermore, these two kinds of loss are not at the same ratio. Heating value is lost faster than the mass. The energy loss at 300 °C (33%) is about 2.8 times of the energy loss at 250 °C (12%); while regarding anhydrous weight loss this number is 2.3. So in order to preserve energy in the torrefied material, lower torrefaction temperature and/or shorter residence time are preferred. On the other hand, if energy condensed material is desired, it is better to have more severe torrefaction condition.

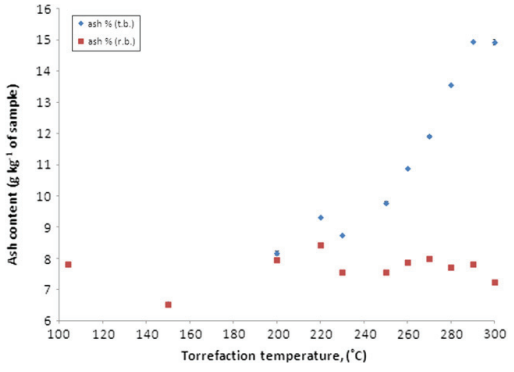

Fig. 7 – Ash content of wheat straw torrefied at different temperatures (denoted as 'ash% (t.b.)'), and calculated ash content of raw materials (denoted as 'ash% (r.b.)'). All data are on dry material basis.

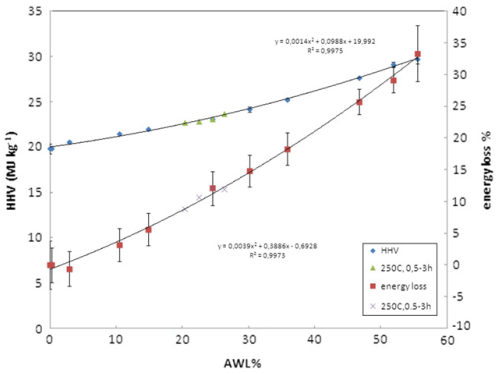

Fig. 8 – Higher heating value and percent of energy loss of wheat straw torrefied at different degrees (150, 200, 220, 230, 250, 260, 270, 280, 290, 300 °C for 2 h '250 °C, 0.5–3 h' represents the data collected at 250 °C torrefaction temperature with different residence time of 0.5, 1, 2, and 3 h). All data are on dry and ash free basis.

4. Conclusion

By comparing the HGI of wheat straw samples torrefied at different temperatures, it can be seen that there is almost no improvement of the grindability for samples torrefied below 200 °C. In the torrefaction temperature range between 230 °C and 300 °C, the HGI value increases sharply. In the same range, tensile failure stress decreases from about 24 MPa to 4 MPa, which shows a close relation between the two properties. The FTIR analysis suggests that the removal of hemicelluloses, the degradation of which starts at 200–250 °C and finishes at about 300 °C, is the main reason for the improvement of grindability in this temperature range. Following grinding of the wheat straw torrefied at a temperature of 230 °C, the samples produce similar mass fraction of fine particles (<75 μm) as the tested wet coal sample (with 9.0% moisture content on wet basis), while similar percentages of fine particles as produced from 'totally dried coal' (with 0% moisture content) can be achieved at a torrefaction temperature of 260 °C.

However, tensile strength test was not proved to be more reproducible and repeatable than the HGI test. But on the other hand, strain energy measured from tensile failure strength suggests that about 80–85% of the energy can be saved when comparing torrefied wheat straw (250 °C, 2 h) with oven dried samples in the breaking process. Such numbers cannot be derived from HGI results.

By looking at the relationship between energy loss and weight loss, it is found that the percent of energy loss increases faster than the weight loss when torrefaction condition gets more severe and is probably because the degradation of lignin and cellulose happen at 270–300 °C. So in order to preserve energy in the torrefied material, lower torrefaction temperature and shorter residence time are preferred. On the other hand, if energy condensed material is desired, it is better to have more severe torrefaction condition.

Acknowledgment

This work was financially supported by ENERGINET.DK and the ForskEL program. The authors express their appreciation to Mr. Hans Lilholt for kindly introduction and valuable comments on tensile strength tests. Thanks are also due to Mr. Frank Adrian for help on finding the proper material to prepare the specimens in the tensile strength tests.

REFERENCES

[1] Bridgeman TG, Jones JM, Williams A, Waldron D. An investigation of the grindability of two torrefied energy crops. Fuel 2010;89(12):3911–8.
[2] Bridgeman TG, Jones JM, Shield I, Williams PT. Torrefaction of reed canary grass, wheat straw and willow to enhance solid fuel qualities and combustion properties. Fuel 2008; 87(6):844–56.
[3] Arias B, Pevida C, Fermoso J, Plaza MG, Rubiera F, Pis JJ. Influence of torrefaction on the grindability and reactivity of woody biomass. Fuel Process Technol 2008;89(2):169–75.
[4] Bergman PCA. Combined torrefaction and pelletisation: the TOP process. Petten, The Netherlands: Energy Research Centre of the Netherlands (ECN); 2005 Jul. 29 [pp. Report No.: ECN-C–;05–073].
[5] Bridgeman TG, Jones JM, Williams A, Waldron D. Using existing coal milling technologies to process thermally pre-treated biomass. In: Biomass conference and exhibition. EU BC&E 2009: Proceedings of the 17th European Biomass Conference and Exhibition; 2009 June 29–July 3; Hamburg, Germany. Italy: ETA-Renewable Energies (Ed.); 2009. pp. 1689–1693.
[6] Abdullah H, Wu H. Biochar as a fuel: 1. Properties and grindability of biochars produced from the pyrolysis of mallee wood under slow-heating conditions. Energy Fuels 2009;23(8):4174–81.
[7] Bergman PCA, Boersma AR, Kiel JHA, Prins MJ, Ptasinski KJ, Janssen FJJG. Torrefaction for entrained-flow gasification of biomass. Available at: www.ecn.nl/docs/library/report/2005/c05067.pdf; 2005 [Accessed 13.01.2012].
[8] Deng J, Wang G, Kuang J, Zhang Y, Luo Y. Pretreatment of agricultural residues for co-gasification via torrefaction. J Anal Appl Pyrolysis 2009;86(2):331–7.
[9] Sadaka S, Negi S. Improvements of biomass physical and thermochemical characteristics via torrefaction process. Environ Prog Sustain Energy 2009;28(3):427–34.
[10] Repellin V, Govin A, Rolland M, Guyonnet R. Energy requirement for fine grinding of torrefied wood. Biomass Bioenergy 2010;34(7):923–30.
[11] Sun RC. Cereal straw as a resource for sustainable biomaterials and biofuels: chemistry, extractives, lignins, hemicelluloses and cellulose. 1st ed. UK: Elsevier; 2010.
[12] Svoboda K, Pohořelý M, Hartman M, Martinec J. Pretreatment and feeding of biomass for pressurized entrained flow gasification. Fuel Process Technol 2009;90(5):629–35.
[13] Beall F, Blankenhorn P, Moore G. Carbonized wood-physical properties and use as an SEM preparation. Wood Sci 1974;6: 212–9.
[14] ACARP Publication. Hardgrove grindability index. Available at: http://www.acarp.com.au/Downloads/ACARPHardgroveGrindabilityIndex.pdf; 2008 [Accessed 13.01.2012].
[15] Joshi NR. Relative grindability of bituminous coals on volume basis. Fuel 1979;58(6):477–8.
[16] Agus F, Waters P. Determination of the grindability of coals, shales and other minerals by a modified Hardgrove-machine method. Fuel 1971;50(4):405–31.
[17] Yigit E. Three mathematical comminution models based on strain energy. Int J Miner Process 1976;3(4):365–74.
[18] O'Dogherty MJ, Huber JA, Dyson J, Marshall CJ. A study of the physical and mechanical properties of wheat straw. J Agric Eng Res 1995;62(2):133–42.
[19] Timoshenko S, MacCullough GH. Elements of strength of materials. 3a ed. Toronto; London: D. Van Nostrand Co.; 1949.
[20] Mucsi G. Fast test method for the determination of the grindability of fine materials. Chem Eng Res Design 2008; 86(4):395–400.
[21] ASTM E 1758–01. Determination of carbohydrates in biomass by high performance liquid chromatography. In: Annual Book of ASTM Standards, vol. 11.05. West Conshocken, PA: ASTM International; 2003.
[22] Kaar WE, Cool LG, Merriman MM, Brink DL. The complete analysis of wood polysaccharides using HPLC. J Wood Chem Technol 1991;11(4):447–63.
[23] Barsberg S. Prediction of vibrational spectra of polysaccharides-simulated IR spectrum of cellulose based on density functional theory (DFT). J Phys Chem B 2010;114(36): 11703–8.
[24] Liang C, Marchessault R. Infrared spectra of crystalline polysaccharides. II. Native celluloses in the region from 640 to 1700 cm^{-1}. J Polym Sci 1959;39(135):269–78.
[25] Pandey K. A study of chemical structure of soft and hardwood and wood polymers by FTIR spectroscopy. J Appl Polym Sci 1999;71(12):1969–75.
[26] Gierlinger N, Goswami L, Schmidt M, Burgert I, Coutand C, Rogge T, et al. In situ FT-IR microscopic study on enzymatic treatment of poplar wood cross-sections. Biomacromolecules 2008;9(8):2194–201.
[27] Kristensen JB, Thygesen LG, Felby C, Jørgensen H, Elder T. Cell-wall structural changes in wheat straw pretreated for bioethanol production. Biotechnol Biofuels 2008;1(5): 1754–6834.
[28] Stelte W, Holm JK, Sanadi AR, Barsberg S, Ahrenfeldt J, Henriksen UB. A study of bonding and failure mechanisms in fuel pellets from different biomass resources. Biomass Bioenergy 2011;35(2):910–8.
[29] O'Dogherty M. A review of the mechanical behaviour of straw when compressed to high densities. J Agric Eng Res 1989;44:241–65.
[30] Limpiti S. Effect of moisture content and stage of maturity on mechanical properties of wheat straw. Thai J Agric Sci 1980; 13:277–83.
[31] Kronbergs E. Mechanical strength testing of stalk materials and compacting energy evaluation. Ind Crop Prod 2000; 11(2–3):211–6.
[32] Burmistrova M, Komol'kova I, Klemm N, Panina M, Polunochev I, P'yankov A. Physicomechanical properties of agricultural crops. National Science Foundation (U.S.); 1963 [Israel Program for Scientific Translations].
[33] Almeida G, Brito J, Perré P. Alterations in energy properties of eucalyptus wood and bark subjected to torrefaction: the potential of mass loss as a synthetic indicator. Bioresour Technol 2010;101(24):9778–84.

PAPER II

Physical and chemical property changes of 3 biomass fuels caused by torrefaction

Lei Shang, Wolfgang Stelte, Jesper Ahrenfeldt, Jens Kai Holm, Rui-zhi Zhang, Yong-hao Luo, Helge Egsgaard, Søren Barsberg, Tobias Thomsen, Lars Stougaard Bach, Ulrik B. Henriksen

Submitted for publication

Physical and chemical property changes of 3 biomass fuels caused by torrefaction

*Lei Shang [*a], Wolfgang Stelte [a], Jesper Ahrenfeldt [a], Jens Kai Holm [b], Rui-zhi Zhang [c], Yong-hao Luo [c], Helge Egsgaard [a], Søren Barsberg [d], Tobias Thomsen [a], Lars Stougaard Bach [a], Ulrik B Henriksen [a]*

** Corresponding author: Phone: +45 2132 4979, Fax: +45 4677 4109, E-mail: lesh@kt.dtu.dk*

[a] Department of Chemical and Biochemical Engineering, Technical University of Denmark, 2800 Kgs. Lyngby, Denmark.

[b] Chemical Engineering, DONG Energy Thermal Power A/S, Nesa Alle 1, 2820 Gentofte, Denmark

[c] School of Mechanical Engineering, Shanghai Jiaotong University, 200240 Shanghai, China

[d] Biomass and Ecosystem Science, Faculty of Life Sciences, University of Copenhagen, Rolighedsvej 23, 1958 Frederiksberg, Denmark

Abstract

Pine chips, Scots pine pellets and wheat straw were torrefied at 200-300 ˚C in an inert atmosphere. The higher heating value (HHV) of chips and pellets increased from about 20 MJ kg^{-1} to 29-30 MJ kg^{-1}; while the HHV of straw was about 0.8 MJ kg^{-1} lower than other two fuels on a dry and ash free basis. Steep reductions in grinding energy were observed for torrefied chips and pellets with mass loss of 25% and 10% during torrefaction, respectively. Hardgrove Grindability Index was proved not able to predict the level of grinding energy under practical conditions. The hygroscopicity results showed biomass torrefied at higher temperature takes up less moisture. The gas products evolving from biomass torrefaction, as detected *in situ* using a mass spectrometer

coupled TGA, matched well with the degradation of biomass. The cumulative releases of gas products from the three biomass species at 300 ˚C were compared.

Keywords: Torrefaction, Hardgrove, Grindability, wood chips, pellet, wheat straw

1. Introduction

The role of sustainability in the heat and electricity production continues to increase worldwide. The European Commission has set a binding target of a 20% share of renewables in the energy consumption by 2020 [1]. Wood pellets, wood chips and wheat straw are three widely used biomass fuels in power plants in Denmark [2]. However, these biomass fuels are more challenging to utilize than coal. Wood chips and wheat straw suffer from a low heating value and low bulk density [3]. The typical energy density (on a lower heating value base) of softwood chips and wheat straw is about 2800 MJ $m^{-3}$and 1740 MJ m^{-3}, respectively. Wood pellets have a much higher value of 9840 MJ m^{-3} [4]. However, they are still not comparable to coal (~ 32500 MJ m^{-3}) [5]. This causes higher transportation and storage costs for biomass fuels compared to coal, and also reduces the thermal capacity in boilers when co-fired with coal [6]. Furthermore, the high moisture content present in biomass fuels and their ability to absorb moisture from the surrounding atmosphere increase the costs of thermochemical conversion due to the drying stage [7]. The tenacious and fibrous nature of biomass fuels, especially for wheat straw and wood chips, is another important issue when it comes to grinding the fuels before utilization.

Torrefaction is a mild thermal (200-300 ˚C) pre-treatment of biomass in an inert atmosphere, which has received increased attention in recent years [8]. During the process, biomass first looses moisture at the drying stage (~100 ˚C) and at higher temperatures gas products are released due to the dehydration and decarboxylation reactions of the long polysaccharide chains [9]. Typically, 70% of the mass is retained as a solid product, containing 90% of the initial energy content. Thus, energy densification can be achieved. Pellets made from torrefied biomass can reach an even higher energy density of 14000 MJ m^{-3}, similar to a low rank coal [10]. In addition, the energy consumption during grinding of torrefied biomass can be reduced by 70-90% compared to

43 untreated biomass [10,11]. Furthermore, torrefied biomass is proved to be hydrophobic [7,12]. All these
44 property changes favor the replacement of fossil fuels with torrefied biomass in connection with co-milling and
45 co-firing with coal in large scale utility boilers. Phanphanich and Mani also reported that torrefied biomass may
46 produce less tar during gasification because of low moisture content and low hemicelluloses concentration [13].

47 The aim of this study was to gain an understanding of how torrified biomass properties depend on torrefaction
48 temperature. Furthermore, comparisons among three biomass fuels (pine chips, Scots pine pellets, and wheat
49 straw) were made. Torrefaction were performed in an oven at 6 different temperatures in the range of 200 to 300
50 ˚C with 20 ˚C intervals. The higher heating value (HHV) was determined using a bomb calorimeter with the aim
51 of establishing a relationship between energy loss and mass loss during torrefaction. Grindability was studied
52 based on a modified Hardgrove Grindability Index (HGI), HGI_{equiv}, which is a simple and trustable measure of
53 grindability for materials that have very different bulk densities [14,15]. The main difference between HGI_{equiv}
54 and standard HGI is that the former uses the same fixed volume (50 cm^3) while the later one uses a fixed mass
55 (50 g) for each grinding test. In the present study, particle size distribution of fines collected after the Hardgrove
56 grindability tests was also measured as a complement to HGI results, because the HGI value is only based on the
57 amount of sample passing through a 75 μm sieve. It needs to be noticed that the HGI test requires that the
58 material is in the size range of 0.6 to 1.18 mm, which means that samples were ground and sieved prior to the
59 test. This procedure could raise the question if the dominant bonding mechanisms of particles in the range of 0.6
60 - 1.18 mm are the same as for the whole sample. This problem is especially relevant for pellets, which are made
61 by compressing sawdust or pre-ground woody biomass together. It is known that high mechanical strength of
62 wood pellets is a result of strong inter particle bonding. The major bonding mechanisms in densified biomass
63 products can be summarized as molecular forces (f.x. hydrogen bonding, van der Waals forces, etc), fiber
64 interlocking, and solid polymer bridges between adjacent wood particles due to polymer softening and
65 interpenetration of polymer chains i.e. lignin [16,17]. Furthermore, these mechanisms may be changed due to
66 molecular structural change caused by torrefaction. For example, hydroxyl groups, responsible for hydrogen

bonding and hydrophilicity, are probably converted. Hence bonding decreases with increasing torrefaction degree. In order to confirm this and to confirm the assumption that the bonding strength in small particles and whole pellets is different, the energy consumption during grinding the whole pine chips and pellets was measured on a bench scale disc mill and compared with the HGI results. The hygroscopicity was studied by measuring the equilibrium moisture contents (EMCs) of torrefied biomass under three different relative humidities.

Gas products evolved from the biomass during torrefaction was analyzed using simultaneous thermal analysis coupled with mass spectrometry (STA-MS). Unlike traditional gas chromatography, which requires sampling and is a discontinuous analysis, STA-MS provides information on the identification of major volatile species and the typical temperature range of release in one continuous measurement. Since each ion detected in the mass spectrometry has its own response factor, the intensities of the same mass to charge ratios (*m/z*) can therefore be compared for different samples after a normalization procedure [18]. However, profiles of different gases released during torrefaction of a single material can be compared only qualitatively, giving information on the temperature range and the evolution behavior for each compound. In this work, the results of STA-MS analysis of three biomass materials are studied, the main volatile compounds are identified and compared, and the main volatilization step is characterized. This information will be useful for utilizing the evolved gas to supply the heat of the process.

2. Experimental

2.1. Materials

Winter wheat straw (*Triticum aestivum* L.) was used which was the most grown wheat species in Denmark in 2008. It was harvested on the island of Funen, Denmark (55°21′ N 10°21′ E) in August 2008 and cut by hand and stored indoors packed in paper bags. Pellets made from pine wood were supplied by Verdo's pellet factory in Scotland. The diameter of the pellets were 6 mm. Wood chips were Danish pine wood from various sources

on Zealand, Denmark (55° 30′ N 11° 45′ E). The size of the chips varied from 30×30×20 mm to 100×100×30 mm. The chips were stored for several months in a shielded container with air circulation and had a constant moisture content of around 16% on wet mass basis.

2.2. Torrefaction

Samples were dried in the oven at 104 ˚C for 24 hours, and subsequently placed in an air tight metal reactor (15×31×10 cm) with a nitrogen gas in and outlet, and a thermocouple centered in the reactor. The reactor was placed in an oven (type S 90, Lyngbyovnen, Denmark) controlling the torrefaction temperature. The heating rate for the oven was 6 ˚C min^{-1}. Nitrogen flow was adjusted to 0.5 dm^3 min^{-1} at room temperature. The residence time is the period from when the thermocouple inside the reactor has reached the set temperature and the start of the cooling down period. Torrefaction was carried out at different temperatures spanning from 200 to 300 ˚C at 20 ˚C intervals for 2 h (residence time). However, for grinding energy consumption measurements pine chips were torrefied at 200, 250, 275 and 300 ˚C for 2 h and pellets at 230, 250 and 270 ˚C for 1 h.

The anhydrous weight loss (AWL, %) means the mass fraction lost during torrefaction, and it was determined based on Equation (1), where m_b is the mass of the original dry sample and m_a is the residual mass after torrefaction of the dried sample.

$$AWL = 100 \times \left(1 - \frac{m_a}{m_b} \right) \quad (1)$$

2.3. Cell wall composition analysis

The content of the cell wall (lignin, cellulose and hemicelluloses) was determined for both untorrefied biomass and biomass torrefied at 300 ˚C for 2 hours according to ASTM E 1758-01 [19] and Kaar et al. [20]. A representative sample smaller than 1 mm was dissolved in 72 % H_2SO_4 at room temperature and then hydrolyzed in dilute acid (4 % H_2SO_4) at 121 ˚C by autoclaved for 60 minutes. Hemicelluloses and cellulose contents were determined by HPLC (Aminex HPX-87H, Bio-Rad, Hercules, CA, USA) analysis of liberated sugar monomers

in the filtered liquids, such as xylose, arabinose, galactose, mannose, and glucose, respectively. Details of HPLC analysis refer to [21]. Klason lignin content was determined based on the residual filter cake corrected for the ash content. Ash was determined as the residue left after 550 ˚C incineration for 3 h.

2.4. Proximate analysis

The contents of moisture, volatile matter, and fixed carbon of the three biomass species were determined on a simultaneous thermogravimetric analyzer (STA 449F1, NETZSCH, Germany) according to [22,23]. Thermogravimetric analysis was carried out under a nitrogen purge at constant rate of 50 cm^3 min^{-1}. About 3 mg samples smaller than 0.09 mm were first heated up to 105 ˚C at a heating rate of 10 ˚C min^{-1}, maintained at 105 ˚C for 10 min, then raised to 900 ˚C at the rate of 50 ˚C min^{-1}. The mass evolved at 105 ˚C is mainly moisture, whereas the mass evolved at temperatures between 105 and 900 ˚C is mainly volatile matter. All mass remaining after heating to 900 ˚C consists of fixed carbon and ash. Ash content was measured separately as described in section 2.3. For both thermogravimetric analysis and determination of ash content two measurements were conducted for each biomass sample.

2.5. Heating value

A bomb calorimeter (6300, Parr Instrument Company, USA) was used to determine the higher heating value (HHV, MJ kg^{-1}). Torrefied biomass was milled in a cutting mill (SM2000, Retsch, Germany) and particles smaller than 0.6 mm was chosen for the test. Initially, the calorimeter was calibrated using benzoic acid tablets. Sample particles were placed in the crucible and fired inside the bomb calorimeter using an ignition wire in the presence of oxygen. At least 2 samples were tested for each temperature condition. Ash content was determined as described in section 2.3. Dry material content (DM, %) was determined by a moisture analyzer (Halogen moisture analyzer, Mettler Toledo, Switzerland). All data were calculated on dry and ash free basis (daf).

$$AWL_{(daf)} = \frac{AWL}{\left(1 - m_{ash}/m_b\right)} \quad (2)$$

$$HHV_{(daf)} = \frac{HHV / DM}{\left(1 - m_{ash} / m_a\right)} \quad (3)$$

$$Energy\ yield_{(daf)} = \frac{HHV_{(daf)}}{HHV_{104°C(daf)}} \times \left(100 - AWL_{(daf)}\right) \quad (4)$$

Where m_{ash} denotes the mass of ash in the sample, m_b is the mass of the original dry sample and m_a is the residual mass after torrefaction of the dried sample. *Energy yield* is defined as the fraction of heating value retained in the biomass samples after the torrefaction treatment. $HHV_{104°C}$ means the higher heating value of oven dried (104 ˚C, 24 h) biomass.

2.6. Equivalent Hardgrove Grindability Index (HGI_{equiv})

Determination of grindability was performed in a standard Hardgrove grinder (3200LB, AUBEMA, Germany) pursuant to the ASTM D 409-51 (1961) standard. The test feed was 50 cm^3 with particle size between 0.6-1.18 mm. The loading on the top grinding ring was 290 N and the grinding time was 3 min (at a speed of 2.09 rad s^{-1}). After the grinding, the mass of particles passing the sieve of 75 μm mesh size was used to calculate the equivalent Hardgrove Index by using Equation (5), which was obtained in our earlier work from the reference coal samples (RUKUZN, supplied by DONG Energy, Denmark) [14]:

$$HGI_{equiv} = \frac{\left(x + 5.2521\right)}{0.3577} \quad (5)$$

Where x is the percentage of the ground product passing the 75 μm sieve.

2.7. Energy consumption during grinding

Samples of pine chips (2-8 mm) and pellets (6 mm diameter) were ground in a bench scale disc mill (Kenia, Mahlkönig, Germany) with a screw conveyer feeding system and a disc grinding system. The finest grinding condition was chosen for the grinding tests. The energy consumed was measured using a wattmeter (THII, Denmark) connected to a data logging system (NI USB-6009, National Instruments, USA).

Approximately 50 g sample was fed into the feed hopper and the time required to finish the grinding was recorded along with the energy consumed. The idling energy was measured before the material was introduced. The specific energy required for grinding was determined by integrating the area under the power curve corresponding to the time required to grind the sample minus the idling energy [24,25].

Particle size distributions were then determined by sieving using a sieving tower (mesh size of 75, 125, 250, 500, 1000, 1400, 2000, 3150, 5000 μm, Retsch, Germany). The sieving was run for 40 min.

2.8. Hygroscopicity

3 different saturated solutions were prepared in 3 desiccators below the platform using NaCl, KCl, and KNO_3, which gave relative humidity values of 75.5%, 85%, and 92.5% at 25 ˚C, respectively [26,27]. Biomass samples with similar size were selected and packed in one plastic net for each torrefaction temperature. These nets, together with 3 empty nets (which accounted for the net sorption) were then put on the platform in the desiccators, which were placed in a well isolated and temperature monitored water bath. Equilibrium moisture contents (EMC) of the biomass samples were measured about once a week, and they were determined by the increase of the mass in the sample nets subtracting the increase of mass in the reference nets.

2.9. Simultaneous thermal analysis-mass spectrometric analysis (STA-MS)

Torrefaction tests were also carried out using a simultaneous thermogravimetric analyzer (STA 409, NETZSCH, Germany) in the TGA/DSC configuration. Biomass samples were milled and particles smaller than 90 μm were collected and dried in an oven at 104 ˚C. Approximately 10 mg of sample was placed in an aluminum oxide crucible on the microbalance and heated at 10 ˚C min^{-1} under nitrogen (50 cm^3 min^{-1}) to a final temperature of 300 ˚C and kept at this temperature for 1 h. Evolved gasses were analyzed *in situ* by a quadruple mass spectrometer (QMS 403 C, NETZSCH, Germany) connected to the STA. In order to prevent condensation of the evolved gas, the transfer line and inlet system of QMS was kept at about 300 ˚C. A small portion of the evolved gas (together with the purge gas) was led to the ion source of the mass spectrometer, since the pressure drops

from atmospheric pressure in the STA down to high vacuum in the QMS. The ion curves close to the noise level were omitted, the intensities of 9 selected ions (*m/z* = 18, 30, 31, 43, 44, 45, 46, 58, 60) were monitored with the thermogravimetric parameters as functions of time. MS intensities were normalized to the initial sample mass, before the background was subtracted [18,28]. In order to compare the relative intensity of gas products for different samples, the signals were further normalized by the maximum of the total intensity current (TIC) of the experiment [29].

3. Results and discussion

3.1 Weight loss and heating value at different torrefaction temperatures

The three biomass fuels have similar proximate analyses, as listed in Table 1. Results of the sugar composition in the cell walls for both untorrefied biomass and biomass torrefied at 300 ˚C are shown in Table 2. Different monosaccharides were chosen for the determination due to the different biomass species. For wheat straw, hemicelluloses are mainly consisting of a (1→4)-linked β-D-xylan with D-glucopyranosyluronic acid (or 4-O-methyl-α-D-glucopyranosyluronic acid) groups attached at position 2, and L-arabionfuranosyl and D-xylopyranosyl groups attached at position 3 [30]. Hence, only xylose and arabinose were chosen. Glucose is mainly contributed by cellulose; however, it is likely that a small amount of glucose is also present in the hemicelluloses, but this has not been taken into account in this work. It can be seen that the hemicelluloses were totally degraded when torrefied at 300 ˚C (for 2 h) for all 3 biomass species, and cellulose was also strongly degraded under these torrefaction conditions.

Table 1: Proximate analyses of biomass samples.

	Moisture, %	Volatiles, %	Fixed carbon, %	Ash, %
Wheat straw	1.35 ± 0.07	74.78 ± 0.59	19.23 ± 0.66	4.64 ± 0.09
Wood chips	1.06 ± 0.03	82.43 ± 0.44	15.26 ± 0.41	1.25 ± 0.01
Wood pellets	1.52 ± 0.07	78.65 ± 0.47	19.17 ± 0.40	0.66 ± 0.01

Table 2: Mass fraction of cell wall compositions in both oven dried biomass and biomass torrefied at 300 ℃ for 2 h on dry material basis (d.b.).

	Glucose	Xylose	Galactose	Mannose	Arabinose	Acid insoluble fraction	Ash	Mass yield
Wheat straw	34.0	23.4	NDa	ND	3.1	20.3	4.6	100
Wheat straw 300 ˚C	0.9	0.3	ND	ND	0.0	86.5	12.1	44.5
Wood pellet	40.5	4.2	2.4	9.8	2.2	32.2	0.7	100
Wood pellet 300 ˚C	0.2	0.0	0.0	0.0	0.0	98.8	1.1	48.6
Wood chips	42.8	6.9	5.3	3.7	0.0	27.5	1.3	100
Wood chips 300 ˚C	13.0	0.0	0.0	0.0	0.0	84.6	1.6	53.6

[a]ND, not determined

As shown in Figure 1, higher torrefaction temperature resulted in higher anhydrous weight loss (AWL) and HHV. On dry and ash free basis, HHV of Scots pine pellets and pine chips are very close, and HHV of wheat straw is always about 0.8 MJ kg^{-1} lower than the value of pellets and chips at the same AWL. This is in agreement with the experimental results from Prins et al. [31], where straw had the lowest heating value compared to willow, larch and beech, both untreated and at a torrefaction temperature of 250 ˚C. Energy yields of the three biomass species as a function of AWL are also plotted in Figure 1. It is interesting to see that the fraction of energy retained in the torrefied sample as a function of the mass loss is very close to each other for the tested biomass species. It means that the same mass loss during torrefaction corresponds to a similar fraction of energy loss in the samples during torrefaction for the tested biomass.

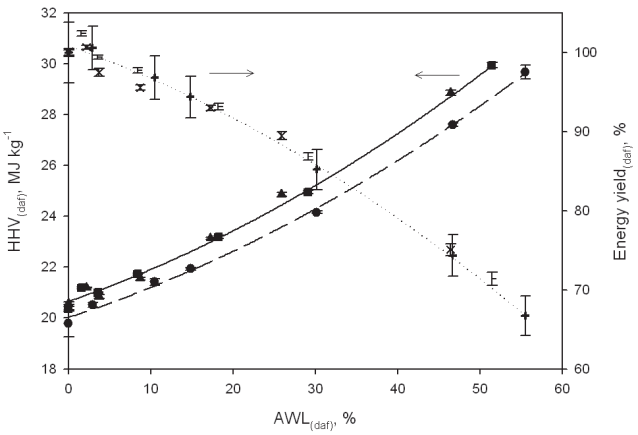

Figure 1: Higher heating value (HHV) for wheat straw (●), Scots pine pellets (■) pine chips (▲), and energy yield for wheat straw (+), Scots pine pellets (-), pine chips (×) vs. anhydrous weight loss (AWL, 0% AWL represents oven dried samples) on dry and ash free basis (daf).

3.2 Equivalent Hardgrove Grindability Index (HGI_{equiv})

Figure 2 shows significant improvement in grindability with increased torrefaction temperature for wheat straw and pine chips; while pellets show very little improvement. In order to achieve similar grindability as wet coal, a torrefaction temperature of about 240 ˚C is needed for wheat straw and pine chips, while for pellets 290 ˚C is required. Below 220 ˚C the grindability of the pellets is almost the same as for pine chips. Above 220 ˚C, the grindability of chips and straw increases dramatically, while pellet grindability improves very modestly.

Based on the HGI results, the grindability of pine chips is almost as good as wheat straw. However, if one takes a look at the particle size distribution results in Figure 3, wheat straw samples have a much higher percentage of fines in the range of 75 to 250 µm compared to pine chips. Therefore particle size distribution measurement is a necessary complement to the HGI test.

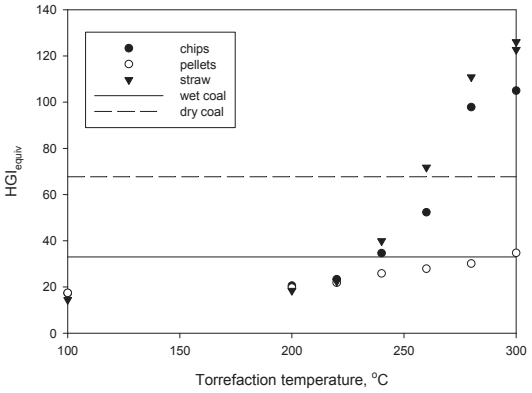

Figure 2: Results of Hardgrove grindability test for oven dried biomass (104 ˚C) and biomass torrefied at different temperatures for 2 h (tests were repeated for wheat straw samples torrefied at 300 ˚C), coal in wet and dry conditions were also tested in the Hardgrove grinder as a reference.

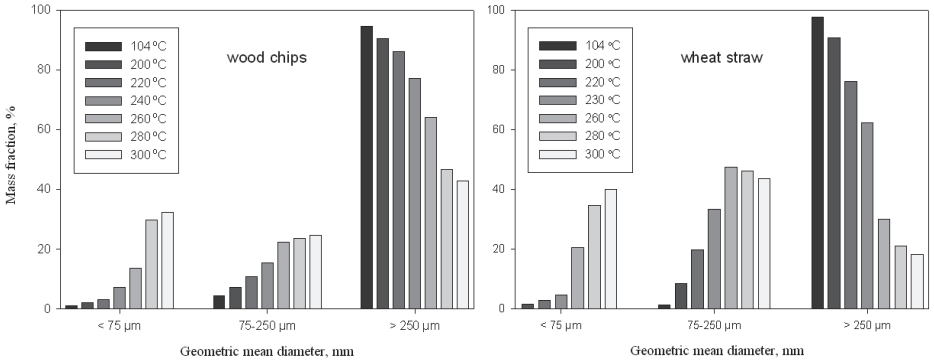

Figure 3: Particle size distribution analysis after Hardgrove test for oven dried biomass (104 ˚C) and biomass torrefied at different temperatures.

3.3 Energy consumption during grinding

Contrary to the HGI results, Figure 4 shows that pine chips consumed more grinding energy than pellets, except for the highest mass loss during torrefaction (about 50% AWL) where energy use in grinding for these two fuels tends to be close. There is a significant difference in creating wood or straw vs. pellets. In pellets, the wood has already been cut into small particles and then compressed together. It would be expected to be easier to

propagate fractures in pellets than in sound cell walls of wood chips. It needs to be noticed that the residence time of torrefaction was different for two materials. Pine chips were torrefied for about 2 h, while pellets were only torrefied for around 1 h. Hence anhydrous weight loss (AWL), which is a parameter to synthesize the effect of torrefaction temperature and duration, is used instead of torrefaction temperature to track the grinding properties.

The energy use for grinding pine chips and pellets showed a sharp decrease up to approximately 25% and 10% AWL, respectively. Therefore, these two mass loss fractions can be suggested as the optimal torrefaction conditions to achieve the maximum energy saving during grinding while maintaining as much energy yield as possible. Comparing the results in this study with our earlier work [11], in which the energy consumption of torrefied pellets was measured in the same disc mill but at the coarsest setting, it can be concluded that grinding at the finest setting requires ten times as much energy as at the coarsest setting. An exponential decrease of grinding energy with torrefaction was observed for both coarse and fine grinding.

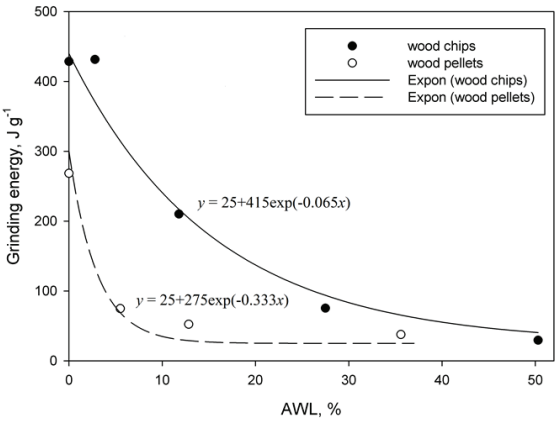

Figure 4: The specific energy required for grinding pellets (torrefied at 230, 250, and 270 ˚C for ca. 1 h) and pine chips (torrefied at 200, 250, 275 and 300 ˚C for ca. 2 h) vs. anhydrous weight loss (AWL, 0% AWL represents original pellets and oven dried chips). The grinding energy of a reference coal sample (RUKUZN, in size range of 2-7.1 mm, oven dried at 104 ˚C overnight) was determined with the same procedure, and it was 25 J g^{-1}.

Particle size distribution analysis was also done for the samples after the grinding energy measurement (Figure 5). Consistent with the HGI results, torrefied pine chips ended up with much higher fraction of fines (75 μm) than pellets after grinding and the higher the torrefaction temperature, the higher the percentage of fines. However, increasing torrefaction temperature from 230 to 270 ˚C seems not to improve the particle size distribution of pellets significantly, which is in agreement with the energy consumption results.

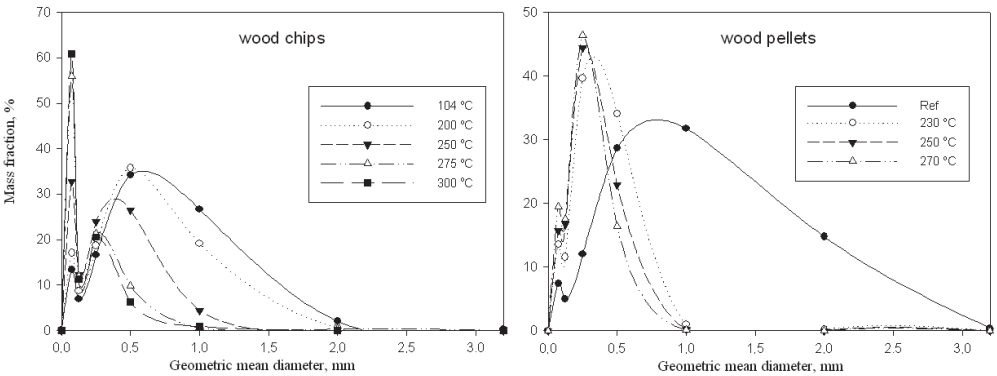

Figure 5: Particle size distribution analysis for oven dried pine chips (noted as '104 ˚C') and original Scots pine pellets (noted as 'Ref') and these two biomass torrefied at different temperatures after grinding.

3.4 Hygroscopicity

Biomass becomes darker with increasing torrefaction temperature, and the biomass has lost its shiny surface and smoothness, especially for pellets torrefied at temperatures higher than 260 ˚C and pine chips torrefied at 300 ˚C. Wheat straw torrefied at 280 ˚C and above became extremely brittle, which led to inaccuracy when determining the EMC.

When the relative humidity was increased, EMC of all samples increased correspondingly. Samples pre-treated at higher torrefaction temperatures absorbed less moisture, although this trend was disturbed for wheat straw torrefied at the highest temperature, due to the experimental error. As shown in Figure 6, EMC of torrefied samples can be reduced by about 5-10%, 7-12% and 13-20% under 75.5%, 85% and 92.5% relative humidity,

respectively. All three biomass samples exhibited similar EMC under a relative humidity of 75.5%. However, when the relative humidity was higher than 75.5% wheat straw samples absorbed most moisture; while Scots pine pellets and pine chips seemed to have similar EMC in most cases. A similar conclusion was also drawn by Reza et al.[32] stating that '*the pelletization process apparently does not affect the EMC*'.

The results shown in Figure 6 were recorded 50 days after the samples were placed at the different relative humidities. For all samples, it took longer to reach the EMC at higher relative humidities. For humidities ranging from 75.5% to 92.5%, it took about 10 to 20 days to reach the EMC, respectively. No special extension of reaching EMC was observed for pellets compared to other 2 biomass, which is in contrast with the results from Reza et al. [32]. One likely reason is that torrefied pellets (in this study) are different from pellets made by compressing torrefied wood (as studied in [32]). Gases formed during torrefaction left the pellets and generated empty sites in the pellets. Therefore the resistance to moisture diffusion in torrefied Scots pine pellets was not as strong as in the pellets compressed from torrefied wood.

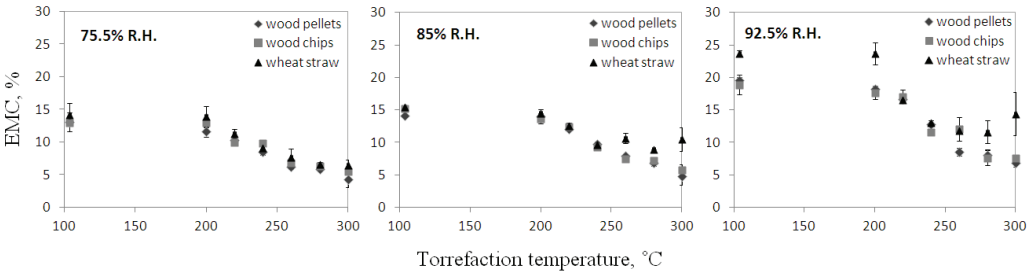

Figure 6: Equilibrium moisture content (EMC, on dry basis) for 3 kinds of biomass torrerfied at different temperatures (temperature at 104 ˚C means oven dried samples) under 3 relative humidities.

3.2 Simultaneous thermogravimetric analysis-mass spectrometric analysis (STA-MS)

The DTG profile shown in Figure 7 (a) is representative of the fraction of mass loss per minute. A small shoulder can be seen for wheat straw at 278 ˚C, this is probably related to the degradation of hemicelluloses. The main peak at 293 ˚C is mainly related to the decomposition of cellulose [33,34]. The corresponding peak for pine

chips and pellets was found at 307 ˚C. This indicates that the thermal decomposition of wheat straw starts at a lower temperature and proceeds at a higher rate than the decomposition of pine chips and pellets, which may explain the better grindability of wheat straw compared to other two species when torrefied at same temperature as observed in HGI test and particle size distribution analysis. Furthermore, the reason of such difference could be related to the high ash content in wheat straw compared to the other two fuels, since inorganic salts lower the decomposition temperature of lignocellulosic materials [35].

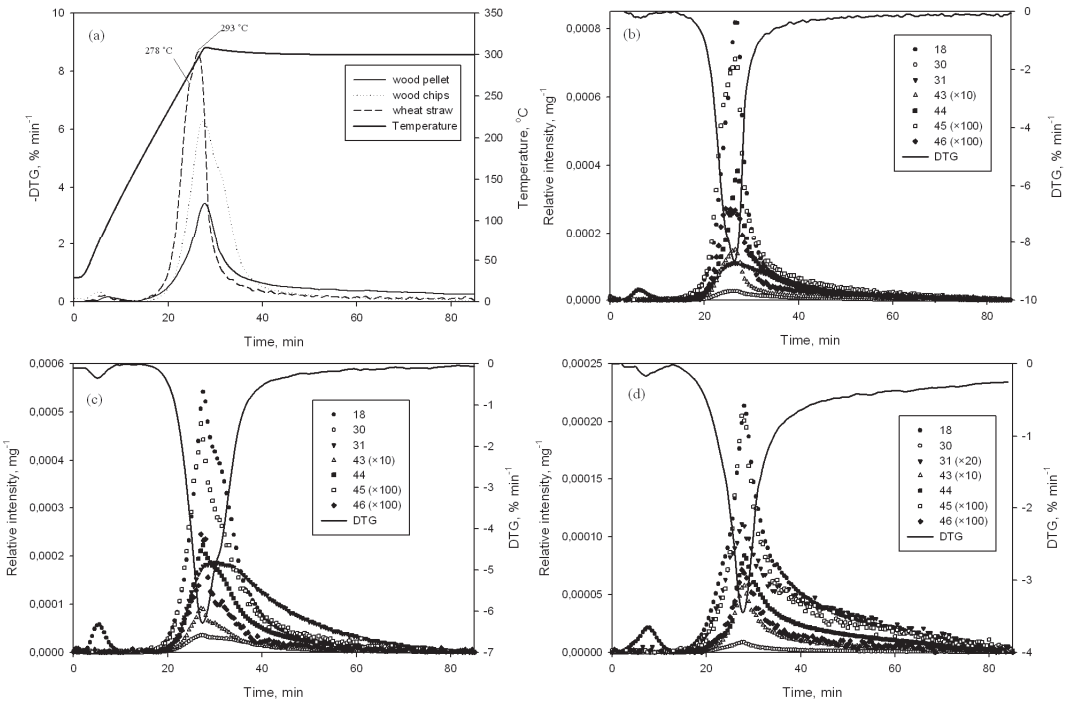

Figure 7: (a) Temperature profile and first derivative of weight loss (DTG) curve during torrefaction of pine chips, Scots pine pellets and wheat straw; derivative weight loss (DTG) curve and MS (18 water, 30 formaldehyde, 31 methanol, 43 acetic acid, 44 carbon dioxide, 45 lactic acid, 46 formic acid) relative intensity of main gases evolved during torrefaction of wheat straw (b), pine chips (c), and pellets (d).

297 **Table 3: Integrated peak areas of the gaseous compounds evolved during torrefaction of three biomass fuels.**

		Integrated relative intensity peak areas $\times 10^5$ (min mg^{-1})		
m/z	Assignation	Wood chips	Wood pellets	Wheat straw
18	H_2O	597.9	299.8	568.2
30	HCHO	67.8	12.0	37.7
31	CH_4O	447.8	11.4	205.2
43	CH_3COOH	9.4	5.9	12.0
44	CO_2	286.4	119.3	310.1
45	$C_3H_6O_3$	5.1	2.5	6.3
46	HCOOH	2.0	0.8	2.8
58	C_3H_6O	0.7	0.4	0.9
60	COS	0.7	0.3	1.0

298 Table 3 shows the most characteristic *m/z* signals and the assigned compounds. In order to make a quantitative
299 comparison of gas products released from different biomass species during torrefaction, integral subtended by
300 the relative intensity of MS curves for different kinds of biomass have been calculated. Gas products during
301 torrefaction of pine chips, Scots pine pellets and wheat straw detected by MS were water (m/z 18), formaldehyde
302 (*m/z* 30), methanol (*m/z* 31), acetic acid (*m/z* 43), carbon dioxide (*m/z* 44), lactic acid (*m/z* 45), formic acid (*m/z*
303 46); traces of acetone (*m/z* 58) and carbonyl sulfide (*m/z* 60) were also found at the torrefaction temperature of
304 300 ˚C. Because N_2 was used as purge gas, it was not possible to distinguish CO (*m/z* 28) in this study. Generally,
305 pellets released the least gas among these 3 kinds of biomass. Wheat straw released more acetic acid, formic
306 acid, lactic acid, acetone, carbonyl sulfide and CO_2 than pine chips. On the other hand, pine chips produced more
307 water, formaldehyde, and methanol than wheat straw and pellets.

308 Figure 7 (b), (c), (d) compare the derivative weight loss curve with the MS relative intensity profiles of gaseous
309 species released as a function of time for the three biomass fuels. The evolution of gas products started almost
310 simultaneously when temperature reached about 200 ˚C. In agreement with the literature [36,37], the dominant
311 product is water for all three biomass. The shape of most MS profiles resembles that of the DTG curves, except

312 for methanol (*m/z* 31). More than half of the methanol was evolved after 30 min and the evolution lasted until
313 almost the end of the torrefaction. This phenomenon is most pronounced for pine chips.

314 4. Conclusion

315 Wheat straw had the highest ash content (4.6%) while Scots pine pellets had the lowest content (0.7%) on a dry
316 basis. Pellets and pine chips showed similar heating values and weight loss characteristics during torrefaction.
317 On a dry and ash free basis, the higher heating value (HHV) of the two fuels increased from about 20 MJ kg^{-1}
318 for oven dried samples to 29 – 30 MJ kg^{-1} for samples torrefied at 300 ˚C, and the corresponding mass losses
319 during torrefaction were around 50%. For wheat straw, The HHV was always about 0.8 MJ kg^{-1} lower than the
320 values for the other two fuels. The correlation between mass loss and energy loss is very similar for the three
321 tested biomass fuels. The chemical analysis showed that hemicelluloses were significantly degraded from all
322 three biomass species after being torrefied at 300 ˚C for 2 h, and cellulose was also strongly degraded at such
323 torrefaction conditions.

324 The grindability of torrefied pellets was not improved to a satisfying level. It only reached same HGI level as
325 wet coal at torrefaction temperature of about 290 ˚C. The grindability of wheat straw showed the best response
326 to the torrefaction treatment. In order to achieve similar grindability as coal, a medium torrefaction temperature
327 (240 – 260 ˚C) is enough for wheat straw and pine chips. By comparing the HGI and energy consumption results,
328 it can be concluded that it requires more energy to grind small particles (e.g. 0.6-1.18 mm) in pellets than chips
329 and torrefaction affects the grinding of these small particles less than larger particles. Thus HGI is a useful
330 method to estimate the amount of fine particles after grinding under similar conditions, but does not predict the
331 level of energy use during grinding in real situation, where feedstock is usually in larger particle size. In this case,
332 large energy reductions were observed when grinding both torrefied pine chips and pellets in a bench scale disc
333 mill, especially up to 25% and 10% mass loss during torrefaction, respectively.

The hygroscopicity study showed that samples torrefied at higher temperatures absorbed less moisture. The equilibrium moisture content (EMC) of torrefied samples can be about 5% to 20% less than the untreated samples under relative humidities ranging from 75.5% to 92.5%. By comparing the cumulative release of gas products during the whole torrefaction reaction for the three tested biomass fuels, it can be concluded that pellets released the lowest amount of gas. Wheat straw released more acetic acid, formic acid, lactic acid, acetone, carbonyl sulfide and CO_2 than pine chips. Pine chips produced more water, formaldehyde, and methanol than wheat straw and pellets.

Acknowledgment

This work was financially supported by ENERGINET.DK and the ForskEL program (Project 2009-1-10202, Torrefaction of Biomass). We would also like to thank Brian Brun Hansen for the assistance of performing the proximate analysis, and Tomas Fernqvist for conducting the cell wall composition analysis.

Reference

[1] Cremers M. IEA Bioenergy Task 32 Deliverable 4 Technical status of biomass co-firing. 2009; Available at: http://ieabcc.nl/publications/09-1654%20D4%20Technical%20status%20paper%20biomass%20co-firing.pdf. Accessed 26.06.2012.

[2] Sander B. Properties of Danish biofuels and the requirements for power production. Biomass Bioenergy 1997;12(3):177-83.

[3] Gilbert P, Ryu C, Sharifi V, Swithenbank J. Effect of process parameters on pelletisation of herbaceous crops. Fuel 2009;88(8):1491-7.

[4] Van Loo S, Koppejan J. The handbook of biomass combustion and co-firing. UK: Earthscan/James & James; 2008.

[5] Demirbaş A. Sustainable cofiring of biomass with coal. Energy Conversion and Management 2003;44(9):1465-79.

[6] Sami M, Annamalai K, Wooldridge M. Co-firing of coal and biomass fuel blends. Progress in energy and combustion science 2001;27(2):171-214.

[7] Acharjee TC, Coronella CJ, Vasquez VR. Effect of thermal pretreatment on equilibrium moisture content of lignocellulosic biomass. Bioresour Technol 2011;102(7):4849-54.

[8] Bridgeman TG, Jones JM, Shield I, Williams PT. Torrefaction of reed canary grass, wheat straw and willow to enhance solid fuel qualities and combustion properties. Fuel 2008;87(6):844-56.

[9] Stelte W, Clemons C, Holm JK, Sanadi AR, Ahrenfeldt J, Shang L, et al. Pelletizing properties of torrefied spruce. Biomass and Bioenergy 2011;35(11):4690-8.

[10] Bergman PCA. Combined torrefaction and pelletisation: the TOP process. Petten, The Netherlands: Energy Research Centre of the Netherlands (ECN); 2005 Jul. 29 p. Report No.: ECN-C--05-073.

[11] Shang L, Nielsen NPK, Dahl J, Stelte W, Ahrenfeldt J, Holm JK, et al. Quality effects caused by torrefaction of pellets made from Scots pine. Fuel Process Technol 2012;101:23-8.

[12] Arias B, Pevida C, Fermoso J, Plaza MG, Rubiera F, Pis JJ. Influence of torrefaction on the grindability and reactivity of woody biomass. Fuel Process Technol 2008;89(2):169-75.

[13] Phanphanich M, Mani S. Impact of torrefaction on the grindability and fuel characteristics of forest biomass. Bioresour Technol 2011;102(2):1246-53.

[14] Shang L, Ahrenfeldt J, Holm JK, Sanadi AR, Barsberg S, Thomsen T, et al. Changes of chemical and mechanical behavior of torrefied wheat straw. Biomass Bioenergy 2012;40:63-70.

[15] Bridgeman TG, Jones JM, Williams A, Waldron D. Using existing coal milling technologies to process thermally pre-treated biomass. In: Biomass conference and exhibition. EU BC&E 2009: Proceedings of the 17th European Biomass Conference and Exhibition; 2009 June 29 - July 3; Hamburg, Germany. Italy: ETA-Renewable Energies (Ed.); 2009. p. 1689-1693 .

[16] Kaliyan N, Morey RV. Natural binders and solid bridge type binding mechanisms in briquettes and pellets made from corn stover and switchgrass. Bioresour Technol 2010;101(3):1082-90.

[17] Stelte W, Holm JK, Sanadi AR, Barsberg S, Ahrenfeldt J, Henriksen UB. A study of bonding and failure mechanisms in fuel pellets from different biomass resources. Biomass Bioenergy 2011;35(2):910-8.

[18] Senneca O, Ciaravolo S, Nunziata A. Composition of the gaseous products of pyrolysis of tobacco under inert and oxidative conditions. J Anal Appl Pyrolysis 2007;79(1-2):234-43.

[19] ASTM E 1758-01. Determination of carbonhydrates in biomass by high performance liquid chromatography. In: Annual Book of ASTM Standards, vol.11.05. West Conshocken, PA: ASTM International; 2003.

[20] Kaar WE, Cool LG, Merriman MM, Brink DL. The complete analysis of wood polysaccharides using HPLC. J Wood Chem Technol 1991;11(4):447-63.

391 [21] Sárossy Z, Tenkanen M, Pitkänen L, Bjerre AB, Plackett D. Extraction and chemical characterization of rye
392 arabinoxylan and the effect of β-glucan on the mechanical and barrier properties of cast arabinoxylan films.
393 Food Hydrocolloid 2012 doi: 10.1016/j.foodhyd.2012.05.022.

394 [22] Mayoral M, Izquierdo M, Andres J, Rubio B. Different approaches to proximate analysis by
395 thermogravimetry analysis. Thermochimica Acta 2001;370(1):91-7.

396 [23] Yan W, Acharjee TC, Coronella CJ, Vásquez VR. Thermal pretreatment of lignocellulosic biomass.
397 Environ Prog Sustainable Energy 2009;28(3):435-40.

398 [24] Adapa P, Tabil L, Schoenau G. Grinding performance and physical properties of non-treated and steam
399 exploded barley, canola, oat and wheat straw. Biomass Bioenergy 2010;35(1):549-61.

400 [25] Mani S, Tabil LG, Sokhansanj S. Grinding performance and physical properties of wheat and barley straws,
401 corn stover and switchgrass. Biomass Bioenergy 2004;27(4):339-52.

402 [26] Winston PW, Bates DH. Saturated solutions for the control of humidity in biological research. Ecology
403 1960;41(1):232-7.

404 [27] Apelblat A, Korin E. The vapour pressures of saturated aqueous solutions of sodium chloride, sodium
405 bromide, sodium nitrate, sodium nitrite, potassium iodate, and rubidium chloride at temperatures from 227 K to
406 323 K. The Journal of Chemical Thermodynamics 1998;30(1):59-71.

407 [28] Zhang R, Luo Y, Duan J, Liu C, Chen Y. Experimental Study on Releasing Characteristics of Products in
408 Biomass Pyrolysis. Journal of Power Engineering 2009;29(6):590-5.

409 [29] Arenillas A, Rubiera F, Pis J. Simultaneous thermogravimetric–mass spectrometric study on the pyrolysis
410 behaviour of different rank coals. J Anal Appl Pyrolysis 1999;50(1):31-46.

411 [30] Sun RC. Cereal straw as a resource for sustainable biomaterials and biofuels: chemistry, extractives, lignins,
412 hemicelluloses and cellulose. 1st ed. UK: Elsevier; 2010.

413 [31] Prins MJ, Ptasinski KJ, Janssen FJJG. Torrefaction of wood: Part 2. Analysis of products. J Anal Appl
414 Pyrolysis 2006;77(1):35-40.

415 [32] Reza MT, Lynam JG, Vasquez VR, Coronella CJ. Pelletization of biochar from hydrothermally carbonized
416 wood. Environmental Progress & Sustainable Energy 2012;31(2):225-34.

417 [33] Tihay V, Gillard P. Pyrolysis gases released during the thermal decomposition of three Mediterranean
418 species. J Anal Appl Pyrolysis 2010;88(2):168-74.

419 [34] Biagini E, Barontini F, Tognotti L. Devolatilization of biomass fuels and biomass components studied by
420 TG/FTIR technique. Ind Eng Chem Res 2006;45(13):4486-93.

421 [35] Szabó P, Várhegyi G, Till F, Faix O. Thermogravimetric/mass spectrometric characterization of two energy
422 crops, *Arundo donax* and *Miscanthus sinensis*. J Anal Appl Pyrolysis 1996;36(2):179-90.

[36] Gu P, Hessley RK, Pan WP. Thermal characterization analysis of milkweed flos. J Anal Appl Pyrolysis 1992;24(2):147-61.

[37] DeGROOT WF, Pan WP, Rahman MD, Richards GN. First chemical events in pyrolysis of wood. J Anal Appl Pyrolysis 1988;13(3):221-31.

PAPER III

Pelletizing properties of torrefied spruce

Wolfgang Stelte, Craig Clemons, Jens Kai Holm, Anand R. Sanadi, Jesper Ahrenfeldt, Lei Shang, Ulrik B. Henriksen

Reprinted from *Biomass and Bioenergy* (2011), 35, 4690-4698,

BIOMASS AND BIOENERGY 35 (2011) 4690–4698

Available online at www.sciencedirect.com

SciVerse ScienceDirect

http://www.elsevier.com/locate/biombioe

Pelletizing properties of torrefied spruce

Wolfgang Stelte [a,*], *Craig Clemons* [b], *Jens K. Holm* [c], *Anand R. Sanadi* [d], *Jesper Ahrenfeldt* [a], *Lei Shang* [a], *Ulrik B. Henriksen* [a]

[a] *Biosystems Department, Risø National Laboratory for Sustainable Energy, Technical University of Denmark, Frederiksborgvej 399, DK-4000 Roskilde, Denmark*

[b] *Forest Products Laboratory, United States Department of Agriculture, 1 Gifford Pinchot Dr., Madison, WI 53726-2398, USA*

[c] *Chemical Engineering, DONG Energy Power A/S, Nesa Alle 1, DK-2820, Gentofte, Denmark*

[d] *Biomass and Ecosystem Science, Faculty of Life Sciences, University of Copenhagen, Rolighedsvej 23, DK-1958 Frederiksberg C, Denmark*

ARTICLE INFO

Article history:
Received 8 January 2011
Received in revised form
29 September 2011
Accepted 30 September 2011
Available online 21 October 2011

Keywords:
Torrefaction
Wood
Spruce
Pellet
Bonding mechanism
SEM

ABSTRACT

Torrefaction is a thermo-chemical conversion process improving the handling, storage and combustion properties of wood. To save storage space and transportation costs, it can be compressed into fuel pellets of high physical and energetic density. The resulting pellets are relatively resistant to moisture uptake, microbiological decay and easy to comminute into small particles. The present study focused on the pelletizing properties of spruce torrefied at 250, 275 and 300 °C. The changes in composition were characterized by infrared spectroscopy and chemical analysis. The pelletizing properties were determined using a single pellet press and pellet stability was determined by compression testing. The bonding mechanism in the pellets was studied by fracture surface analysis using scanning electron microscopy. The composition of the wood changed drastically under torrefaction, with hemicelluloses being most sensitive to thermal degradation. The chemical changes had a negative impact, both on the pelletizing process and the pellet properties. Torrefaction resulted in higher friction in the press channel of the pellet press and low compression strength of the pellets. Fracture surface analysis revealed a cohesive failure mechanism due to strong inter-particle bonding in spruce pellets as a resulting from a plastic flow of the amorphous wood polymers, forming solid polymer bridges between adjacent particles. Fracture surfaces of pellets made from torrefied spruce possessed gaps and voids between adjacent particles due to a spring back effect after pelletization. They showed no signs of inter-particle polymer bridges indicating that bonding is likely limited to Van der Waals forces and mechanical fiber interlocking.

1. Introduction

The utilization of wood and agricultural biomass residues for sustainable heat and power production is an important part of future energy concepts [1]. One of the major challenges of biomass utilization for heat and power production is its unfavorable handling properties. Biomass is a bulky and inhomogeneous material, making it both difficult and expensive to store and transport. Furthermore, it is difficult to comminute into small particles and has a relatively low energy density (compared to fossil fuels) and high moisture contents. An ancient process to improve the combustion properties of wood is the manufacturing of charcoal, resulting in a product that burns at higher temperature, is

* *Corresponding author*. Tel.: +45 2132 5175; fax: +45 4677 4109.
E-mail addresses: stelte@gmail.com, wost@risoe.dtu.dk (W. Stelte).
0961-9534/$ – see front matter © 2011 Elsevier Ltd. All rights reserved.
doi:10.1016/j.biombioe.2011.09.025

easier to ignite, and can be stored easier due to its better moisture resistance. Nevertheless, charcoal contains only 20–55% of the raw material's energy content, depending on how well the process is carried out [2]. Torrefaction is an advance of this process, in which wood is roasted under controlled conditions (heating rate, temperature, time) in an inert atmosphere, retaining most of its energy [3]. The process results in an attractive fuel, with improved heating value, low moisture content and ease of size reduction [4]. Torrefaction is usually carried out between 230 and 300 °C [5] and removes moisture, carbon dioxide and volatiles from the biomass. Volatiles such as hydroxymethylfurfural, furfural and aldehydes are formed during the dehydration and decarboxylation reactions of the long polysaccharide chains [6]. The oxygen-to-carbon ratio is lowered significantly and the energy density of the biomass is increased, making it an ideal fuel for gasification processes where high oxygen contents are disadvantageous [7]. The value of torrefied biomass can be further improved by mechanical compression into pellets of high physical and energetic density [8]. The pelletization of biomass reduces its handling costs and results in a solid fuel of standardized shape and size that can be fed automatically in industrial and household size boilers being used for heat and power production. At present, there is a solid interest for utilizing torrefied wood pellets in existing large-scale combined heat and power (CHP) plants to replace coal with a biofuel without major changes in the power plant design [9].

The global production of fuel pellets from biomass was estimated to be about 13 Mt in 2009 with strong growth rates, and it is expected that Europe alone will reach a consumption of 50 million tons per year by the year 2020 [10]. Consequently, the variety of raw materials used for pellet production has greatly increased in recent years and is expected to further increase in the future. The production of mixed biomass pellets produced from many different agricultural and forestry residues is increasing [11]. Biomass composition has a great effect on the pellet quality [12] and the pelletizing process itself [13].

Few studies have been published on using thermally pretreated biomass in the pelletizing process [14,15] but to the best of the authors knowledge none have so far studied in detail the impact of thermal degradation of the wood polymers on the pellet quality and integrity. In the present work, pellets were produced from Norway spruce and after torrefaction at 250, 275 and 300 °C. The chemical changes after torrefaction were investigated and their effect on the friction in the press channel of a pellet mill was studied using a laboratory scale single pellet press unit. The pellet stability was determined by compression testing and the internal bonding of the pellets was studied by fracture surface analysis using scanning electron microscopy (SEM).

2. Experimental

2.1. Materials

The raw material used in this study was Norway spruce (*Picea abies K*), harvested in southern Sweden (Skåne/Småland) during 2007. Wood stems were collected in autumn, debarked and comminuted into wood chips. The material was dried in a warehouse by free air circulation for four weeks and further chopped into particles < 5 mm in diameter using a hammer mill (Model 55, Jensen and Sommer Aps, Denmark). The material was packed in paper bags permeable to air and moisture and stored for 24 month in a dry storage. The used samples had a particle size between 1 and 2.8 mm and the mass fraction of water was about 8.2%.

2.2. Torrefaction

A lab scale torrefaction unit was constructed and built for this research similar to the one developed by Pimchuai et al. [5]. A metal box with a volume of about 2 L and two openings (5 mm in diameter) for nitrogen inlet and gas outlet was used as reactor. The box was installed in a programmable muffle furnace (S90, Lyngbyoven, Denmark) and connected to a nitrogen cylinder with pressure and flow regulator, water seal valve and fittings and pipes for gas inlet, outlet and temperature sensors. A temperature sensor (iron-constantan thermocouple) was installed in the center of the metal reactor and connected to a thermometer (52 kJ, John Fluke, USA) and a computer system controlling the heating of the oven. A torrefaction time of two hours and maximum temperature (T_{max}) of 250, 275 and 300 °C have been chosen according to Pimchuai et al. [5].

About 450 g of wood particles were weighed in and sealed in the metal box. The box was put in the oven and heated at a rate of 2 °C min^{-1} until T_{max} was reached and kept constant for 2 h. Afterward the oven was switched off and the samples were allowed to cool. Nitrogen was flushed through the box at a rate of 0.5 L min^{-1} until the samples were cooled to ambient conditions. Dry weight was determined before and after torrefaction and was used to calculate the mass loss. The torrefied samples were conditioned in climate chambers at 27 °C at 65, 80 or 90% relative humidity until a constant weight was reached. The samples were termed T250, T275 and T300 according to the T_{max} reached during torrefaction.

2.3. Attenuated total reflectance infrared spectroscopy (ATR-FTIR)

ATR-FTIR spectra of the pellet fracture surfaces were recorded at 30 °C using a Fourier transform infrared spectrometer (Nicolet 6700 FT-IR, Thermo Electron Corporation, USA), equipped with a temperature-adjustable ATR accessory (Smart Golden Gate diamond ATR accessory, Thermo Electron Corporation, USA). Samples were dried at 105 °C for 4 h and stored in airtight containers until used for testing. A minimum of five measurements per sample was performed. To ensure good contact, all hard, solid samples were pressed against the diamond surface using a metal rod and consistent mechanical pressure. All spectra were obtained with 200 scans for the background (air), 100 scans for the sample and with a resolution of 4 cm^{-1} from 500 to 4000 cm^{-1}. Spectra were normalized at around 760–790 nm where the spectra were free of any distinct IR bands.

2.4. Biomass characterization

A fiber analysis to study the biomass composition (cellulose, lignin, hemicelluloses and ash content) was conducted according to the procedure used by Davis et al. [16] and can be summarized as follows. About 10 g per sample were milled to pass through a screen with a mesh size of 0.84 mm and then vacuum-dried at 45 °C. Approximately 100 mg sample were hydrolyzed in 1 mL sulfuric acid (13.5 mol L^{-1}) for 1 h at 30 °C. The samples were diluted to a sulfuric acid concentration of 0.75 mol L^{-1} by adding distilled water. Fucose was added as an internal standard, and a secondary hydrolysis was performed for 1 h at 121 °C. To control for sugar degradation during secondary hydrolysis, a standard mixture of sugars was hydrolyzed in parallel with each batch of samples. Material loss during primary hydrolysis was minimal and therefore ignored. The following secondary hydrolysis samples were immediately filtered through tared Gooch porcelain crucibles containing glass fiber filters (934-AH, Whatman, USA). The filtrate and three washes with 5 mL distilled water were collected in 100 mL volumetric flasks and brought to volume with water. The acid-insoluble residue (Klason lignin and insoluble degradation products) was washed for additional six times with 10 mL hot distilled water and its weight determined gravimetrically. Klason lignin values were corrected for ash content by gravimetric measurement following incubation of the lignin at 575 °C for > 3 h. Sugar contents of the hydrolyzates were determined by anion exchange high performance liquid chromatography using pulsed amperometric detection. After filtration through 0.45 μm PTFE membranes, acid hydrolyzates (sulfuric acid concentrations ranging between 0.2 and 0.75 mol L^{-1}) were injected with no further treatment. The chromatographic system consists of an autosampler (AS50, Dionex, USA) a quaternary gradient high pressure pump (GS50, Dionex, USA), and a pulsed amperometric detector (ED50, Dionex, USA). Sugar separation was achieved with guard and analytical columns (Carbo-Pac PA1, Dionex, USA) connected in series. Sugars were eluted with distilled water at a flow rate of 1.1 mL min^{-1} and a temperature of 18 °C. For detection, sodium hydroxide solution (0.3 mol L^{-1}) as added as a post-column reagent at a flow rate of ca. 0.3 mL min^{-1}. Prior to each injection, the anion exchange columns were conditioned with 400 mL sodium acetate solutions 0.24 mol L^{-1} and then equilibrated with distilled water. Sugars were quantitated using an internal standard method. Results are reported in terms of percent of the original sample mass dry matter.

Moisture uptake was studied by spreading 5 g of each material on a tray and conditioning in climate chambers (USDA Forest products lab, USA) at 27 °C and a relative moisture content of 65, 80 and 90%. Equilibrium moisture content was determined after the weight of the sample was constant for three days in a row. The moisture content was calculated based on weight loss after oven drying the material for 8 h at 105 °C.

2.5. Pellet preparation and determination of pelletizing pressure P_x in the channel of the pellet press

The pellets were prepared as described in [12], using a single pellet press (invented and constructed at the workshop of the Technical University of Denmark, Denmark). The press consisted of a cylindrical die 7.8 mm in diameter, made of hardened steel, lagged with heating elements and thermal insulation. The temperature was controlled using a thermocouple connected to a control unit. The end of the die was closed using a removable backstop. Pressure was applied using a metal piston. The entire pellet press was mounted in a material test system (MTS 810 Material Test system, MT Systems Corporation, USA) so that piston movement could be controlled and the force could be measured using a 100 kN load cell. The die was rinsed with acetone, and wiped clean using a paper towel before each use, and when changing raw materials. To simulate the pelletizing process within a commercial pellet mill, the pellet had to be built up in sequential layers [17]. The die was heated to 100 °C. Spruce and torrefied spruce particles equilibrated at 65% relative humidity (see Fig. 3 for moisture content) were loaded stepwise in amounts less than 0.25 g into the unit, and then compressed at a rate of 2 mm s^{-1} until a maximum pressure of 200 MPa was reached. The pressure was released after five seconds, the piston removed, and more biomass was loaded and compressed until the pellet had a length of about 16 mm. This results in a layered structure, similar to pellets obtained by commercial units, although there are some differences. The most significant difference is that the lower part of the pellet is pressed repeatedly, and the upper layers are pressed fewer times, with the top layer being pressed only once. For determination of pelletizing pressure in the press channel of the pellet mill, P_x, the pellets were removed from the die by removing the backstop and pushing out the pellet at a rate of 2 mm s^{-1}. The applied maximum force was logged and P_x was calculated based on the pellet surface area.

2.6. Determination of pellet strength

The internal strength of the manufactured pellets was analyzed by compression testing and determined as the force at break. Pellets 16 mm (±1 mm) in length and between 7.9 and 8.2 mm in diameter were produced in the single pellet press, stored at a relative humidity of 50% and 20 °C for three weeks, and tested under the same conditions. The pellets were placed on their side (the pellet's cylindrical shape oriented horizontally) in the same material tester as was used for pellet preparation. Compression tests were performed using a disc shaped metal probe with a ball bearing of 50 mm in diameter and attached to a 100 kN load cell. The test was run at a compression rate of 20 mm min^{-1} and was stopped after pellet failure. The average force at break and its standard deviation were calculated based on 5 replications per test condition.

2.7. Scanning electron microscopy (SEM)

SEM was used to study the bonding mechanism of the prepared biomass pellets by fracture surface analysis of failed pellets. The compression test resulted in total disintegration of the pellets, and therefore fracture surfaces were prepared by manually breaking a pellet into two parts. Care was taken to replicate the way each pellet was broken and that it took place in the same region. A tiny notch was cut in the center of

the pellet using a razor blade, and the pellets were snapped into two. Care was taken to examine the fracture surface away from the notch. The two halves of the fractured pellet were attached to metal stubs using a conductive silver paste (Conductive silver paste plus, SPI Supplies, USA) that was carefully applied below and around the sample to prevent electric charging of the specimen. The upper surface was coated with a thin layer of gold using a sputter coater (Desk-1 sputter coater, Denton, USA). Electron micrographs were recorded using a scanning electron microscope (LEO EVO 40 SEM, Carl Zeiss, Germany) operated at 5–15 kV. Multiple samples were observed for each type of pellet and representative images were selected for each sample type.

2.8. *Pellet density*

The obtained pellets were stored at 50% relative humidity at 20 °C for one month. The unit density of the pellets was calculated by determination of the pellets weight and dimensions for at least 5 samples for pellets pressed at each condition.

3. Results and discussion

The torrefaction of spruce at 250, 275 and 300 °C resulted in three products of light brown, dark brown and black color as shown in Fig. 1. The color change is mainly attributed to chemical changes of the lignin, i.e. the formation of chromaphoric groups, mainly the increase of carbonyl groups [18]. The loss of dry matter (anhydrous weight loss) through volatilization during torrefaction was 25% at 250 °C, 34% at 275 °C and 53% at 300 °C.

The chemical analysis of the torrefied spruce shows a strong decrease of hemicellulose and cellulose content and is attributed to the thermal degradation of the carbohydrate polymers into volatile compounds and the evaporation of water and carbon dioxide [19]. Hemicelluloses are well known to undergo a two step thermal degradation where light volatiles i.e. mono and polysaccharides, followed by their catalytic degradation into CO and CO_2 [20]. Lignin undergoes depolymerization, mainly β-aryl-ether linkages and re-condensation reactions that lower its average molecular weight [6]. The relative increase in the acid-insoluble fraction with torrefaction temperature is likely due to both the volatilization of some of the carbohydrate fraction as well as the formation of acid-insoluble degradation products from them [21]. For example, cellulose can undergo scission reactions with aromatization and cross-linking, resulting in an insoluble solid [22].

The chemical changes occurring during torrefaction have been studied using ATR-FTIR-spectroscopy and the results are shown in Fig. 2.

The IR spectra of spruce and torrefied spruce at 250 and 275 °C have several features in common, while the spectra of spruce torrefied at 300 °C has very different characteristics. The broad band in the OH stretching vibration region at about 3600–3200 cm^{-1} is due to intra- and inter molecular hydrogen bonds and bands characteristic of crystalline cellulose [23–25]. The intensity of these bands decreases with increasing torrefaction temperature and has almost disappeared at 300 °C. This indicates that the torrefied material contains less water and hydrogen bonding sites due to the degradation of hemicelluloses and cellulose, which is supported by the chemical analysis data (Table 1). A lignin vibration can be found at about 1269 cm^{-1} (the aromatic C-O stretching of methoxyl and phenyl propane units) and at 1516 cm^{-1} and 1508 cm^{-1} (C=C aromatic ring vibrations) [23,26,27].These bands were present in the raw material and after treatment at 250 and 275 °C at same intensity but has disappeared after treatment at 300 °C, this suggests that the lignin, to large extent, has been degraded at this high temperature. Vibrations at about 1735 cm^{-1} are related to C=O stretching vibrations of the carboxylic acids of hemicelluloses (i.e. xyloglucan, arabinoglucuronoxylan and galactoglucomannan) [23,28]. This vibration is only present in the raw material. The torrefied samples show a band at about 1700 cm^{-1} which is attributed to a degradation product formed during the torrefaction. This indicates that hemicelluloses are degrading already at 250 °C, which agrees with the chemical analysis data (Table 1). The band at 1160 cm^{-1} is celluloses antisymmetric stretching of C–O–C glycosidic linkages [29] its intensity is strongest for untreated spruce and decreases with increasing torrefaction temperature. The band is not present at 300 °C, which indicates that most cellulose has degraded at this temperature.

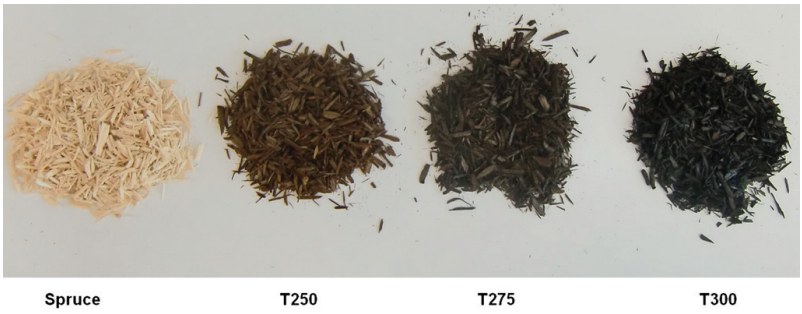

Fig. 1 – Color change during the torrefaction process. (For interpretation of the references to colour in this figure legend, the reader is referred to the web version of this article.)

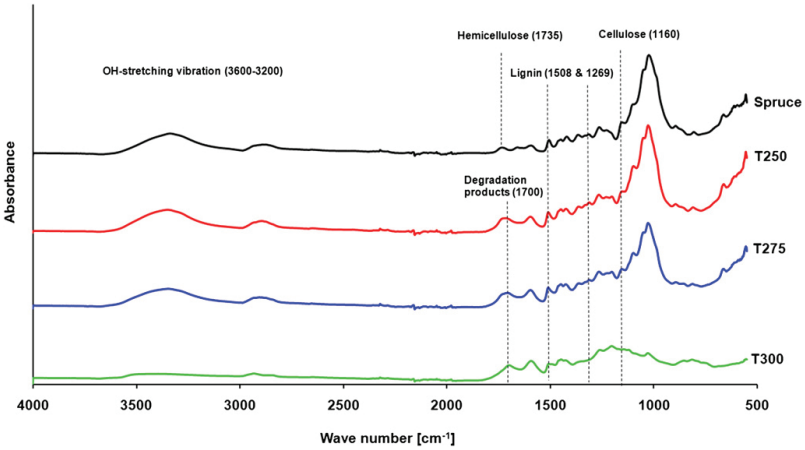

Fig. 2 – ATR-FTIR spectra of dry spruce and torrefied spruce at 250,275 and 300 °C. For better comparability, the scale of the y-axis was adjusted.

Torrefaction has been reported to have a strong effect on the mechanical stability and combustion properties of biomass [2–4].

Since the IR data has shown that most of the hydrogen-bonding hydroxyl groups have been removed during torrefaction, the moisture uptake of torrefied biomass is expected to decrease. The results presented in Fig. 3 show that the spruce absorbed twice as much water as it did after torrefaction at 250 °C. The ability to absorb water decreased further after the 275 and 300 °C treatment.

There are three different types of bound water in wood [30]. *Non-freezing bound water* is specifically bound to the hydroxyl groups of the wood polymers, especially the hemicelluloses. *Freezing bound water* is loosely bound to hydroxyl groups organized in clusters and can be found at high humidity in nanovoids and on the wall lining of macro- and microvoids. *Free water* is held in macro- and microvoids and bound by capillary forces but not to specific sorption sites. Since hemicelluloses are degraded during the heat treatment and most hydroxyl groups are removed, it is likely that water in torrefied wood is mainly bound as free water in macro- and micro-sized voids where it is held in place by capillary forces. This supports the observation, made during this study, that torrefied wood reaches equilibrium moisture content much faster than untreated wood.

The differences in composition and water content have also a strong effect on the pelletizing properties for spruce and the torrefied spruce. The pelletizing pressure in the press channel of the pellet mill (P_x) is a crucial parameter in pelletizing processes in terms of process energy consumption and pellet quality [15,31].

P_x increases drastically when comparing spruce and torrefied spruce (Fig. 4). This increase is most likely attributed to the lack of water and low hemicelluloses content in the torrefied spruce. Water acts as a plasticizer, lowering the

Table 1 – Composition of spruce and spruce torrefied at 250 °C (T250), 275 °C (T275) and 300 °C (T300) in percentage of total dry matter (average of two replicates).

	Cellulose	Hemicellulose	Acid insoluble fraction	Ash
Norway Spruce	43.7	23.3	28.9[a]	0.1
T250	43.6	6.6	43.2	0.1
T275	32.7	0.7	62.2	0.3
T300	0.2	0.0	99.0	0.6

a In case of spruce the acid insoluble fraction is defined as Klasson lignin content.

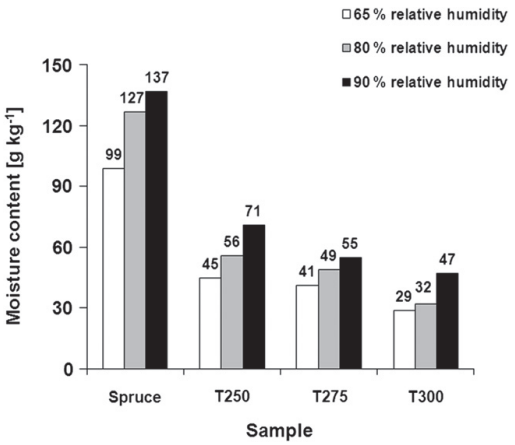

Fig. 3 – Moisture content of spruce and torrefied spruce after three weeks storage at 27 °C and 65, 80 and 90% relative humidity.

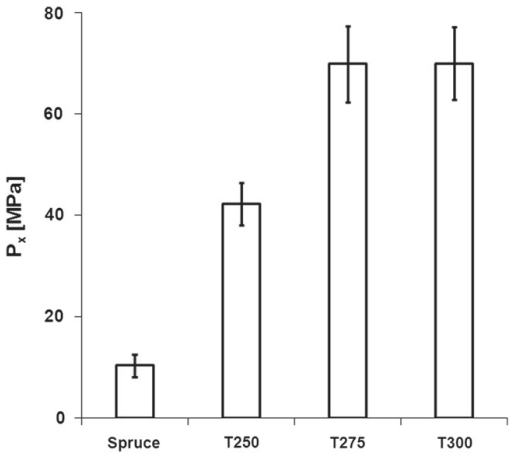

Fig. 4 – Pressure (P_x) during the pelletization of spruce and torrefied spruce.

softening temperature of the wood polymers. In nature, hemicelluloses bind lignin and cellulose fibrils and provides flexibility in the plant cell wall [32]. Their degradation embrittles wood, making it easier to comminute into small particles [4,33]. The degradation of the hemicelluloses, cellulose and the lignin are likely to affect important pelletizing parameters such as the friction coefficient and Poisson ratio which are directly correlated to P_x [15].

It is likely that extractives are removed during the torrefaction process. Extractives have been shown to play an important role during the pelletizing process [12] and are likely to act as lubricant lowering the friction in the press channel.

The pellets were very different in their quality (Fig. 5). No pellets could be made from spruce torrefied at 300 °C and even at 275 °C the pellets exhibits many defects. The pellet length (after one month storage) increased with an increasing degree of torrefaction from 19.3 ± 0.3 mm for spruce pellets to 23.9 ± 1.1 mm for spruce torrefied at 250 °C and 28.5 ± 1.2 mm for spruce torrefied at 275 °C. The unit density decreased with an increasing torrefaction temperature from 1090 ± 19 kg m^{-3} (untreated spruce) to 832 ± 39 kg m^{-3} for pellets made from spruce torrefied at 250 °C and to 698 ± 30 kg m^{-3} for pellets made from material torrefied at 275 °C. This attributes to a spring-back effect and is a sign of poor adhesion between the particles [34].

Fig. 6 shows a strong decrease in pellet compression strength as a result of torrefaction. Pellets made from T300 were too weak to be tested. Yildiz et al. [33] have tested the compression strength of spruce that had been heat treated between 130 and 200 °C for 2–10 h. They found that the compression strength of their samples decreased both with treatment time and temperature and concluded that the strength loss is connected to the degradation of hemicelluloses.

In an earlier work [12], the bonding and failure mechanisms in fuel pellets made from spruce, beech and straw was studied by means of fracture surface analysis using SEM. This method was applied to pellets made from torrefied spruce (Fig. 7).

The low and medium magnification images show more inter-particle gaps and voids with increasing torrefaction temperature, indicating poor adhesion between adjacent particles and/or spring back effects [12,34,35]. Images taken at higher magnification, (Fig. 7c,f and i) provide a deeper insight into the bonding and failure mechanisms of the pellets. The failure surface of spruce pellet (Fig. 7c) indicates a cohesive failure with a high energy absorption. Fiber ends and particles are sticking out of the surface and few voids are found. This suggests that lignin and hemicelluloses have exceeded their glass transition temperatures at the pelletization conditions (e.g., moisture content, temperature and pressure), allowing them sufficient mobility to flow into cracks and crevices and establish solid bridges between adjacent particles. The pellets from torrefied wood, T250 (Fig. 7f) and T275 (Fig. 7i), have flatter failure surfaces than those of the spruce pellets, indicating a minimized polymeric flow. The amount of hydrogen binding sites decreases gradually with the torrefaction temperature and the torrefied biomass contains less moisture, thus both hydrogen bonding between polymer chains of adjacent particles and a polymeric flow of the lignin and hemicelluloses (forming solid bridges) can be assumed less likely to occur. According to Rumpf [36] who has studied the binding mechanisms in biomass granules and agglomerates it is likely that Van der Waals forces and fiber interlocking remain as the major forces keeping a pellet together. Since these forces are weak compared to covalent bonds and hydrogen bonding this could be an explanation both for the observed spring back

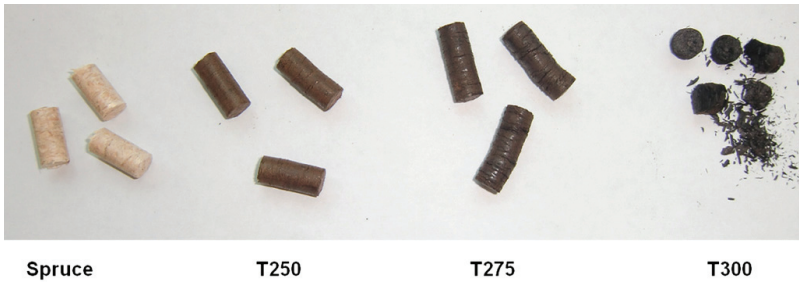

Fig. 5 – Pellets made from spruce and torrefied spruce. From left to right: Spruce and torrefied spruce at 250, 275 and 300 °C.

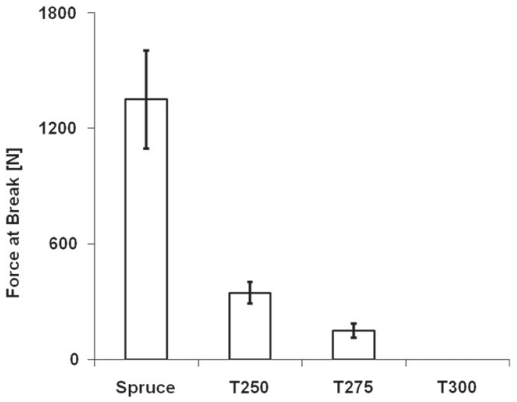

Fig. 6 – Compression strength of spruce and torrefied spruce pellets.

effect (Fig. 5) as well as for the low compression strength of pellets made from torrefied spruce (Fig. 6).

It is well known that a combination of torrefaction time and temperature determine the degree of polymer degradation and the mechanical properties of heat treated wood [33,35]. The mechanical properties of a pellet have been shown to depend on the one hand on the biomass composition i.e. moisture and extractives content and on the other hand on the processing conditions i.e. temperature and pressure [12,37-40]. Since hemicelluloses and lignin are both subject to thermal degradation during torrefaction and the amount of available hydrogen bonding sites is reduced, it can be expected that the pellet strength of torrefied pellets is lower compared to pellets made from untreated spruce. Furthermore, the moisture content of the torrefied wood is lower which results in an increase in the glass transition temperatures of the remaining hemicelluloses and lignin [41]. This may reduce the interdiffusion of the wood polymers between adjacent particles in a pellet and thus the formation of solid bridges between them. The resulting pellets are brittle and less stable than pellets made from untreated wood. To increase the mechanical properties of torrefied biomass pellets it is necessary to establish a better bonding between the particles. One possibility is to add an additive that compensates for the lost bonding sites and ideally binds between the hydrophobic surface of the biomass and remaining polar groups on the wood polymer surface such as short fatty acids or mono glycerides. Another option could be to adjust the torrefaction parameters so that less of the wood polymers are degraded to

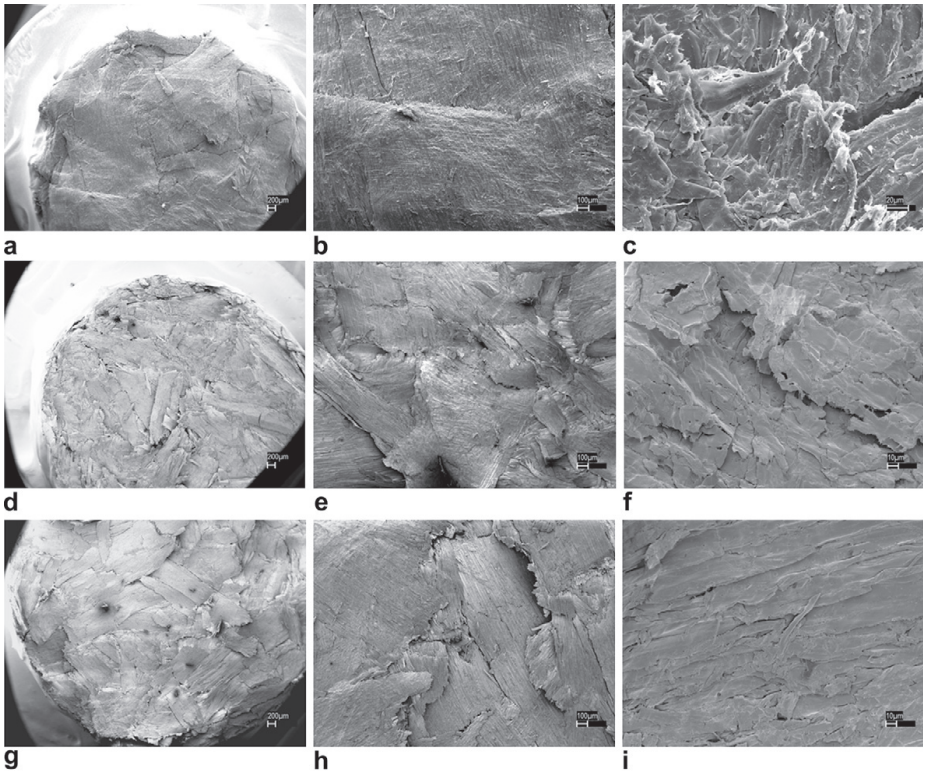

Fig. 7 – Low, medium, and high magnification, respectively, of a pellet fracture surface for spruce (a–c), spruce torrefied at 250 °C (d–f) and spruce torrefied at 275 °C (g–i).

ensure sufficient hydroxyl groups on the wood polymer chains to form strong inter particle bonds. This could be achieved by shorter treatment time, lower torrefaction temperature, different torrefaction medium (e.g. wet torrefaction) or surface increase (e.g. steam explosion conditions).

The development of a combined torrefaction pelletization concept requires that both processes are adjusted to each other. An interesting recent work reports improved mechanical stability and moisture resistance for pellets made from steam exploded Douglas fir [14] performed at temperatures between 200 and 220 °C for 5–10 min. The water vapor grants a fast heat transfer and the short treatment time and relatively low temperature (compared to our study) preserves sufficient amounts of amorphous polymers that can be plasticized during pelletization and form solid inter-particle bridges.

Future, studies have to investigate the optimal torrefaction conditions to obtain a raw material that both has the beneficial properties of torrefied biomass and also can be pelletized into stable pellets. Furthermore the impact of raw material composition on the torrefaction and pelletizing process has to be investigated.

4. Conclusions

The torrefaction of biomass degrades hemicelluloses, cellulose and lignin and removes moisture from the material. Both effects have a strong effect on the pelletizing properties of the biomass. The friction in the press channel of a pellet mill increases, resulting in high pelletizing pressures which increase the energy uptake of the mill and might result in a decrease of capacity and in worst case an overheating (risk of fire) of a blockage of the mills press channels.

Torrefaction breaks down the carbohydrates and therefore the ability to establish hydrogen bonds between polymer chains of adjacent particles can be assumed to be strongly reduced. The lack of moisture increases the glass transition temperature of the remaining carbohydrate polymers and restricts the ability of polymeric flow and the establishment of solid bridges between particles. There are several options to overcome this lack of bonding capacity. For example, an additive with a high bonding capacity could be introduced after the torrefaction process that would compensate for the lost hydrogen bonding sites due to torrefaction.

Acknowledgments

The present study was conducted under the framework of the Danish Energy Agency's EFP project: "Advanced understanding of biomass pelletization" ENS-33033-0227. The authors wish to thank Vattenfall Nordic A/S, DONG Energy A/S and the Danish Energy Agency for project funding. The USDA-Forest Products Laboratory in Madison, Wisconsin is thanked for its hospitality and the provision of laboratory space and equipment for this study. Fred Mat, Dan Yelle and Tom Kuster are thanked for help with chemical analysis, the compression testing and scanning electron microscopy. Charles Frihart is greatly acknowledged for his comments and suggestions when planning this study. Tobias Thomsen is thanked for preparation of the torrefied wood samples and Søren Barsberg for help with the infrared spectra.

REFERENCES

[1] Lesage D, Van de Graf T, Westphal K. Global energy governance in a multipolar world. London: Ashgate; 2010. 235 p.
[2] Pentananunt R, Rahman A, Bhattacharya SC. Upgrading of biomass by means of torrefaction. Energy 1990;15(12): 1175–9.
[3] Prins MJ, Ptasinski KJ, Janssen FJJG. Torrefaction of wood - part 1. Weight loss kinetics. J Anal Appl Pyrolysis 2006;77(1): 28–34.
[4] Arias B, Pevida C, Fermoso J, Plaza MG, Rubiera F, Pis JJ. Influence of torrefaction on the grindability and reactivity of woody biomass. Fuel Process Technol 2008;89(2):169–75.
[5] Pimchuai A, Dutta A, Basu P. Torrefaction of agriculture residue to enhance combustible properties. Energ Fuel 2010; 24:4638–45.
[6] Brosse N, El Hage R, Chaouch M, Petrissans M, Dumarcay S, Gerardin P. Investigation of the chemical modifications of beech wood lignin during heat treatment. Polym Degrad Stabil 2010;95(9):1721–6.
[7] Prins MJ, Ptasinski KJ, Janssen F. More efficient biomass gasification via torrefaction. Energy 2006;31(15):3458–70.
[8] Uslu A, Faaij APC, Bergman PCA. Pre-treatment technologies, and their effect on international bioenergy supply chain logistics. Techno-economic evaluation of torrefaction, fast pyrolysis and pelletization. Energy 2008;33(8):1206–23.
[9] Blakeslee TR. Fuel free!: living well without fossil fuels. Seattle: Createspace; 2009. 152 pp.
[10] Pirraglia A, Ronalds G, Daniel S. Wood pellets: an expanding market opportunity. Biomass Mag 2010;6:68–75.
[11] Sultana A, Kumar A, Harfield D. Development of agri-pellet production cost and optimum size. Bioresour Technol 2010; 101(14):5609–21.
[12] Stelte W, Holm JK, Sanadi AR, Barsberg S, Ahrenfeldt J, Henriksen UB. A study of bonding and failure mechanisms in fuel pellets from different biomass resources. Biomass Bioenerg 2011;35(2):910–8.
[13] Nielsen NPK, Gardner DJ, Poulsen T, Felby C. Importance of temperature, moisture content, and species for the conversion process of wood into fuel pellets. Wood Fiber Sci 2009;41(4):414–25.
[14] Lam PS, Sokhansanj S, Bi X, Lim J, Melin S. Energy input and quality of pellets made from steam-exploded douglas fir (pseudotsuga menziesii). Energy Fuels 2011;25(4): 1521–8.
[15] Gilbert P, Ryu C, Sharifi V, Swithenbank J. Effect of process parameters on pelletization of herbaceous crops. Fuel 2009; 88(8):1491–7.
[16] Davis MW. A rapid modified method for compositional carbohydrate analysis of lignocellulosics by high pH anion-exchange chromatography with pulsed amperometric detection (HPAEC/PAD). J Wood Chem Technol 1998;18(2): 235–52.
[17] Holm JK, Henriksen UB, Hustad JE, Sorensen LH. Toward an understanding of controlling parameters in softwood and hardwood pellets production. Energy Fuel 2006;20(6): 2686–94.
[18] Gonzalez-Pena MM, Hale MDC. Colour in thermally modified wood of beech, Norway spruce and Scots pine. Part 1: colour

evolution and colour changes. Holzforschung 2009;63(4): 385–93.
[19] Gonzalez-Pena MM, Curling SF, Hale MDC. On the effect of heat on the chemical composition and dimensions of thermally-modified wood. Polym Degrad Stabil 2009;94(12): 2184–93.
[20] Gaur S, Reed TB. Thermal data for natural and synthetic materials. New York: Marcel Dekker; 1998.
[21] Yan W, Acharjee TC, Coronella CJ, Vasquez VR. Thermal pretreatment of lignocellulosic biomass. Environ Prog Sustain Energ 2009;28(3):435–40.
[22] Agrawal RK. Kinetics of reactions involved in pyrolysis of cellulose. 1. The 3-reaction model. Can J Chem Eng 1988; 66(3):403–12.
[23] Stevanic JS, Salmen L. Characterizing wood polymers in the primary cell wall of Norway spruce (Picea abies (L.) Karst.) using dynamic FT-IR spectroscopy. Cellulose 2008;15(2): 285–95.
[24] Fengel D. Influence of water on the valency range in deconvoluted FTIR spectra of cellulose. Holzforschung 1993; 47(2):103–8.
[25] Sugiyama J, Persson J, Chanzy H. Combined infrared and electron-diffraction study of the polymorphism of native cellulose. Macromolecules 1991;24(9):2461–6.
[26] Akerholm M, Salmen L. The oriented structure of lignin and its viscoelastic properties studied by static and dynamic FT-IR spectroscopy. Holzforschung 2003;57(5):459–65.
[27] Agarwal UP, Ralph SA. FT-Raman spectroscopy of wood: Identifying contributions of lignin and carbohydrate polymers in the spectrum of black spruce (Picea mariana). Appl Spectrosc 1997;51(11):1648–55.
[28] Gierlinger N, Goswami L, Schmidt M, Burgert I, Coutand C, Rogge T, et al. In situ FT-IR microscopic study on enzymatic treatment of poplar wood cross-sections. Biomacromolecules 2008;9(8):2194–201.
[29] Pandey KK. A study of chemical structure of soft and hardwood and wood polymers by FTIR spectroscopy. J Appl Polym Sci 1999;71(12):1969–75.
[30] Berthold J, Desbrieres J, Rinaudo M, Salmen L. Types of adsorbed water in relation to the ionic groups and their counterions for some cellulose derivatives. Polymer 1994; 35(26):5729–36.
[31] Holm JK, Henriksen UB, Wand K, Hustad JE, Posselt D. Experimental verification of novel pellet model using a single pelleter unit. Energy Fuel 2007;21(4):2446–9.
[32] Jones L, Milne JL, Ashford D, McQueen-Mason SJ. Cell wall arabinan is essential for guard cell function. P Natl Acad Sci USA 2003;100(20):11783–8.
[33] Yildiz S, Gezer ED, Yildiz UC. Mechanical and chemical behavior of spruce wood modified by heat. Build Environ 2006;41(12):1762–6.
[34] Kaliyan N, Morey RV. Natural binders and solid bridge type binding mechanisms in briquettes and pellets made from corn stover and switchgrass. Bioresour Technol 2010;101(3): 1082–90.
[35] Odogherty MJ, Wheeler JA. Compression of straw to high-densities in close cylindrical dies. J Agr Eng Res 1984;29(1): 61–72.
[36] Rumpf H. The strength of granules and agglomerates. In: Knepper WA, editor. Agglomeration. New York: John Wiley and Sons; 1962. p. 379.
[37] Shi JL, Kocaefe D, Zhang J. Mechanical behaviour of quebec wood species heat-treated using thermowood process. Holz Roh Werkst 2007;65(4):255–9.
[38] Kaliyan N, Morey RV. Factors affecting strength and durability of densified biomass products. Biomass Bioenerg 2009;33(3):337–59.
[39] Larsson SH, Thyrel M, Geladi P, Lestander TA. High quality biofuel pellet production from pre-compacted low density raw materials. Bioresour Technol 2008;99(15):7176–82.
[40] Nielsen NPK, Gardner DJ, Felby C. Effect of extractives and storage on the pelletizing process of sawdust. Fuel 2010;89(1): 94–8.
[41] Stelte W, Clemons C, Holm JK, Ahrenfeldt J, Henriksen UB, Sanadi A. Thermal transitions of the amorphous polymers in wheat straw. Ind Crop Prod 2011;34(1):1053–6.

PAPER IV

Quality effects caused by torrefaction of pellets made from Scots pine

Lei Shang, Niels Peter K. Nielsen, Jonas Dahl, Wolfgang Stelte, Jesper Ahrenfeldt, Jens Kai Holm, Tobias Thomsen, Ulrik B. Henriksen

Reprinted from *Fuel Processing Technology* (2012), 101, 23-28,

Fuel Processing Technology 101 (2012) 23–28

Contents lists available at SciVerse ScienceDirect

Fuel Processing Technology

journal homepage: www.elsevier.com/locate/fuproc

Quality effects caused by torrefaction of pellets made from Scots pine

Lei Shang [a,*], Niels Peter K. Nielsen [c], Jonas Dahl [c], Wolfgang Stelte [a], Jesper Ahrenfeldt [a], Jens Kai Holm [b], Tobias Thomsen [a], Ulrik B. Henriksen [a]

[a] Department of Chemical and Biochemical Engineering, Technical University of Denmark, 2800 Kgs. Lyngby, Denmark
[b] Chemical Engineering, DONG Energy Power A/S, Nesa Alle 1, 2820 Gentofte, Denmark
[c] Renewable Energy and Transport, Danish Technological Institute, Gregersensvej 3, 2630 Taastrup, Denmark

ARTICLE INFO

Article history:
Received 19 January 2012
Received in revised form 9 March 2012
Accepted 20 March 2012
Available online 25 April 2012

Keywords:
Wood pellets
Torrefaction
Durability
Strength
Grinding

ABSTRACT

The purpose of the study was to investigate the influence of torrefaction on the quality of Scots pine pellets. Pellet samples were torrefied at 230, 250 and 270 °C for 1 h in nitrogen atmosphere. Higher heating value (HHV) was increased from 18.37 MJ kg^{-1} to 24.34 MJ kg^{-1}. The energy to crush a pellet by mechanical compression was determined using a material tester and results showed a rapid decrease before torrefaction temperature reached 250 °C. Slightly further decrease was observed when increasing the temperature up to 270 °C. The strength loss was confirmed by determining the energy required for grinding the pellet samples in a bench scale disc mill. Particle size distribution measurements after grinding indicated a significant increase of small particles (diameter<ca. 1 mm) for torrefied pellets at a torrefaction temperature of 230 °C and further increase of temperature resulted in steep decrease of large particles (diameter>ca. 2 mm). To further analyze the effect on strength, the mechanical durability of pellets was tested according to wood pellet standards, EN 15210-1. The results have shown a good correlation between pellet durability and compression strength, and indicated that the pellet durability can be estimated based on compression strength data of about 25 pellets.

1. Introduction

Wood pellets are the only solid biofuels which have a global market. The global production of fuel pellets from biomass was estimated to be about 13 million tons in 2009 with strong growth rates, and pellet consumption in Europe is expected to reach 50 million tons per year by 2020 [1]. Since pellets are very suitable for long-distance transport, the pellet price is sensitive to the transportation cost. In case of Canada, data from 2004 has shown that local transportation, storage and oversea shipment (for example to Rotterdam harbor) cost 3.2 € GJ^{-1}, which is more than half of the market price of pellets (5.9 € GJ^{-1}) [2]. As a consequence, high energy density combined with easy handling properties, i.e. low dust formation, is desired when producing pellets. The energy density of wood pellets can be increased by means of torrefaction, which is a mild temperature (200-300 °C) pretreatment process of biomass in an inert atmosphere [3]. During the process, the biomass looses water and a proportion of its volatile content, becoming dry, brittle and darker in color. Torrefied biomass is more hydrophobic, has a higher calorific value and is easier to grind when compared to untreated biomass [4,5]. Torrefaction can reduce the energy consumption required for size reduction up to 70–90% compared to untreated biomass [5]. Nevertheless, it has been shown earlier that torrefaction can lower the pellets mechanical properties, which might result in problems during transportation and handling. Therefore it is important to investigate the changes of mechanical properties induced by torrefaction at different temperatures. European standards such as the ENPlus set high demands for the pellets mechanical properties i.e. durability and dust formation. According to a defined test protocol the pellet durability may not fall below 97.5% [6], meaning that less than 2.5% dust may be formed during the test. Several studies [5,7–10] have been made investigating the pelletizing properties of torrefied biomass. Two studies made by Stelte et al. [10] and Gilbert et al. [9] indicate that pellet production from torrefied biomass can be challenging and can result in problems during processing and pellet quality. It was shown that torrefaction of biomass increases the friction in the press channel of a pellet mill and that the manufactured pellets are more brittle and less strong compared to conventional pellets. However, no studies have been reported so far for pellets that are torrefied subsequent to pelletization.

Wood pellets made from untreated biomass have high mechanical properties which arise from the thermal softening of lignin, its subsequent flow and the formation of what can be referred to as an "entanglement network of molten polymers" [11]. The interpenetration of lignin polymer chains results in strong bonds upon cooling and solidification of the pellet. The idea behind the present study was to investigate whether these strong bonds outlast the torrefaction process and whether this might be a feasible method to produce pellets of a

* Corresponding author. Tel.: +45 2132 4979; fax: +45 4677 4109.
E-mail address: lesh@kt.dtu.dk (L. Shang).

0378-3820/$ – see front matter © 2012 Elsevier B.V. All rights reserved.
doi:10.1016/j.fuproc.2012.03.013

high mechanical stability and high energy density. In the present work, Scots pine pellets were torrefied at 230, 250, and 270 °C with residence time of 1 hour under nitrogen atmosphere. Higher heating value (HHV) was determined using a bomb calorimeter. The mechanical properties were determined by compression testing, milling in a bench scale disc mill and durability testing according to a standard protocol.

2. Material and methods

2.1. Torrefaction of pellets

Scots pine (*Pinus sylvestris*, L.) pellets, 6 mm in diameter were supplied by a commercial pellet factory. Samples were dried in the oven at 104 °C for 24 h, and subsequently placed in an air tight metal reactor (15×31×10 cm) with a gas in and outlet. The reactor was placed in an oven (type S 90, Lyngbyovnen, Denmark) and heated up to the desired torrefaction temperature. The heating rate programmed for the oven was 6 °C min^{-1}. Nitrogen flow through the reactor was adjusted to 0.5 L min^{-1} to create an inert atmosphere. A thermocouple placed in the middle of the reactor was used for temperature control of the oven. The residence time of the torrefaction process was started when the thermocouple inside the reactor has reached the set temperature. After one hour at the desired temperature the oven was shut down and the reactor was allowed to cool down. Torrefaction was carried out at 230, 250, and 270 °C with residence time of 1 hour. The total weight loss (TWL, %) was determined based on Eq. (1), where m_b is the mass (kg) of original sample before drying and m_a is the mass (kg) of residues after torrefaction.

$$TWL = 100 \times \left(1 - \frac{m_a}{m_b}\right) \quad (1)$$

2.2. Heating value

A bomb calorimeter (6300, Parr Instrument Company, USA) was used to determine the higher heating value (HHV, MJ kg^{-1}). Initially, the calorimeter was calibrated using benzoic acid tablets. Samples were prepared by grinding in a commercial coffee grinder (Kenia, Mahlkönig, Germany); 1 g of material was placed in the crucible and fired inside the bomb calorimeter using an ignition wire in the presence of oxygen. The measurements were repeated 2 times. The determination of energy loss was based on Eq. (2).

$$Energyloss = \frac{m_b \times HHV_{ref} - m_a \times HHV}{m_b \times HHV_{ref}} \times 100 = \left[1 - \frac{HHV}{HHV_{ref}} \times \left(1 - \frac{TWL}{100}\right)\right] \times 100 \quad (2)$$

Where HHV_{ref} is the heating value of untreated pellets in the unit of MJ kg^{-1}.

Table 1
Mass fraction of hemicelluloses, cellulose and lignin in oven dried pellets and pellets torrefied at 300 °C (dry and ash free basis).

	Lignin	Cellulose	Hemicellulose	Ash
Oven dried wood pellet	32.5	39.5	20.1	0.7
Wood pellet torrefied at 300°C	100.7	0.1	0.0	0.9

2.3. Biomass composition

The content of lignin, cellulose and hemicelluloses was determined according to the ASTM standard E 1758-01 [12], and Kaar et al. [13]. A representative sample smaller than 1 mm was first made soluble in strong acid (72% H_2SO_4) at room temperature; and then it was hydrolyzed in dilute acid (4% H_2SO_4) at 121 °C by autoclavation. Hemicelluloses and cellulose contents were determined by HPLC analysis of liberated sugar monomers. Klason lignin content was determined based on the filter cake (the residues from the strong acid hydrolysis), minus the ash content of the filter cake determined by 550 °C incinerating for 3 h.

2.4. Pellet compression energy

Pellets were tested individually by compressing between two smooth metal platens in a material tester (AG250kNx, Shimadzu, Japan). The pellet was laid horizontally on the lower platen, and the upper platen was then moved down to compress the pellet. The upper platen was mounted on a load cell, and run with a compression speed of 25 mm min^{-1}. The upper platen traveled to 4.5 mm above the lower platen before returning to its initial position. As the pellet diameter was 6 mm it means that the pellets were compressed 1.5 mm, which caused an irreversible deformation (crushing). To quantify the pellet strength, the force and the corresponding position (displacement) of the upper plate was logged (10 ms logging interval). The data was used to calculate the energy required for compressing the pellet. 25 pellets were used for each sample. Prior to compressing, the length and pellet mass were determined.

2.5. Grinding energy

Energy consumption for grinding pellets was determined using a commercial coffee grinder (Kenia, Mahlkönig, Germany) with a screw conveyer feeding system and a disc grinding system, as shown in Fig. 1. The distance between the two separate discs could be adjusted manually and was set to maximum for all tests. The power consumption of the coffee grinder in operation was determined using a wattmeter (THII, Denmark). The meter was connected to a data logging system (NI USB-6009, National Instruments, USA).

Approximately 200 g pellets were manually fed into the feed hopper while the grinder was running. The time required to grind the pellet and the energy used by the grinder were recorded and used for calculating the specific energy required for grinding. The idling energy was measured before the material was introduced. The specific energy required for grinding was determined by integrating the area under the power

Fig. 1. Picture of the inside of the coffee grinder.

Fig. 2. Images of untreated Scots pine pellets and pellets torrefied at different temperatures for 1 h.

demand curve for the total time required to grind the sample minus the idling power [14,15]. The energy reduction during grinding was calculated according to Eq. (3):

$$energyreduction = \frac{\Delta E}{E_{ref}} \times 100 = \frac{E_{ref} - E_{samp}}{E_{ref}} \times 100 \quad (3)$$

where E_{ref} is the specific energy ($J\,g^{-1}$) required for grinding untreated pellets, E_{samp} is the specific energy ($J\,g^{-1}$) required for grinding pellets torrefied at different temperatures.

Particle size distribution was calculated based on sieve separation of the obtained biomass fraction using a sieve shaker (Retsch, Germany) with nine different sieves (mesh size of 75, 125, 250, 500, 1000, 1400, 2000, 3150, 5000 μm). The sieve shaker was run for 40 minutes and the weight of the individual fractions was determined subsequently.

2.6. Standard durability test

The pellet durability was determined according to the EN 15210-1 standard [16], also known as tumbling can test, where a defined mass of pellets is filled into a metal container and exposed to impacts by rotating the containers for a defined period of time. The amount of fines formed during this test, is used to quantify the pellet durability. Prior to the testing, pellets were sieved through a 3.15 mm screen (round holes) to remove fines and dust from the samples. The amount of dust is referred to as 'dust in sample', and quantified as the difference in weight of the pellet sample before and after sieving, in percent of the sample before sieving. 500 g dust free pellets were then loaded into the chamber of the standard durability tester and exposed to 500 rotations within a time interval of 10 min. The amount of fines formed during the test was determined by sieving the treated sample again through the 3.15 mm screen and determination of the weight difference before and after sieving. The durability value was calculated as the mass fraction of dust free pellets after the treatment in the pellets that was loaded into the tester.

3. Results and discussion

3.1. Torrefaction

The composition of the Scots pine pellets used in this study is listed in Table 1. Images of untreated pellets (noted as 'reference') and pellets torrefied at different temperatures are shown in Fig. 2. The pellets became darker with an increasing torrefaction temperature and the pellet surface has lost its shine and smoothness, especially for the pellets torrefied at 270 °C. The color change of thermally modified wood was studied by González-Peña and Hale [17], and they concluded that color change is linked to changes in the acid-insoluble lignin substance rather than in the carbohydrate fraction.

Results for the HHV, ratio between HHV of reference pellets and torrefied pellets, TWL, corresponding energy loss are listed in Table 2. The results indicate that in case of weight based charging of transportation fees for pellets about 10–25% of the cost can be saved by transporting the same amount of heating value of torrefied pellets compared to regular wood pellets. To account for the correlation between energy loss and weight loss, a second-order polynomial regression has been made and is shown in Fig. 3. A good correlation was found between energy loss and weight loss. By increasing torrefaction temperature from 250 to 270 °C, both weight loss and energy loss increased sharply. Based on our previous studies of torrefaction effects on spruce [10] and wheat straw [18] , this is mainly due to the extensive thermal degradation of hemicelluloses and partial degradation of cellulose at elevated temperatures. Thus, in order to preserve energy in the pellets, a torrefaction temperature of about 250 °C might be a critical upper limit.

Table 2
Data of higher heating value (HHV), total weight loss (TWL on wet basis), energy loss, and ratio between HHV of untreated pellets and pellets torrefied at different temperatures for 1 hour.

Temperature	HHV, MJ kg^{-1}	TWL[a] (w.b.), %	Energy loss, %	HHV_{ref}/HHV
Reference	18.37 (0.01)[b]	0	0 (0.05)	1
230 °C	20.42 (0.02)	14.8	5.30 (0.10)	0.90
250 °C	21.35 (0.08)	21.3	8.54 (0.35)	0.86
270 °C	24.34 (0.03)	41.9	23.02 (0.09)	0.75

[a] Pellet samples had a moisture content of 9.8% (w.b.) determined by drying at 104 °C for 24 hours.
[b] Number enclosed in parenthesis are standard errors of the mean values listed.

3.2. Compression energy

Pellet before and after compression in the universal materials test are illustrated in Fig. 4.

Fig. 5 shows force/displacement curves for compression of 25 reference pellets. The plots illustrate the position (Displacement, mm) of the compression platen from 2 mm above the pellet to 5.5 mm, from where the platen returned to its starting point. It can be seen that the platen meets the pellet at position 4 mm, where the force increased as the pellet was crushed. The energy (in J) required for compressing the pellets to 75% of the initial diameter (4.5 mm vs. 6 mm) was calculated based on the area under the plots. Since the pellets had different lengths, the compression energy of the distinct pellets was different. To account for this, linear regressions of strength (in J) vs. length were made (see Fig. 6). It can be seen that the longer the pellet, the higher the energy required for compressing. The regression parameters were used to predict the strength of a model pellet with the length of

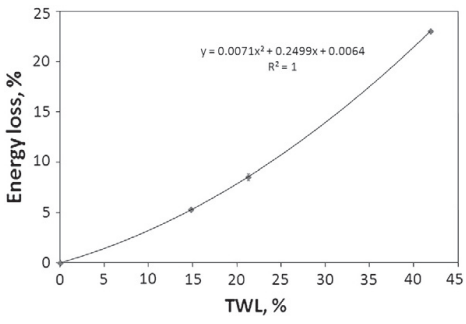

Fig. 3. Energy loss vs. total weight loss (TWL) during drying and torrefaction of pellets torrefied at different temperatures.

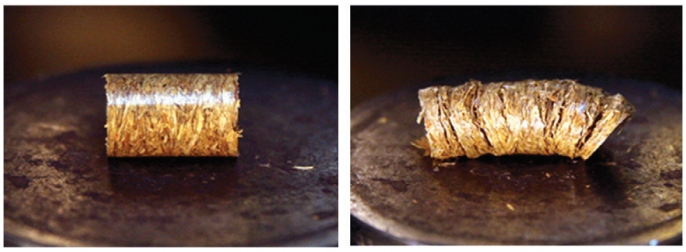

Fig. 4. Pellet before and after compression in the universal material machine.

15 mm. This strength of compressing single pellet was further converted to weight based strength by the mass. Results are presented in Table 3.

3.3. Grinding energy

Fig. 7 shows the relationship between the specific energy requirement of grinding pellets and the total weight loss (TWL). Results of the single pellet compression strength are also presented in this figure. Both results show the similar trend of energy decreasing when the TWL increases. Fig. 8 plots energy reduction against pellets' energy loss, which is listed in Table 2. It can be seen that about 73% of the energy used in the grinding process can be saved by losing 9% of the pellets' heating value due to torrefaction, but further increase of the pellets' energy loss does not reduce the grinding energy a lot. However, the absolute value of the thermal energy lost from the pellets ($1653\ J\ g^{-1}$) is much higher than the electrical energy saved during grinding ($19.6\ J\ g^{-1}$) in this case. The fraction of grinding energy saved due to torrefaction in torrefied pellets' HHV was also plotted in Fig. 8 for different torrefaction temperatures. Since the energy consumption during grinding depends on the end particle size, a higher absolute value of energy saving can be expected with decreasing particle size, when fine grinding is chosen.

Mass fractions of the particles retained on each test sieve in relation to the geometric mean diameter of the particles on each sieve are shown in Fig. 9. An obvious increase (8% compared to reference sample) of small particles (about 1 mm) occurs already at a torrefaction temperature of 230 °C. Further increase of torrefaction temperature (from 230 to 270 °C) resulted only in slight increase of small particles (+ 5%), but steep decrease of big particles (- 10%).

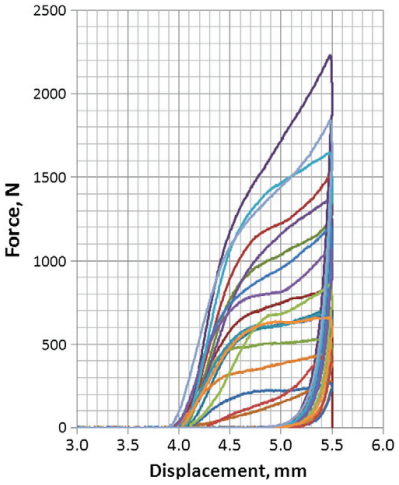

Fig. 5. Plot illustrating the compression strength analysis of 25 reference pellets.

3.4. Standard durability test

The results from the standardized mechanical durability test are presented in Fig. 10. It can be seen that the torrefaction resulted in pellets with more dusts and lower durability when exposed to mechanical loads. And this effect increases with increasing torrefaction temperature.

Fig. 11 illustrates the correlation between the durability and the compression energy. It is seen that an exponential function fits the correlation well. This indicates that if the compression energy is known, a reasonable estimate for the durability can be made and vice versa. It must also be noted that the analysis was based on pellets with a diameter of 6 mm only, which means the diameter parameter has not been taken into account, and that the present parameters may not fit i.e. 8 mm pellet. However in this case, if pellets of 15 mm lengths have compression strength higher than 0.6 J ($1.53\ J\ g^{-1}$ pellet

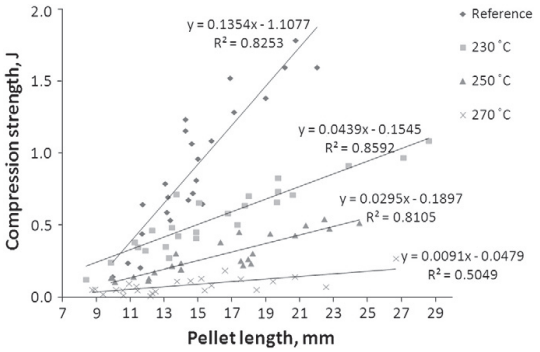

Fig. 6. Linear regressions of compression strength as y-axis (in J) vs. pellet length as x-axis (in mm).

Table 3
The compression strength of a model pellet (15 mm long) based on the linear regressions in Fig. 6.

Sample	Strength, J pellet^{-1}	Strength, J g-pellet^{-1}
Reference	0.92 (0.20)[a]	2.25 (0.50)
230 °C	0.50 (0.09)	1.34 (0.25)
250 °C	0.25 (0.06)	0.76 (0.19)
270 °C	0.09 (0.04)	0.35 (0.18)

[a] Number enclosed in parenthesis are standard errors of predicted strength from the regression parameters in Fig. 6.

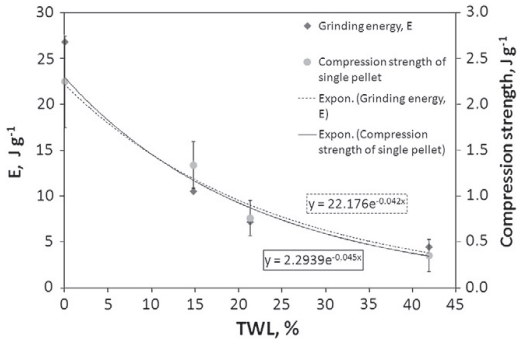

Fig. 7. The specific energy required for grinding pellets (E, J g^{-1}) and the compression strength of single 15-mm-long pellet (J g^{-1}) vs. total weight loss (TWL) of pellet samples after torrefaction.

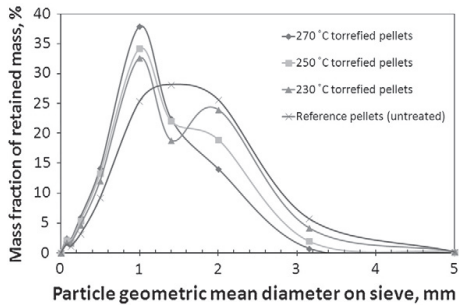

Fig. 9. Particle size distribution of fines after the energy consumption measurement.

according to Table 3), it is likely the batch from which they are taken has durability higher than 97.5%.

4. Conclusion and discussion

The study has shown that higher torrefaction temperature resulted in higher weight and energy loss. A steep increase of total weight loss (from 21% to 42%) and energy loss (from 9% to 23%) occurred when the torrefaction temperature was increased from 250 to 270 °C. In order to preserve energy in the pellet, torrefaction temperatures higher than 250 °C should be avoided. However, if shorter residence time is used in production, torrefaction temperature higher than 250 °C could be relevant.

Both single pellet compression energy and energy required for disc mill grinding showed a similar exponential decrease when TWL increases. Rapid decreases happened in the first 20% TWL; however reduction was less when TWL increased from 20% to 40%. The particle size distribution after disc mill grinding showed that an obvious increase of small particles with diameter of about 1 mm happened already at torrefaction temperature of 230 °C, whereas further increase of temperature resulted in only slight increase of small particles but extensive decrease of large particles with diameter of about 2 mm.

The pellet durability showed negative relationship with torrefaction temperature, and good correlation was shown among pellet durability, the compression strength measured in a universal materials tester, and the energy requirement for grinding. It means that compression strength of single pellet can be used as a product quality control method to predict the durability of the whole batch pellets and the energy use in grinding and vice versa.

In order to produce pellets (with diameter of 6 mm) with durability higher than 97.5% as required by ENPlus, compression strength of 0.6 joule per pellet with length of 15 mm (or 1.53 joule per gram pellet with length of 15 mm) is needed, and grinding energy of about 15.3 J g^{-1} is expected. At this condition, energy reduction in grinding compared with untreated pellets is 43% (11.6 J g^{-1}), and the energy loss due to the torrefaction of pellets is about 4% (730 J g^{-1} based on original mass). However, the higher heating value (HHV) is increased by about 1600 J g^{-1} from 18.4 MJ kg^{-1} for reference pellets to 20.0 MJ kg^{-1}, which corresponds to a torrefaction temperature of a bit lower than 230 °C with residence time of 1 h.

On the other hand a previous work [10] has shown that pellets pressed from torrefied spruce increase significantly in length after pelletization, which indicates worse quality of inter-particle bonding with correlation to higher torrefaction temperatures. The pellets produced in this study (put the torrefaction step after the pelletization step) exhibit better durability, no spring back effect or disintegration was observed for pellets even torrefied at 270 °C. Similar conclusions of low durability and low mass density were also drawn for pellets made from pine wood torrefied at 300 °C by Reza et al. [19] in a recent study, although they succeeded making mechanically durable pellets from hydrothermally carbonized pine wood without additives. However, there is lack of results for pellets made from biomass torrefied at temperatures below 250 °C. Furthermore, all pellets made by pelletizing torrefied biomass reviewed here [9,10,19] are from single pellet press, which works in a different way compared to commercial

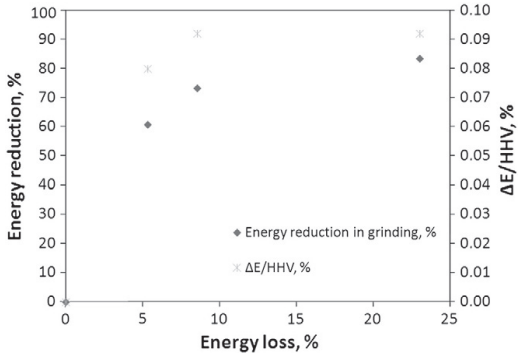

Fig. 8. Energy reduction during grinding and the fraction of reduced grinding energy (ΔE) in sample's higher heating value (HHV) vs. pellets' energy loss due to torrefaction.

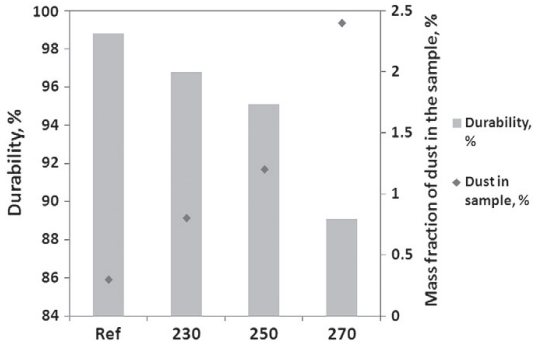

Fig. 10. The results from the standard durability test and mass fraction of dust in the sample prior to the test.

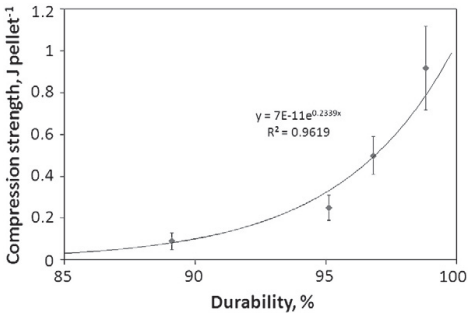

Fig. 11. Plot of compression strength of single 15 mm-long pellet (J pellet^{-1}) vs. durability. The fit of an exponential function is illustrated.

pellet mills. In fact, a variety of pellets made from torrefied biomass are available in markets and they possess very good durability, which means the pellet quality can still be enhanced by adding additives or improving the torrefaction process, for example wet torrefaction.

Acknowledgment

This work was financially supported by ENERGINET.DK and the ForskEL program (Project 2009-1-10202, Torrefaction of Biomass). We would also like to thank VERDO Renewables Limited for supplying the wood pellets.

References

[1] A. Pirraglia, R. Gonzalez, D. Saloni, J. Wright, Wood pellets: an expanding market opportunity, Available at: http://www.biomassmagazine.com/articles/3853/wood-pellets-an-expanding-market-opportunity 2010. Accessed 17.01.2012.
[2] M. Junginger, T. Bolkesjo, D. Bradley, P. Dolzan, A. Faaij, J. Heinimo, B. Hektor, O. Leistad, E. Ling, M. Perry, Developments in international bioenergy trade, Biomass and Bioenergy 32 (2008) 717–729.
[3] T.G. Bridgeman, J.M. Jones, I. Shield, P.T. Williams, Torrefaction of reed canary grass, wheat straw and willow to enhance solid fuel qualities and combustion properties, Fuel 87 (2008) 844–856.
[4] B. Arias, C. Pevida, J. Fermoso, M.G. Plaza, F. Rubiera, J.J. Pis, Influence of torrefaction on the grindability and reactivity of woody biomass, Fuel Processing Technology 89 (2008) 169–175.
[5] P.C.A. Bergman, Combined torrefaction and pelletisation: the TOP process, Energy Research Centre of the Netherlands (ECN), Petten, The Netherlands, 2005, Report No.: ECN-C--05-073 (2005 Jul. 29 pp.).
[6] European Pellet Council, Handbuch für die Zertifizierung von Holzpellets für Heizungszwecke Available at: http://www.enplus-pellets.de/downloads/Enplus Handbuch.pdf. Accessed 11.10.2011.
[7] A. Uslu, A.P.C. Faaij, P.C.A. Bergman, Pre-treatment technologies, and their effect on international bioenergy supply chain logistics. Techno-economic evaluation of torrefaction, fast pyrolysis and pelletisation, Energy 33 (2008) 1206–1223.
[8] M.N. Nimlos, E.B.M.J. Looker, R.J. Evans, Biomass torrefaction studies with a molecular beam mass spectrometer, Preprint Papers - American Chemical Society, Division of Fuel Chemistry 48 (2003) 590.
[9] P. Gilbert, C. Ryu, V. Sharifi, J. Swithenbank, Effect of process parameters on pelletisation of herbaceous crops, Fuel 88 (2009) 1491–1497.
[10] W. Stelte, C. Clemons, J.K. Holm, A.R. Sanadi, J. Ahrenfeldt, L. Shang, U.B. Henriksen, Pelletizing properties of torrefied spruce, Biomass and Bioenergy 35 (2011) 4690–4698.
[11] B. Gfeller, M. Zanetti, M. Properzi, A. Pizzi, F. Pichelin, M. Lehmann, L. Delmotte, Wood bonding by vibrational welding, Journal of Adhesion Science and Technology 17 (2003) 1573–1589.
[12] ASTM E 1758-01, Determination of carbonhydrates in biomass by high performance liquid chromatography, Annual Book of ASTM Standards, vol.11.05, ASTM International, West Conshocken, PA, 2003.
[13] W.E. Kaar, L.G. Cool, M.M. Merriman, D.L. Brink, The complete analysis of wood polysaccharides using HPLC, Journal of Wood Chemistry and Technology 11 (1991) 447–463.
[14] P. Adapa, L. Tabil, G. Schoenau, Grinding performance and physical properties of non-treated and steam exploded barley, canola, oat and wheat straw, Biomass and Bioenergy 35 (2010) 549–561.
[15] S. Mani, L.G. Tabil, S. Sokhansanj, Grinding performance and physical properties of wheat and barley straws, corn stover and switchgrass, Biomass and Bioenergy 27 (2004) 339–352.
[16] EN 15210-1: Solid biofuels – Determination of mechanical durability of pellets and briquettes – Part 1: Pellets, European Committee for Standardization, 2010.
[17] M.M. González-Peña, M.D.C. Hale, Colour in thermally modified wood of beech, Norway spruce and Scots pine. Part 1: Colour evolution and colour changes, Holzforschung 63 (2009) 385–393.
[18] L. Shang, J. Ahrenfeldt, J.K. Holm, A.R. Sanadi, S. Barsberg, T. Thomsen, W. Stelte, U.B. Henriksen, Changes of chemical and mechanical behavior of torrefied wheat straw, Biomass and Bioenergy (2012), doi:10.1016/j.biombioe.2012.01.049.
[19] M.T. Reza, J.G. Lynam, V.R. Vasquez, C.J. Coronella, Pelletization of biochar from hydrothermally carbonized wood, Environmental Progress & Sustainable Energy (2012), doi:10.1002/ep.11615.

PAPER V

Intrinsic kinetics and devolatilization of wheat straw during torrefaction

Lei Shang, Jesper Ahrenfeldt, Jens Kai Holm, Søren Barsberg, Rui-zhi Zhang, Yong-hao Luo, Helge Egsgaard, Ulrik B. Henriksen

Reprinted from *Journal of Analytical and Applied Pyrolysis* (2013), 100, 145-152,

Journal of Analytical and Applied Pyrolysis 100 (2013) 145–152

Contents lists available at SciVerse ScienceDirect

Journal of Analytical and Applied Pyrolysis

journal homepage: www.elsevier.com/locate/jaap

Intrinsic kinetics and devolatilization of wheat straw during torrefaction

Lei Shang[a,*], Jesper Ahrenfeldt[a], Jens Kai Holm[b], Søren Barsberg[c], Rui-zhi Zhang[d], Yong-hao Luo[d], Helge Egsgaard[a], Ulrik B. Henriksen[a]

[a] Department of Chemical and Biochemical Engineering, Technical University of Denmark, 2800 Kgs., Lyngby, Denmark
[b] Chemical Engineering, DONG Energy Thermal Power A/S, Nesa Alle 1, 2820 Gentofte, Denmark
[c] Biomass and Ecosystem Science, Faculty of Life Sciences, University of Copenhagen, Rolighedsvej 23, 1958 Frederiksberg, Denmark
[d] School of Mechanical Engineering, Shanghai Jiaotong University, Shanghai 200240, China

ARTICLE INFO

Article history:
Received 27 September 2012
Received in revised form
22 November 2012
Accepted 11 December 2012
Available online 24 December 2012

Keywords:
Torrefaction
Kinetics
TGA-MS
Wheat straw

ABSTRACT

Torrefaction is a mild thermal treatment (200–300 °C) in an inert atmosphere, which is known to increase the energy density of biomass by evaporating water and a proportion of volatiles. In this work, the degradation kinetics and devolatilization of wheat straw was studied in a thermogravimetric analyzer by coupling with a mass spectrometer. The kinetic parameters obtained by applying a two-step reaction in series model and taking initial dynamic heating period into account can accurately describe the experimental results with different heating programs. Activation energies and pre-exponential parameters obtained for the two steps are: 71.0 and 76.6 kJ mol^{-1}, 3.48×10^4 and 4.34×10^3 s^{-1}, respectively. The model and these parameters were also proven to be able to predict the residual mass of wheat straw in a batch scale torrefaction reactor. By analyzing the gas products in situ, the formation of water, carbon monoxide, formic acid, formaldehyde, methanol, acetic acid, carbon dioxide, methyl chloride, traces of hydrogen sulfide and carbonyl sulfide were found at torrefaction temperatures of 250 and 300 °C.

1. Introduction

Torrefaction is a mild temperature (200–300 °C) pretreatment in an inert atmosphere to upgrade ligno-cellulosic biomass to a high quality biofuel. During the process, biomass releases water and a part of the volatiles, causing a decrease in mass but an increase in energy density [1–3]. Our earlier work also showed improved grindability of wheat straw torrefied above 200 °C [3]. The loss of hemicelluloses, the degradation of which starts at 200–250 °C and cease at about 300 °C, is the main reason for the improvement of grindability in this temperature range. Degradation of the other two main components, lignin and cellulose, detected by ATR (attenuated total reflectance) – Fourier transform infrared spectroscopy occurs at 270–300 °C. This results in a higher energy loss from the wheat straw in this temperature range. So in order to control and optimize the process, it is desired to know the residence times required for complete conversion of the hemicelluloses but only minor degradation of cellulose and lignin in the biomass. The residence time is the result of heat, mass transfer and solid degradation rate in the reacting environment [4]. Therefore, it is important to know the chemical kinetics to predict the thermal decompositions of wheat straw. Thermogravimetric analysis (TGA) is the most common technique in solid-phase thermal degradation studies [5–7]. However, the use of TGA to determine kinetic parameters for the thermal degradation of biomass is complicated in that TGA only provides general information on the overall reaction kinetics while biomass decomposition represents a number of reactions in parallel and series. In practice, the aim of the kinetic evaluation of the thermogravimetric data is to obtain relatively simple models, describing the torrefaction of biomass [8]. There are plenty of research data [9] relating to pyrolysis of biomass under both dynamic conditions (non-isothermal) and steady-state (isothermal) conditions. The main advantage of determining kinetic parameters by non-isothermal methods rather than by isothermal studies is that only a single sample is required to calculate the kinetics over an entire temperature range in a continuous manner. However, it is widely agreed that multiple heating rates should be adopted to enhance the accuracy of the non-isothermal method [9].

In case of torrefaction, all kinetic studies [10–12] were conducted under isothermal condition. Prins et al. [12] used a two-step reaction in series model to describe the weight loss kinetics of willow torrefaction. This model, as shown in scheme (1), was earlier introduced by Di Blasi and Lanzetta [4] for studying the intrinsic kinetics of isothermal xylan degradation under inert atmosphere in the temperature range of 200–340 °C. They found that a one-step global reaction did not fit the experimental results satisfactorily, as the time derivative of the solid mass fraction as a function of temperature exhibited a double peak. In both steps, a competitive

* Corresponding author. Tel.: +45 2132 4979; fax: +45 4677 4109.
E-mail address: lesh@kt.dtu.dk (L. Shang).

0165-2370/$ – see front matter © 2012 Elsevier B.V. All rights reserved.
http://dx.doi.org/10.1016/j.jaap.2012.12.010

volatile and solid formation was taken into account. In the later study done by Branca and Di Blasi on beech wood [13], it was suggested that the first step is due to the degradation of extractives and the most reactive fractions of hemicelluloses, and the second step is due to the degradation of cellulose and part of lignin and hemicelluloses. For temperatures higher than 327 °C there is a third step, which can be attributed to the degradation of lignin and small fractions of the other two constituents. It was observed from both studies that the first step is much faster than the second step. Di Blasi and Lanzetta [4] pointed out the usual limitation encountered in order to attain the isothermal stage is that by using slow heating rates to avoid intra-particle temperature gradients usually result in non-negligible weight loss in the heating stage. Therefore high heating rate (40–70 °C s^{-1}) was adopted, and the char yield was determined as a function of the sample size prior to the tests to ensure no influence from the temperature spatial gradients. Constant char yields were attained for sample thickness around 100 μm, so particle size of 50 μm was chosen for the test. The results showed that the faction of mass loss for the beginning of isothermal stage is in the range of 0–0.16. So it was decided that these data can be analyzed by an isothermal model.

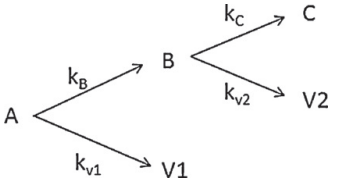

(1)

$$\frac{d[A]}{dt} = -(k_B + k_{v1})[A] \tag{2}$$

$$\frac{d[B]}{dt} = k_B[A] - (k_C + k_{v2})[B] \tag{3}$$

$$\frac{d[C]}{dt} = k_C[B] \tag{4}$$

In scheme (1) the xylan is denoted '*A*', and '*B*' is the intermediate compound, which is a solid with a reduced degree of polymerization. '*V1*' and '*V2*' are volatiles; '*C*' is the solid residue. From the proposed model, rate equations, as shown in Eqs. (2)–(4), can be obtained for solids by assuming first order reactions [4,12], where k is the rate constant for each step, and is expressed as s^{-1}. Integrate the above differential equations, with the initial condition that only *A* is present at the beginning of the reactions, expression for the solid residual, *M*, as a function of the two steps of the reaction mechanism can be given:

$$\frac{M - M_\infty}{M_0} = \lambda_1 e^{-K_1 t} + \lambda_2 e^{-K_2 t} \tag{5}$$

where

$$\frac{M}{M_0} = [A] + [B] + [C] \tag{6}$$

$$\lambda_1 = 1 + \left[\frac{k_B \cdot K_1 - k_B \cdot k_C}{K_1 \cdot (K_2 - K_1)}\right], \quad \lambda_2 = \frac{-k_B \cdot K_2 + k_B \cdot k_C}{K_2 \cdot (K_2 - K_1)} \tag{7}$$

$$\frac{M_\infty}{M_0} = \frac{k_B \cdot k_C}{K_1 \cdot K_2} \tag{8}$$

$$K_1 = k_B + k_{v1}, \quad K_2 = k_C + k_{v2} \tag{9}$$

M_0 is the initial sample mass on ash free basis; M_∞ is the final char yield [*C*] when time is sufficiently long. M/M_0 can be determined experimentally by:

$$\left(\frac{M}{M_0}\right)_{\exp} = \frac{m_{TGA} - m_{ash}}{m_0 - m_{ash}} \tag{10}$$

where m_0 is the initial sample mass, m_{ash} is mass of ash in the sample and m_{TGA} is the mass measured by TGA as a function of time.

Di Blasi and Lanzetta [4] used graphical method to determine kinetic parameters by taking logarithm of Eq. (5).

$$\ln\left(1 - \frac{M_0 - M}{M_0 - M_{B^*}}\right) = -K_1 \cdot t \tag{11}$$

$$\ln\left(1 - \frac{M_{B^*} - M}{M_{B^*} - M_\infty}\right) = -K_2 \cdot (t - t^*) \tag{12}$$

where t^* is demarcation time, which separates the first and the second step. Consequently, M_{B^*} is the maximum value of the reaction intermediate mass, which occurs at time t^*. If the left side of Eqs. (11) and (12) is plotted against time for different temperatures, K_1 and K_2 can then be obtained from the slope of these sets of straight lines. Arrhenius plots are then used to get activation energies, Ea, and pre-exponential factors, *A*.

$$ln\, k = \ln(A) - \frac{Ea}{RT} \tag{13}$$

Prins et al. [12] mentioned that an exact demarcation time is difficult to establish for their results due to overlapping of the reaction steps. They used a numerical approach (MATLAB) to fit all kinetic parameters by minimizing the sum of squares function:

$$F = \sum_i \left[\left(\frac{M}{M_0}\right)_{\exp,i} - \left(\frac{M}{M_0}\right)_{\text{theor},i}\right]^2 \tag{14}$$

Different from Di Blasi and Lanzetta [4], bigger particle size (0.7–2.0 mm) and a much lower heating rate (10 °C min^{-1} to reach the isothermal part) was used in the experiments to obtain the kinetic parameters. However, the model fit the results obtained with the higher heating rate (100 °C min^{-1} at 260 °C) well in the first 14 min.

Repellin et al. [11] proposed that torrefaction is kinetically controlled and neglected heat transfer within wood chips in their study, because the time taken for the center of a wood chip to reach the temperature imposed at the surface of these chips is short compared to the heating rate and the residence time of torrefaction (e.g. at 200 °C, this characteristic time was 8 s for beech and 11 s for spruce). It was also concluded that for a residence time of more than 20 min, the anhydrous weight loss (AWL) depends almost entirely on the torrefaction temperature, because AWL is composed of two stages. The first stage is completed within 20 min with a rapid increase, the second one matches with a slow increase. They used activation energies found in the literature and adjusted kinetic constants for the three models to fit the calculated weight loss to the experimental data using a minimization of least squares method. The models used were a global one-step reaction model, a Di Blasi and Lanzetta model [4], and a Rousset model [14]. The Rousset model assumes that lignin and cellulose hardly react; hence the decomposition of hemicelluloses is the reason for the overall AWL of wood. However, Repellin et al. only compared the final AWL with experimental results; no comparison was conducted on the degradation of wood as a function of time.

Chen and Kuo [10] analyzed the thermal decompositions of the three constituents (hemicelluloses, cellulose and lignin) separately using TGA at 200–300 °C with 1 h residence time. Kinetic parameters (activation energy, pre-exponential factor and reaction order) were derived by applying a global one-step reaction model to the weight loss curve for these three constituents. With the assumption of no interaction among hemicelluloses, cellulose and lignin, the torrefaction of a mixture of these constituents can be described by the superimposed kinetics. The limitation of this model is that the heating period is not taken into account, and that the conversion of the components, especially hemicellulose and xylan, is already as

high as 70% at the beginning of torrefaction at 300 °C. So the interpretation of the data lacks an important part of the whole process. And hence the use of this model will be limited if different heating rates are applied. Moreover, as the assumption of a constant ratio of char to volatile yields is made; one-step mechanisms cannot be applied to predict product distribution [4].

Therefore, the present study uses a two-step reaction in series model as shown in Eq. (1) and includes the non-isothermal part of torrefaction in the model. Wheat straw sample (<0.09 mm) was tested on TGA at heating rates of 10 and 50 °C min^{-1} to obtain intrinsic kinetic parameters. Afterwards this model and parameters were examined by comparing the residual mass predicted by the model and experimental data from a batch scale reactor. Secondly, devolatilization of wheat straw during torrefaction (at 250 and 300 °C) was studied by coupling a mass spectrometer with the TGA and detecting the gas products *in situ*. The relative quantity of each gas product from the two torrefaction temperatures was also compared. The objective of this study is to develop a kinetic expression that can predict the mass loss and gas evolution during torrefaction of wheat straw under real production conditions.

2. Experimental

2.1. Materials

The wheat straw used in this study is from winter wheat (*Triticum aestivum* L.), which was the most grown wheat species in Denmark in 2008. The straw was cut by hand in the field on the island of Funen, Denmark (55°21′N, 10°21′E) in August 2008, and stored indoors packed in paper bags. Prior to the TGA experiment, wheat straw were milled and particles smaller than 90 μm were collected. The cell wall composition and proximate analysis of the wheat straw raw material are listed in Table 1, and detailed descriptions of the analysis methods can be found in previous work [3,15].

2.2. Thermogravimetric analysis

Torrefaction of wheat straw (in the range of 250 and 300 °C) at heating rates of both 10 and 50 °C min^{-1} were carried out on a TGA (TG 209 F3, NETZSCH, Germany) with a nitrogen flow rate of 40 cm^3 min^{-1}. Sample weight varied from 3 to 5 mg, and ceramic crucible was used for the test. In each test, the sample was first heated up to 105 °C at 20 °C min^{-1} and held for 3 min for complete drying, then heated to the desired torrefaction temperature and held for 90 min. Afterwards, purge gas was switched from nitrogen to air and the sample was heated to 850 °C at 50 °C min^{-1}, and kept at this temperature for 5 min for complete combustion. The residual mass is the ash content, and data was obtained using Eq. (10). Two tests were conducted for each condition, and good reproducibility was achieved.

2.3. Thermogravimetric/mass spectrometric analysis

Torrefaction tests were also carried out using a thermal analyzer (STA 409, NETZSCH, Germany) in the TGA/DSC configuration mode. Prior to the experiment, wheat straw particles were dried in the oven at 100 °C overnight. Approximately 10 mg of the sample was placed on the microbalance and heated at 10 °C min^{-1} under 50 cm^3 min^{-1} argon, to a final temperature of 250 or 300 °C, and kept at this temperature for 1 h. Evolved gas was analyzed online by a quadrupole mass spectrometer (QMS 403 C, NETZSCH, Germany) coupled to the TGA. In order to prevent condensation of the evolved gas, the transfer line and inlet system of QMS was kept at ca. 300 °C. A small portion of the evolved gas together with the purge gas was led to the ion source of the mass spectrometer, since the pressure drops from atmospheric pressure in the TGA down to high vacuum in the QMS.

The analysis was focused on selected ions (m/z), in particular those which had been detected with high intensity. Since it is difficult to assign a given fragment to a single compound without confirmation by complimentary methods, the main detected m/z values were associated with the chemical species that are commonly present in gas products of wheat straw torrefaction or early stages of pyrolysis. A maximum number of 64 ions could be monitored as a function of time. The mass spectrometric intensities were normalized by the initial sample mass, and the background was subtracted. In order to compare the relative intensity of gas products at different temperatures, the signals were further normalized by the total intensity current (TIC) of the experiment [16]. However no specific response factors were applied. In order to reach the most reasonable association, the ion traces of both parent and fragment ions of most species have been considered. Furanes and phenols (tar), e.g. furfural and guaiacol, were not detected.

The quantification analysis of gaseous products released during torrefaction was only performed for H_2O in this study based on the methods used by Tihay and Gillard [17]. The concentration of H_2O was directly deduced from the ion intensities by:

$$[H_2O] = \frac{I_{18}}{F_A} \tag{15}$$

where I_{18} is the ion intensity for m/z 18 (H_2O), F_A is the calibration factor for H_2O. Correction due to $^{36}Ar^{2+}$ was not required.

2.4. Torrefaction in batch scale

In order to verify the model and kinetic parameters from the TGA test, torrefaction of wheat straw was conducted in a batch scale reactor as shown in Fig. 1. For each test, wheat straw (whole stalk, about 50 g) was first dried in the oven at 104 °C for 24 h prior to the torrefaction, and subsequently placed in an air tight metal reactor (15 cm × 31 cm × 10 cm) with nitrogen gas in and outlet, and a thermocouple centered in the reactor. The reactor was placed in an oven (type S 90, Lyngbyovnen, Denmark) with heating rate of 6 °C min^{-1}. Nitrogen flow was adjusted to 500 cm^3 min^{-1}, and a heater was used for gas outlet to avoid condensation. Torrefaction was carried out at temperatures spanning from 200 to 300 °C for about 2 h residence time (from the thermocouple inside the reactor reached the torrefaction temperature until the start of cooling down period). Ash content was determined by placing the samples in a muffle furnace at 550 °C for 3 h. Before the measurement, sample crucibles were ashed and dried. Two measurements were taken for each condition.

3. Results and discussion

3.1. Thermal decomposition characteristics

The differential thermogravimetric (DTG) curves at 250 °C and 300 °C are shown in Fig. 2, which allows observing the different torrefaction stages. The first peak between 50 °C and 150 °C is usually called drying stage, and corresponding to the vaporization of moisture, to the desorption of water and to the emission of volatile organic compounds [17]. The shoulder around 280 °C during torrefaction at 300 °C can be attributed to the hemicellulose degradation. The maximum peak, which occurs when temperature reaches 300 °C, corresponds to the main step of cellulose degradation (depolymerization). No shoulder is observed for torrefaction conducted at 250 °C, which means the reaction temperature of 250 °C is not high enough for the degradation of cellulose. This is in agreement with the conclusion drawn from our early work [3], where the degradation temperature of cellulose in wheat straw

Table 1
Chemical and proximate analysis (d.b.) of oven dried wheat straw.

	Cell wall composition			Proximate analysis			
	Lignin	Cellulose	Hemicellulose	Moisture	Volatiles	Fixed carbon	Ash
Wheat straw	20.3	34.0	26.5	1.35	74.78	19.23	4.6

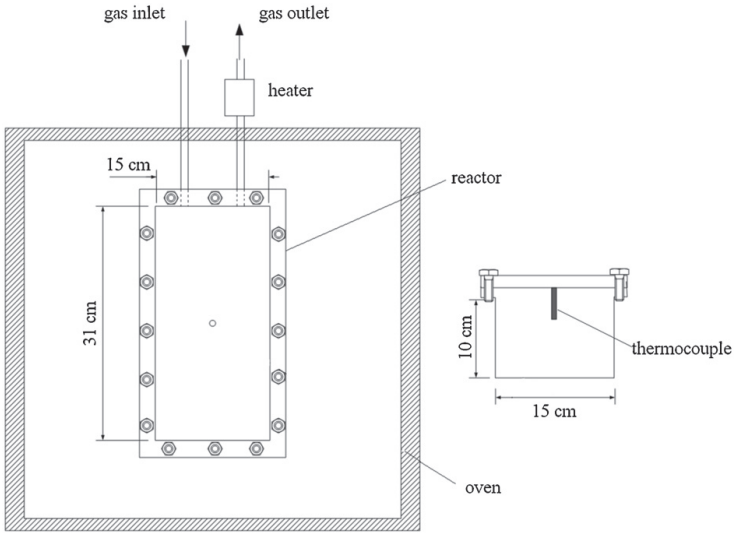

Fig. 1. Drawing of the torrefaction reactor.

was found to be between 270 and 300 °C. This also confirms the hypothesis of two-step reaction in serial models.

3.2. Kinetic model for torrefaction

The two-step reaction series model, as shown in scheme (1), was chosen for this study. In contrast to Di Blasi and Lanzetta [4], slow heating rate was used in this study to avoid intra-particle temperature gradients. Therefore, weight loss during heating stage needs to be taken into account when deriving the kinetic parameters from the isothermal stage:

at $t = 0$, $\quad [A] = [A]_0$, $\quad [B] = [B]_0$, $\quad [C] = [C]_0$

Integration of Eqs. (2)–(4) with the above mentioned initial conditions gives:

$$[A] = [A]_0 \exp(-K_1 t) \tag{16}$$

$$[B] = \frac{k_B[A]_0}{K_1 - K_2} [\exp(-K_2 t) - \exp(-K_1 t)] + [B]_0 \exp(-K_2 t) \tag{17}$$

$$[C] = [C]_0 + \frac{k_C (k_B[A]_0 + K_1[B]_0)}{K_1 K_2} + \frac{k_B k_C [A]_0 \exp(-K_1 t)}{K_1 (K_1 - K_2)} - \frac{k_B k_C [A]_0 \exp(-K_2 t)}{K_2 (K_1 - K_2)} - \frac{k_C [B]_0 \exp(-K_2 t)}{K_2} \tag{18}$$

$$\left(\frac{M}{M_0}\right)_{\text{theor}} = [A] + [B] + [C] \tag{19}$$

A schematic drawing of the algorithm taking into account the chemical composition change at the onset of the isothermal period is shown in Fig. 3. In the first iteration it was assumed that the entire solid is A, with no B and C. With this initial assumption and a starting guess of k_B, k_{V1}, k_C, k_{V2}, which were based on values found from [12], nonlinear optimization using the MATLAB (version R2008b) command 'lsqcurvefit' was made with the default tolerance settings. The 'lsqcurvefit' is based on the Niedler–Mead optimization algorithm and used to minimize the root mean square of the difference between the calculated and experimental data. Following this, at each temperature the four pre-exponential factors (A) and activation energies (Ea) were calculated by means of Arrhenius plot

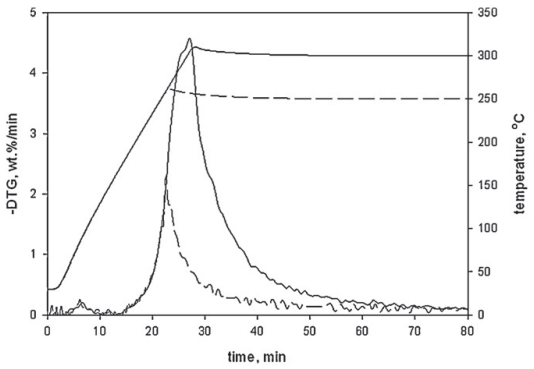

Fig. 2. Temperature and DTG profile of wheat straw torrefied at 250 °C (dash line) and 300 °C (solid line) at heating rate of 10 °C min^{-1}.

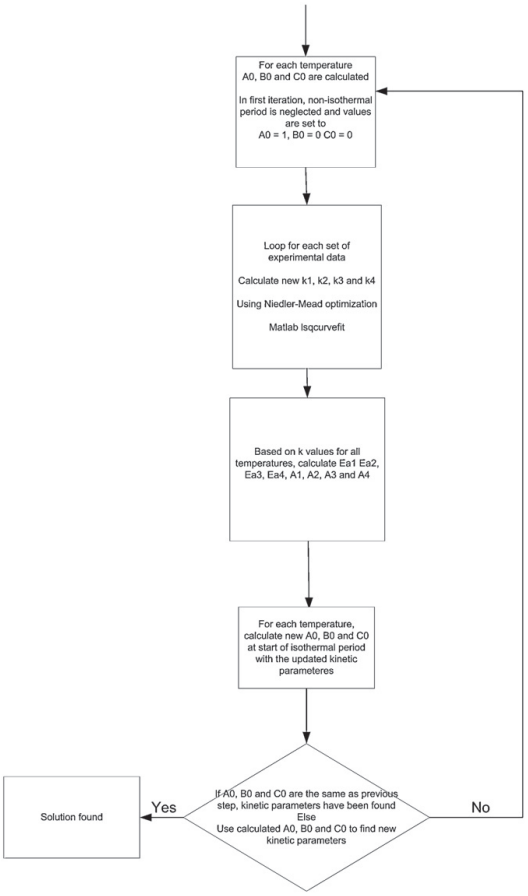

Fig. 3. Diagram of algorithm used in MATLAB for calculating kinetic parameters of wheat straw torrefaction.

as shown in Eq. (13). With these calculated values the initial concentration of the isothermal period for *A*, *B*, and *C* can be obtained, and then used as input for the optimization. The calculations were done by numerical solution of the three coupled first order differential equations, as shown in Eqs. (2)–(4). To account for the heating rate, the chain rule was used to transform the equations into the temperature dependent form shown in Eqs. (20)–(22). From the second iteration and onwards the calculated *A* and Ea were used to provide the starting guess for the Niedler–Mead optimization. The procedure was repeated until stable values for the *A* and Ea were reached, as shown in Fig. 4.

$$\frac{d[A]}{dT} = \left(\frac{dt}{dT}\right) \cdot \left\{-(k_B + k_{v1})[A]\right\} = \frac{1}{\beta} \cdot \left\{-(k_B + k_{v1})[A]\right\} \quad (20)$$

$$\frac{d[B]}{dT} = \frac{1}{\beta} \cdot \left\{k_B[A] - (k_C + k_{v2})[B]\right\} \quad (21)$$

$$\frac{d[C]}{dT} = \frac{1}{\beta} \cdot \left\{k_C[B]\right\} \quad (22)$$

where β is the heating rate in $^{\circ}C\,s^{-1}$.

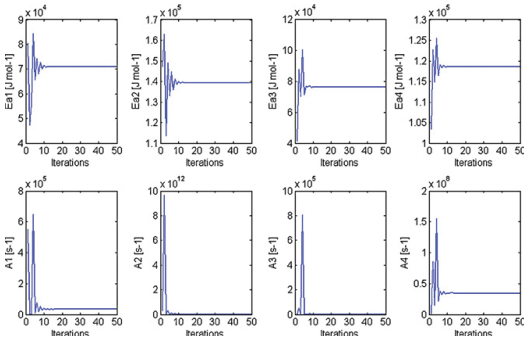

Fig. 4. Plot of activation energies (Ea) and pre-exponential factors (*A*) from each iteration when deriving kinetic parameters for k_B, k_{V1}, k_C, k_{V2} (from left to right).

3.3. Kinetic parameters and model verification

The kinetic parameters obtained by fitting the experimental data at 250, 260, 275 °C (at heating rate of 10 °C min^{-1}) and at 250, 260, 275, 280 (at heating rate of 50 °C min^{-1}) are as follows:

$$k_B = 3.48 \times 10^4 \exp\left(\frac{-70999}{RT}\right) \quad (23)$$

$$k_{v1} = 3.91 \times 10^{10} \exp\left(\frac{-139460}{RT}\right) \quad (24)$$

$$k_C = 4.34 \times 10^3 \exp\left(\frac{-76566}{RT}\right) \quad (25)$$

$$k_{v2} = 3.48 \times 10^7 \exp\left(\frac{-118620}{RT}\right) \quad (26)$$

where k is the reaction rate constant in unit of s^{-1}, T is the temperature in K, and R is the universal gas constant in J mol^{-1} K^{-1}. In agreement with literature, the first step is much faster than the second step. Solid yields for the two reaction steps decreased from 85% and 66% at 250 °C to 61% and 46% at 300 °C, respectively.

In order to verify the model, experimental data were compared with the model results for both the non-isothermal part (heating period from 200 °C to final torrefaction at both heating rates) and isothermal part. Due to the similarity, only results from 10 °C min^{-1} are shown in Fig. 5 part (a). Instead, a multiple-step torrefaction was run from 200 °C to 270 °C at different heating rates and held at 270 °C for 1 h. The model and experimental results are shown in Fig. 5(b). It can be seen the model described the reaction accurately.

The model was also tested on torrefaction of wheat straw conducted in a batch reactor, as shown in Fig. 1. The temperature recorded in the center of the reactor was used as the input for the model to calculate the residual mass, assuming heat transfer from the wheat straw surface to the center is much faster than the heating rate of the oven. Model and experimental results are shown in Fig. 6. There is a good correlation between model results and experimental data.

3.4. Gas evolution with MS analysis

Gas products detected during torrefaction of wheat straw based on selected ions were water (18), carbon monoxide (28), formic acid (46, 45), formaldehyde (30, 29), methanol (31, 32), acetic acid (43, 45, 60), carbon dioxide (44), methyl chloride (50, 52). Traces of hydrogen sulfide (34) and carbonyl sulfide (60, 48) were also found. In addition, relatively large quantities of simple aliphatic hydrocarbons were apparently present, C_xH_y and C_xH_{2x} (15, 27, 39, 41).

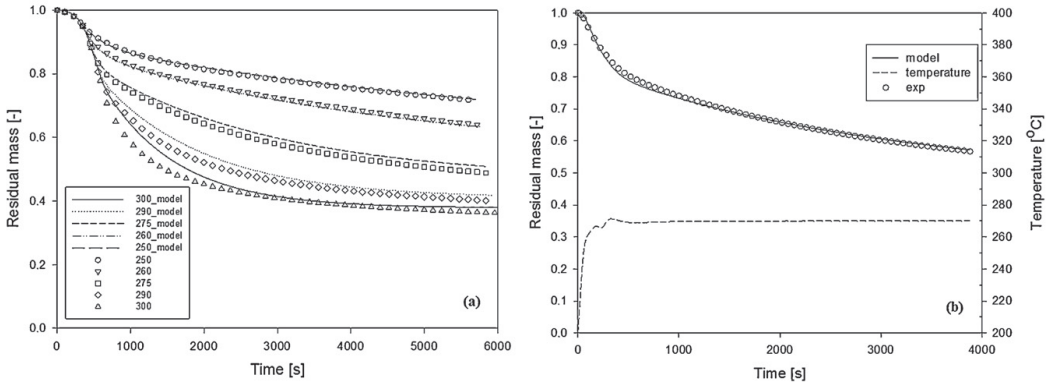

Fig. 5. Experimental and modeled relative weight (on ash free basis) of wheat straw vs. time for (a) at heating rate of 10 K min^{-1}. (b) Multiple-step heating at various rates. Starting weight is defined at 200 °C; heating period from 200 °C to desired torrefaction temperature is included in the plot.

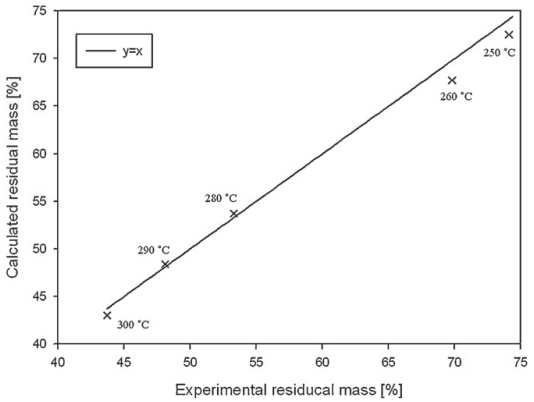

Fig. 6. Correlation between experimental residual mass obtained from torrefaction of wheat straw in a batch reactor and calculated results from the model. Both results are on dry and ash free basis.

Table 2
Fraction of wheat straw overall mass loss at two stages, and calculated mass fraction of water evolved during torrefaction after the drying stage.

%	300 °C	250 °C
Mass loss at 10 min	0.66	0.67
Mass loss at 81.5 min	57.95	21.59
H_2O released from 10 to 81.5 min	26.00	7.94

Since no signals other than water was observed during the early stage (<150 °C), the total weight loss in this period can be attributed to the release of water (the first peak of $m/z = 18$ in Fig. 7). Based on Eq. (15), the cumulative water evolution during torrefaction after drying stage (the second peak of $m/z = 18$), $m_{H_2O,2nd}$, can be calculated by Eq. (27) and results are shown in Table 2. It can be seen that at 300 °C, evolution of water (26.66%) accounts for almost half of the overall mass loss (57.95%). Similar results were reported by Prins et al. [18] that a mass fraction of 5.5% released from straw when torrefied at 250 °C for 30 min was water and water released from willow when torrefied at 300 °C and 250 °C was 13% and 7%, respectively.

$$m_{H_2O,2nd} = m_{H_2O,1st} \times \frac{\int_{10\,min}^{81.5\,min} I_{18}}{\int_{0\,min}^{10\,min} I_{18}} \quad (27)$$

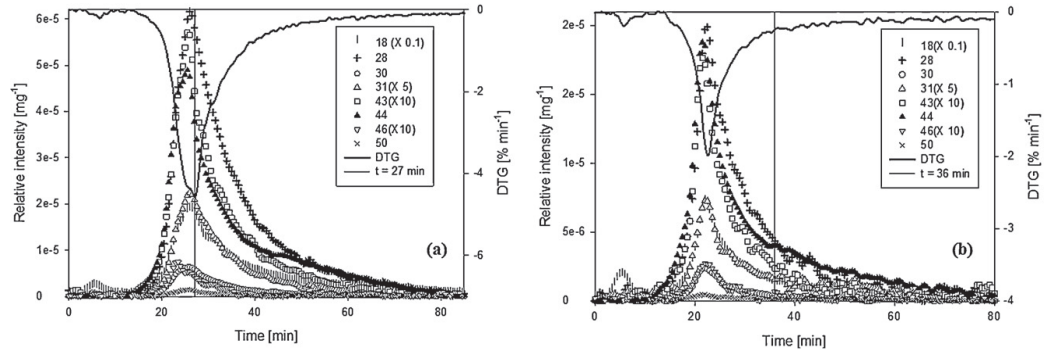

Fig. 7. DTG and MS curves of wheat straw torrefied at 300 °C (a) and 250 °C (b). The straight line refers to the time when yield of the intermediate solid product '*B*' reaches the maximum.

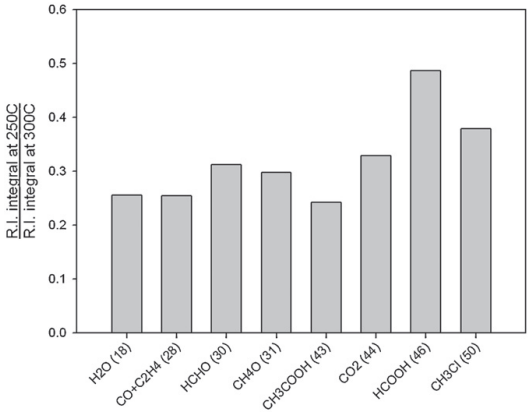

Fig. 8. Ratio of each gas product released from wheat straw at 250 and 300 °C by calculating the relative intensity (RI) integral over the period from 200 °C until the end of torrefaction.

Fig. 8 indicates the relative quantities of each gas released from torrefaction at temperatures of 250 and 300 °C for a residence time of 1 h. It can be seen that the quantities of most of the gas products released at 250 °C was about 30% of the gasses released at 300 °C, except for formic acid (46). It means that formic acid is preferentially released at lower temperatures compared to the other gases. This phenomenon can also be observed from the 300 °C data in Fig. 7, where the peak of this compound appeared before the other products.

4. Discussion

Fig. 9 shows the change of *A*, *B*, and *C* at torrefaction temperatures of 250 and 300 °C with a heating rate of 10 °C min^{-1} from 200 °C. At a torrefaction temperature of 300 °C, the isothermal part of torrefaction starts at 600 s, where $[A]_0$ is as low as 4%. So it is not reasonable to assume that only *A* is present at the beginning of the reaction with a low heating rate such as 10 °C min^{-1} as in [12]. In order to simulate the model with such assumption, 1 iteration instead of 50 was run to derive the kinetic parameters. A comparison of model results and experimental data are shown in Fig. 10.

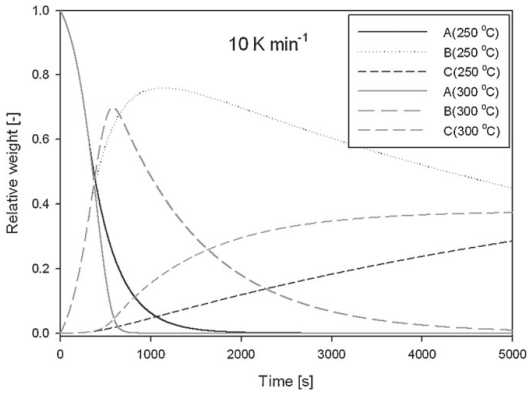

Fig. 9. Yields of *A*, *B*, and *C* at torrefaction temperature of 250 and 300 °C and heating rate of 10 °C min^{-1}. Starting weight defined at 200 °C, heating period from 200 °C is included in the plot.

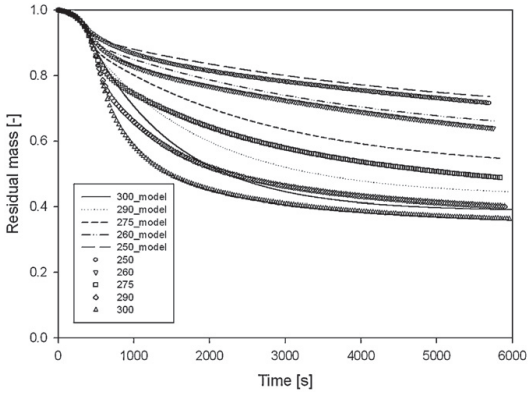

Fig. 10. Same experimental results as in Fig. 5 part (a), but with modeled relative weight using kinetic parameters from only one iteration.

In comparison with Fig. 5, which shows the model results using parameters from 50 iterations, it can be seen that the parameters from 50 iterations gives a better fit to the experimental data.

In this study, experimental data at both heating rates (10 and 50 °C min^{-1}) were used to derive the activation energies (Ea) and pre-exponential factors (*A*), because model with these parameters gives best fit to most experimental results. It can be seen in Fig. 5 that at higher temperature the agreement between model and experimental data is not as good as at lower temperature. This is because the experimental data used to derive the kinetic parameters is only up to 275 °C for 10 °C min^{-1}, and 280 °C for 50 °C min^{-1}. The reason of not including experimental data above 280 °C is due to that the heating rate of the TGA is limited to 80 °C min^{-1}, and thus while being heated to high temperature (e.g. 300 °C) major fraction of *A* will already be transformed to *B* in initial non-isothermal phase of experiments. Another potential problem is the temperature overshooting when reaching the desired temperature in TGA, and the higher the set temperature (and/or the higher the heating rate) the larger the overshoot occurs. For example, the overshoot can be 10 °C for 290 °C with 50 °C min^{-1}. It was also found kinetic parameters obtained by including these experimental data do not fit well with 10 °C min^{-1} experimental data when applied to the model.

According to Fig. 9, the maximum yield of *B* ($[B]_{max}$) is found at 580 and 1140 s for torrefaction temperatures of 300 and 250 °C, respectively. At 300 °C, $[B]_{max}$ locates close to the end of first step reaction and the early stage of the second step reaction, since the yield of *A* decreases to almost zero and the yield of *C* just starts to increase from 0. While for 250 °C $[B]_{max}$ is reached during the second step. The vertical straight lines in Fig. 7 correspond to 580 and 1140 s after reaching 200 °C. Correspondingly, most gases were released before reaching the $[B]_{max}$ for 250 °C, while for 300 °C more than half of the gas products were released after reaching the $[B]_{max}$.

However, when applying the model to a real torrefaction facility, there could be limitations from heat transfer when biomass in other forms (e.g. logs, chips, etc.) or other kinds (e.g. biomass with different compositions that may generate heat during torrefaction) are used as feedstock. In this case, a heat transfer model will need to be coupled to the existing kinetic model for the mass loss calculations.

5. Conclusion

A two-step first order reaction in series model was used to study the kinetics of wheat straw torrefaction in a TGA setup. In contrast

to other studies, which obtained the kinetic parameters from the isothermal part of torrefaction by neglecting the degradation of sample during the heating period, this paper took the mass loss during the heating period into account when deriving the parameters. The results show that parameters obtained in this way are in better accordance with the experimental results. Torrefaction of wheat straw was also conducted in a batch scale reactor at a much lower heating rate; a model with kinetic parameters obtained from TGA gave good prediction of residual mass at the end of the reaction. It means the mass yield and gross chemical state of solids in the real torrefaction facility can be predicted by simply knowing the temperature history of the sample. By analyzing the gas evolution *in situ*, water, carbon monoxide, formic acid, formaldehyde, methanol, acetic acid, carbon dioxide, methyl chloride, and traces of hydrogen sulfide, carbonyl sulfide were found at both 250 and 300 °C. At 300 °C, evolution of water accounts for almost half of the overall mass loss.

Acknowledgements

This work was financially supported by ENERGINET.DK and the ForskEL program (Project 2009-1-10202, Torrefaction of Biomass). The authors express their appreciation to Freddy Christensen, Kristian Estrup, Erik Hansen for the assistance of building the torrefaction reactor and to Tobias Thomsen for performing the torrefaction. Thanks are also due to Tomas Fernqvist for conducting the cell wall composition analysis.

References

[1] M.J.C. van der Stelt, H. Gerhauser, J.H.A. Kiel, K.J. Ptasinski, Biomass upgrading by torrefaction for the production of biofuels: a review, Biomass Bioenergy 35 (9) (2011) 3748–3762.
[2] L. Shang, N.P.K. Nielsen, J. Dahl, W. Stelte, J. Ahrenfeldt, J.K. Holm, et al., Quality effects caused by torrefaction of pellets made from Scots pine, Fuel Processing Technology 101 (2012) 23–28.
[3] L. Shang, J. Ahrenfeldt, J.K. Holm, A.R. Sanadi, S. Barsberg, T. Thomsen, et al., Changes of chemical and mechanical behavior of torrefied wheat straw, Biomass Bioenergy 40 (2012) 63–70.
[4] C. Di Blasi, M. Lanzetta, Intrinsic kinetics of isothermal xylan degradation in inert atmosphere, Journal of Analytical and Applied Pyrolysis 40 (1997) 287–303.
[5] M. Stenseng, A. Jensen, K. Dam-Johansen, Investigation of biomass pyrolysis by thermogravimetric analysis and differential scanning calorimetry, Journal of Analytical and Applied Pyrolysis 5 (2001) 8–59, 765-780.
[6] D.K. Shen, S. Gu, K.H. Luo, A.V. Bridgwater, M.X. Fang, Kinetic study on thermal decomposition of woods in oxidative environment, Fuel 88 (6) (2009) 1024–1030.
[7] K. Ninan, Kinetics of solid state thermal decomposition reactions, Journal of Thermal Analysis and Calorimetry 35 (4) (1989) 1267–1278.
[8] L. Helsen, E. Van den Bulck, Kinetics of the low-temperature pyrolysis of chromated copper arsenate-treated wood, Journal of Analytical and Applied Pyrolysis 53 (1) (2000) 51–79.
[9] J.E. White, W.J. Catallo, Biomass pyrolysis kinetics: a comparative critical review with relevant agricultural residue case studies, Journal of Analytical and Applied Pyrolysis 91 (1) (2011) 1–33.
[10] W.H. Chen, P.C. Kuo, Isothermal torrefaction kinetics of hemicellulose, cellulose, lignin and xylan using thermogravimetric analysis, Energy 36 (11) (2011) 6451–6460.
[11] V. Repellin, A. Govin, M. Rolland, R. Guyonnet, Modelling anhydrous weight loss of wood chips during torrefaction in a pilot kiln, Biomass Bioenergy 34 (5) (2010) 602–609.
[12] M.J. Prins, K.J. Ptasinski, F.J.J.G. Janssen, Torrefaction of wood Part 1: weight loss kinetics, Journal of Analytical and Applied Pyrolysis 77 (1) (2006) 28–34.
[13] C. Branca, C. Di Blasi, Kinetics of the isothermal degradation of wood in the temperature range 528–708 K, Journal of Analytical and Applied Pyrolysis 67 (2) (2003) 207–219.
[14] P. Rousset, I. Turner, A. Donnot, P. Perré, The choice of a low-temperature pyrolysis model at the microscopic level for use in a macroscopic formulation, Annals for Forest Science 63 (2) (2006) 1–17.
[15] L. Shang, W. Stelte, J. Ahrenfeldt, J.K. Holm, R. Zhang, Y. Luo, et al., Physical and chemical property changes of 3 biomass fuels caused by torrefaction. Biomass Bioenergy (under review).
[16] A. Arenillas, F. Rubiera, J. Pis, Simultaneous thermogravimetric-mass spectrometric study on the pyrolysis behaviour of different rank coals, Journal of Analytical and Applied Pyrolysis 50 (1) (1999) 31–46.
[17] V. Tihay, P. Gillard, Pyrolysis gases released during the thermal decomposition of three Mediterranean species, Journal of Analytical and Applied Pyrolysis 88 (2) (2010) 168–174.
[18] M.J. Prins, K.J. Ptasinski, F.J.J.G. Janssen, Torrefaction of wood: Part 2: analysis of products, Journal of Analytical and Applied Pyrolysis 77 (1) (2006) 35–40.

PAPER VI

A method of predicting the heating value of the solid residues during torrefaction

Lei Shang, Jesper Ahrenfeldt, Jens Kai Holm, Ulrik B. Henriksen

Submitted for conference

EU BC&E 2013, June 2013
Subject 3:
3.2 Advanced solid biofuels

A method of predicting the heating value of the solid residues during torrefaction

Lei Shang[§], Jesper Ahrenfeldt[§], Jens Kai Holm[£], Ulrik B. Henriksen[§]*

** Corresponding author: Phone: +45 2132 4979, E-mail: lesh@kt.dtu.dk*

§ Department of Chemical and Biochemical Engineering, Technical University of Denmark, DTU, building 313, Frederiksborgvej 399, DK-4000 Roskilde, Denmark

£ Chemical Engineering, DONG Energy Power A/S, Nesa Alle 1, DK-2820, Gentofte, Denmark

Abstract

Torrefaction is a mild thermal treatment (200-300 ˚C) in an inert atmosphere, which is known to increase the energy density of biomass by evaporating water and a proportion of volatiles. In this work, a two-step first order reaction in series model was used to study the kinetics of wheat straw torrefaction in a thermogravimetric analyzer (TGA) setup. In contrast to other studies, which obtained the kinetic parameters from the isothermal part of torrefaction by neglecting the degradation of sample during the heating period, this work took the mass loss during the heating period into account when deriving the parameters. The results show that parameters obtained in this way are in better accordance with the experimental results, and they can accurately describe the experimental results with different heating programs. Torrefaction of wheat straw was also conducted in a batch scale reactor at a much lower heating rate; a model with kinetic parameters obtained from TGA gave good prediction of residual mass at the end of the reaction. It means the mass yield of solids in the real torrefaction facility can be predicted by simply knowing the temperature history of the sample. Together with the previously measured higher heating value (HHV) and energy yield plot of biomass torrefied at different conditions, it is possible to predict the HHV of the products in advance by just measuring the HHV of the raw material of the feedstock. This could be a reliable method as torrefaction process design in order to produce homogeneous torrefied products in real facilities.

Explanatory pages

The two-step first order reaction in series model, as shown in scheme (1), was chosen for this study. As opposed to the high heating rate of 40-70 K s^{-1} adopted by Di Blasi and Lanzetta [1], slow heating rate (< 100 K min^{-1}) was used to avoid intra-particle temperature gradients. Therefore weight loss during heating stage needs to be taken into account when deriving the kinetic parameters from the isothermal stage. Prins et al. [2] first used this model, Eq. (2)-(4), for studying torrefaction of willow. But the degradation during the heating period was neglected. A schematic drawing of the algorithm taking into account the chemical composition change at the onset of the isothermal period is shown in Figure 1.

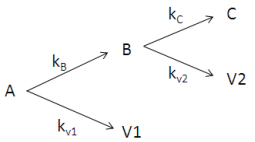

(1)

$$\frac{d[A]}{dt} = -(k_B + k_{v1})[A] \tag{2}$$

$$\frac{d[B]}{dt} = k_B[A] - (k_C + k_{v2})[B] \tag{3}$$

$$\frac{d[C]}{dt} = k_C[B] \tag{4}$$

Where the biomass is denoted ‘A’, and ‘B’ is the intermediate compound, which is a solid with a reduced degree of polymerization. ‘V1’ and ‘V2’ are volatiles; ‘C’ is the solid residue. k is the rate constant for each step, expressed as s^{-1}. And $at \quad t = 0, \quad [A] = A0, \quad [B] = B0, \quad [C] = C0$.

Wheat straw sample (< 0.09 mm) was tested on TGA at heating rates of 10 and 50 ˚C min^{-1} to obtain intrinsic kinetic parameters. The model developed in this study allows predicting the mass yield of the solid by simply knowing the temperature history/profile of the biomass. In order to verify the model, experimental data were compared with model results for both non-isothermal part (heating period from 200 ˚C to final torrefaction at both heating rates) and isothermal part (Figure 2 (a)). The model was also tested on torrefaction of wheat straw conducted in our batch scale torrefaction reactor. The temperature recorded in the center of the reactor was used as the input for the model to calculate the residual mass, assuming heat transfer from the wheat straw surface to the center is much faster than the heating rate of the oven (6 ˚C min^{-1}). Model and experimental results are shown in Figure 2 (b).

Based on the previous studies about the heating value and energy yield of torrefied biomass (wheat straw, wood chips and pellets) (Figure 3), which shows a similar energy yield trend according to mass loss during torrefaction (AWL). It is possible to predict the higher heating value (HHV) of the products in advance by just measuring the HHV of the raw material of the feedstock. This method may supply a solution to the inhomogeneity problem of torrefied products encountered by most torrefaction facilities.

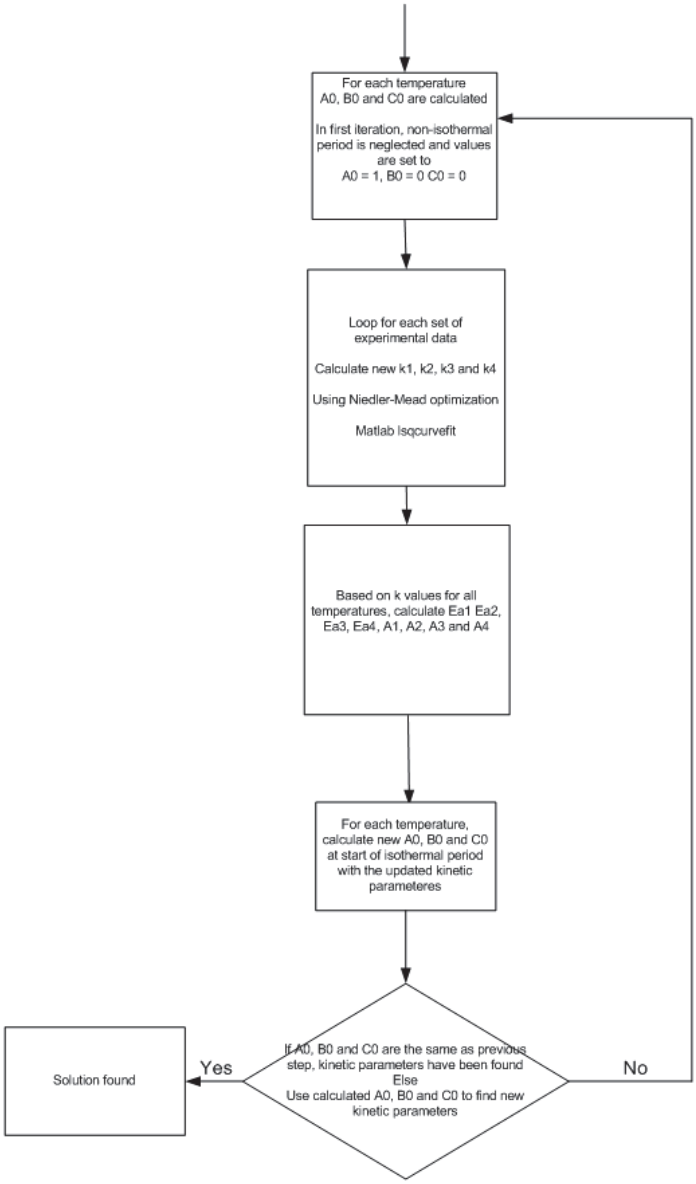

Figure 1: Diagram of algorithm used in MATLAB for calculating kinetic parameters of wheat straw torrefaction [3].

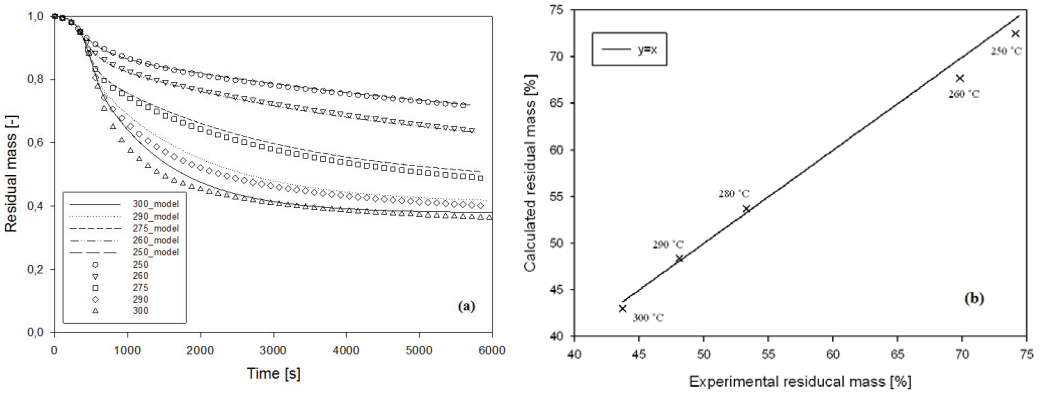

Figure 2: Experimental and modeled relative weight of wheat straw (daf) vs. time for (a) tests run on TGA at heating rate of 10 K min^{-1}; (b) torrefaction of wheat straw in a batch reactor [3].

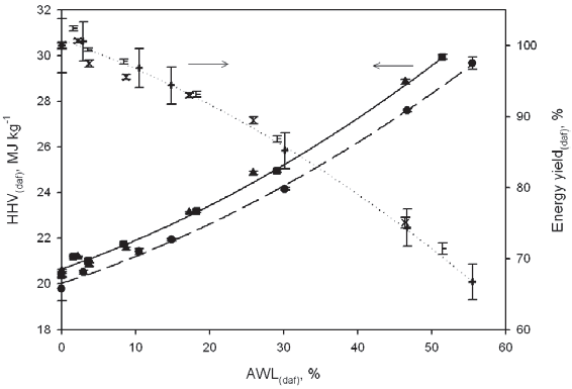

Figure 3: Higher heating value for wheat straw (●), wood pellets (■) wood chips (▲), and energy yield for wheat straw (+), wood pellets (-), wood chips (×) vs. anhydrous weight loss (torrefaction was carried out from 200 to 300 °C with every 20 °C interval) [4].

Reference

[1] Di Blasi C, Lanzetta M. Intrinsic kinetics of isothermal xylan degradation in inert atmosphere. J Anal Appl Pyrolysis 1997;40:287-303.

[2] Prins MJ, Ptasinski KJ, Janssen FJJG. Torrefaction of wood:: Part 1. Weight loss kinetics. J Anal Appl Pyrolysis 2006;77(1):28-34.

[3] Shang L, Ahrenfeldt J, Holm JK, Barsberg S, Zhang RZ, Luo YH, Egsgaard H, Henriksen UB. Intrinsic kinetics and devolatilization of wheat straw during torrefaction. J Anal Appl Pyrol, accepted.

[4] Shang L, Stelte W, Zhang RZ, Thomsen T, Bach LS, Ahrenfeldt J. Physical and chemical property changes of 3 biomass fuels caused by torrefaction, oral presentation: WSED Next: 29.Feb – 2.Mar 2012, Wels, Austria.